UNIVERSIDADE FEDERAL DE SÃO CARLOS
CENTRO DE CIÊNCIAS BIOLÓGICAS E DA SAÚDE
PROGRAMA DE PÓS-GRADUAÇÃO EM GENÉTICA EVOLUTIVA E BIOLOGIA MOLECULAR

Juliana Virginio da Silva

“Microbioma ruminal ativo de Nelore: efeitos da dieta e interações com emissão de metano, eficiência alimentar”

SÃO CARLOS-SP
2025

Juliana Virginio da Silva

Microbioma ruminal ativo de Nelore: efeitos da dieta e interações com emissão de metano, eficiência alimentar

Tese apresentada ao Programa de Pós-Graduação em Genética Evolutiva e Biologia Molecular do Centro de Ciências Biológicas e da Saúde da Universidade Federal de São Carlos, como parte dos requisitos para obtenção do título de Doutor em Ciências, área de concentração: Genética e Evolução.

Orientadora: Drª. Luciana Correia de Almeida Regitano

Coorientador: Dr. Bruno Gabriel Andrade

São Carlos-SP
2025

UNIVERSIDADE FEDERAL DE SÃO CARLOS

Centro de Ciências Biológicas e da Saúde
Programa de Pós-Graduação em Genética Evolutiva e Biologia Molecular

Folha de Aprovação

Defesa de Tese de Doutorado da candidata Juliana Virginio da Silva, realizada em 24/10/2025.

Comissão Julgadora:

Profa. Dra. Luciana Correia de Almeida Regitano (EMBRAPA)

Prof. Dr. Francis de Morais Franco Nunes (UFSCar)

Profa. Dra. Maria Cristina da Silva Pranchevicius (UFSCar)

Profa. Dra. Aline Silva Mello Cesar (ESALQ/USP)

Profa. Dra. Adriana Mércia Guaratini Ibelli (EMBRAPA)

O Relatório de Defesa assinado pelos membros da Comissão Julgadora encontra-se arquivado junto ao Programa de Pós-Graduação em Genética Evolutiva e Biologia Molecular.

DEDICATÓRIA

Dedico esta tese à minha avó Florinda, que começava qualquer pedido com “Você é capaz de…?”. Hoje sei que suas palavras iam muito além das tarefas do dia a dia: eram a forma mais simples e bonita de me ensinar a acreditar em mim.

AGRADECIMENTOS

Agradeço, antes de tudo, à minha família, minha base e meu porto seguro. Aos meus pais Sueli e Donizete, pelo amor incondicional, pelo exemplo de dedicação e por acreditarem em mim mesmo quando eu duvidava. Ao meu irmão Rafael, pela paciência, carinho, conselhos, presença e pelos momentos de leveza e afeto que fizeram toda diferença nos dias difíceis. Eu amo vocês!

A minha orientadora, Luciana Regitano, pela orientação científica, pela confiança depositada em meu trabalho e pelos ensinamentos que levarei além da vida acadêmica. Ao meu coorientador, Bruno Andrade, pelo apoio e pelas contribuições a esta pesquisa.

Aos meus tios, que sempre me apoiaram, oferecendo carinho, conselhos e incentivo em todos os momentos. Aos meus primos, em especial Dudu, Bruna, Renan e Thais, por me acolherem sempre que precisei e por tornarem os dias mais leves. À minha cunhada Ana, por todo o incentivo, pelas palavras de encorajamento e por acreditar em mim. Aos meus primos de coração, Julia, Maria Rita, Peronti, Rafaela e Tamires, pela presença constante, pelas risadas e pelo apoio sincero ao longo dessa trajetória.

A todos os colegas de laboratório que tive o prazer de conhecer ao longo desta jornada, sejam ICs, estagiários, mestrandos, doutorandos, pós-docs ou funcionários, minha gratidão pela companhia, pela troca de experiências e pelo apoio em diferentes momentos deste trabalho.

Agradeço à família que encontrei no laboratório: Liliane, Alex (e André) e Bárbara. Obrigada pelos momentos compartilhados nas viagens, nos treinos, nos Aperolazos e nas partidas de beach tênis. Vocês tornaram os desafios mais leves e as vitórias mais especiais. Em especial, quero agradecer à Liliane pela parceria, pelo apoio, por todos os ensinamentos, pelas reuniões e discussões fora do horário habitual e pelos conselhos que me incentivam a crescer, tanto profissional quanto pessoalmente. Obrigada por ser luz, força e inspiração.

Meus mais sinceros agradecimentos ao Cardigans. Karen e Rebeca, obrigada por serem cura nos dias difíceis, alegria nos momentos cansativos e companhia constante ao longo de todos esses anos. Também quero agradecer aos amigos Camila, Matheus, Rodrigo e Samanta por estarem presentes e tornarem esta caminhada mais leve e especial. Sou imensamente grata por ter vocês ao meu lado.

Aos profissionais Camila, Leticia, Luiza e Renan, por cuidarem da minha saúde física e mental com tanta dedicação. O apoio, a orientação, o acolhimento e a amizade de vocês foram fundamentais para que eu mantivesse o equilíbrio e a serenidade ao longo desta jornada.

Ao Conselho Nacional de Desenvolvimento Científico e Tecnológico (CNPq), processo nº 161516/2021-1, e à Fundação de Amparo à Pesquisa do Estado de São Paulo (FAPESP), processo nº 2021/08079-1, pelo apoio financeiro, por meio das bolsas de fomento que viabilizaram esta pesquisa.

À Embrapa, pela infraestrutura e condições oferecidas para a realização deste trabalho. À UFSCar, pela oportunidade de realização do doutorado no Programa de Pós-Graduação em Genética Evolutiva e Biologia Molecular. Ao Leandro, do CNPTIA, pelo suporte na manutenção do servidor, essencial para a execução das análises. Ao Dr. Sérgio Raposo, por toda a orientação e ajuda prestadas ao longo desta pesquisa.

Ao universo, por agir de forma misteriosa e generosa, proporcionando encontros inesperados que tornaram cada passo deste caminho possível e transformaram desafios em aprendizados e descobertas.

Por fim, agradeço a todos aqueles que, de forma direta ou indireta, contribuíram para a realização deste trabalho. Cada gesto de apoio, incentivo e compreensão foi essencial para que este trabalho se tornasse possível.

“Vamos viver tudo que há pra viver.

Vamos nos permitir.”

Lulu Santos, Tempos Modernos

RESUMO

A crescente demanda global por carne bovina, especialmente proveniente de sistemas de produção em regiões tropicais, exige estratégias inovadoras que aumentem a eficiência alimentar e reduzam os impactos ambientais da pecuária. O microbioma ruminal desempenha um papel central na digestão de carboidratos complexos e na produção de ácidos graxos voláteis, que são a principal fonte de energia para os ruminantes. No Brasil, a raça Nelore (*Bos indicus*) e seus cruzamentos representam cerca de 80% do rebanho nacional. No entanto, estudos funcionais sobre o microbioma ruminal dessa raça ainda são escassos. Avanços nas tecnologias ômicas permitem investigar como a dieta, o microbioma e genoma do hospedeiro afetam a eficiência produtiva e ambiental na pecuária de corte. Devido a isso, este trabalho visou investigar a atividade do microbioma ruminal de uma população de 52 bovinos da raça Nelore, submetidos a duas dietas distintas (convencional e subprodutos) e integrar, de maneira inédita, dados metagenômicos, metatranscriptômicos e de microRNAs da parede ruminal bovina. Para isso, propusemos como objetivos: Caracterizar o perfil funcional ativo do microbioma ruminal em resposta a diferentes dietas, utilizando dados metatranscriptômicos; Avaliar a composição taxonômica e funcional do microbioma ruminal ativo, integrando dados metagenômicos e metatranscriptômicos; Associar o microbioma ativo com a emissão de metano e a eficiência alimentar; Investigar a interação entre o microbioma ativo e o genoma do hospedeiro, integrando dados de expressão de miRNAs da parede ruminal com informações funcionais e taxonômicas do microbioma. A análise metatranscriptômica revelou alterações funcionais importantes no microbioma ruminal, mesmo com uma composição taxonômica relativamente estável entre as dietas. Os componentes de cada dieta influenciaram diretamente o metabolismo microbiano. No grupo convencional, a maior parte das funções expressas esteve associada ao metabolismo de carboidratos facilmente fermentáveis, como amido e manose, presentes no milho e na soja. Em contraste, no grupo com subprodutos, observaram-se atividades microbianas ligadas à degradação de carboidratos complexos, como a celulose da polpa cítrica. Além disso, a inclusão de subprodutos favoreceu vias metabólicas alternativas que competem com a metanogênese, como a via da acetogênese redutiva (por exemplo, *tetrahydrofolate synthase*), capaz de redirecionar H_2 e CO_2 para a produção de acetato. Observou-se também aumento na expressão de *folylpolyglutamate synthase/ dihydropteroate synthase*, possivelmente indicando limitação de metionina e reduzindo a disponibilidade de substratos essenciais para metanogênese como o metanofurano e a metanopterina. Para expandir a compreensão do microbioma, construímos um catálogo de genes procarióticos ruminais que revelou diferenças taxonômicas e funcionais entre o metagenoma total (*Nelore Ruminal Prokaryotic Microbiome Genes* - *NRPMG*) e sua fração

transcricionalmente ativa (active-*Nelore Ruminal Prokaryotic Microbiome Genes - aNRPMG*). Esses resultados indicam que os processos fermentativos no rúmen são moldados principalmente pela atividade funcional das comunidades microbianas, e não apenas por sua presença. Identificamos ainda enzimas e táxons associados à emissão de metano e à eficiência alimentar. Entre eles, destacam-se *Carbohydrate Esterase family 20* (*CE20*) e *Glycoside Hydrolase family 15* (*GH15*), e os gêneros *Monoglobus* e *Halosimplex*, que surgem como potenciais indicadores ou moduladores de características de desempenho do hospedeiro. Por fim, a análise da interação entre hospedeiro e microbioma revelou padrões de coexpressão entre microRNAs da parede ruminal, enzimas e gêneros microbianos ativos, sugerindo uma interação hospedeiro–microbioma. Esses miRNAs podem modular a expressão gênica de enzimas ou de microrganismos envolvidos em funções metabólicas específicas, incluindo processos relacionados ao metabolismo lipídico e à saúde do hospedeiro. Em conjunto, os resultados desta tese reforçam que o microbioma ruminal deve ser compreendido não apenas pela sua composição, mas sobretudo pela sua atividade funcional. A abordagem integrativa adotada evidencia como a interação entre microbioma, hospedeiro e dieta molda processos metabólicos chave, destacando alvos microbianos e moleculares com potencial para embasar estratégias voltadas à mitigação das emissões de metano e ao aprimoramento da eficiência alimentar em bovinos criados em ambientes tropicais.

Palavras-chave: atividade da microbiota; *Bos indicus*; holobionte; metatranscriptoma, metagenoma; microRNA

ABSTRACT

The growing global demand for beef, particularly from production systems in tropical regions, requires innovative strategies that enhance feed efficiency and reduce the environmental impacts of livestock. The ruminal microbiome plays a central role in the digestion of complex carbohydrates and the production of volatile fatty acids, which are the primary energy source for ruminants. In Brazil, the Nelore breed (*Bos indicus*) and its crossbreeds represent approximately 80% of the national herd. However, functional studies on the ruminal microbiome of this breed are still scarce. Advances in omics technologies now allow the investigation of how diet, the microbiome, and the host genome affect productive and environmental efficiency in beef cattle. Therefore, this study aimed to investigate the activity of the ruminal microbiome in a population of 52 Nelore cattle subjected to two distinct diets (conventional and byproducts) and to integrate, in an unprecedented manner, metagenomic, metatranscriptomic, and rumen wall microRNA data. To achieve this, we set the following objectives: Characterize the active functional profile of the ruminal microbiome in response to different diets using metatranscriptomic data; Assess the taxonomic and functional composition of the active ruminal microbiome by integrating metagenomic and metatranscriptomic data; Associate the active microbiome with methane emissions and feed efficiency; Investigate the interaction between the active microbiome and the host genome by integrating rumen wall microRNA expression with functional and taxonomic information of the microbiome. Metatranscriptomic analyses revealed key functional shifts in the rumen microbiome, despite relatively stable taxonomic composition across diets. Dietary components directly influenced microbial metabolism. In the conventional diet group, most expressed functions were associated with the metabolism of readily fermentable carbohydrates such as starch and mannose, present in corn and soybean meal. In contrast, animals receiving the by-product diet exhibited microbial activities linked to the degradation of complex carbohydrates, such as the cellulose found in citrus pulp. Additionally, the inclusion of by-products favored alternative microbial pathways that compete with methanogenesis, such as the reductive acetogenesis pathway (e.g., tetrahydrofolate synthase), which can redirect H_2 and CO_2 toward acetate production. Increased expression of folylpolyglutamate synthase/dihydropteroate synthase was also observed, potentially indicating methionine limitation and reducing the availability of essential substrates for methanogenesis, such as methanofuran and methanopterin. To further deepen our understanding of the rumen microbiome, we constructed a rumen prokaryotic gene catalog that revealed taxonomic and functional differences between the total metagenome (Nelore Ruminal Prokaryotic Microbiome Genes – NRPMG) and its transcriptionally active fraction (active-Nelore Ruminal Prokaryotic Microbiome Genes – aNRPMG). These findings indicate

that fermentative processes in the rumen are shaped primarily by the functional activity of microbial communities, rather than their mere presence. We also identified enzymes and taxa associated with methane emissions and feed efficiency. Among them, Carbohydrate Esterase family 20 (CE20), Glycoside Hydrolase family 15 (GH15), and the genera *Monoglobus* and *Halosimplex* emerged as potential indicators or modulators of host performance traits. Finally, the analysis of host–microbiome interactions revealed co-expression patterns among rumen wall microRNAs, enzymes, and active microbial genera, suggesting meaningful host–microbiome interplay. These microRNAs may modulate the gene expression of enzymes or microorganisms involved in specific metabolic functions, including lipid metabolism and host health processes. Overall, the findings of this thesis reinforce that the rumen microbiome should be understood not only through its composition but, more importantly, through its functional activity. The integrative approach adopted here highlights how the interplay among microbiome, host, and diet shapes key metabolic processes and underscores microbial and molecular targets with potential to support strategies aimed at mitigating methane emissions and improving feed efficiency in cattle raised in tropical environments.

Keywords: *Bos indicus*; holobiont; metagenome; metatranscriptome; microRNA; microbiota activity

SUMMARY

1 Contextual framework of the thesis

1.1 Introduction

The global demand for meat and milk is projected to rise substantially by 2050, driven by several factors including the continued growth of the middle class, rising incomes, rapid urbanization, and notably, a significant increase in the world's population (Henchion et al., 2021; Badhan et al., 2025). Therefore, there is an increasing need to adopt more sustainable and efficient production practices that can maximize the nutritional utilization of forage-based diets while simultaneously mitigating environmental impacts (Cole et al., 2018). Ruminants, particularly the Nelore breed (*Bos indicus*), which accounts for approximately 80% of the Brazilian cattle herd, play a crucial role in maintaining the country's status as one of the world's leading beef producers and exporters (Barbosa et al., 2014; Da Silva et al., 2023).

The rumen is a specialized digestive chamber unique to ruminants that enables the conversion of fibrous feedstuffs, such as forages, into high-quality animal protein (Malmuthuge et al., 2019). This process is mediated by a complex and dynamic microbial community, including bacteria, archaea, and eukaryotes, which produces enzymes capable of breaking down structural polysaccharides. The resulting fermentation generates volatile fatty acids (VFAs), which supply more than 70% of the host's energy requirements (Henderson et al., 2015; Malmuthuge et al., 2019). During fermentation, gases such as CO_2 and H_2 are released; hydrogen is rapidly utilized by methanogenic archaea to produce methane, a reaction that helps maintain favorable thermodynamic conditions. However, this also leads to an energy loss accounting for 2–12% of the dietary intake (Hook et al., 2010). Thus, enhancing ruminal digestion efficiency improves feed efficiency and shortens generation intervals, thereby reducing the environmental footprint. From an economic perspective, this is a key strategy to meet the growing global demand for bovine products such as meat and milk (Badhan et al., 2025). Also, incorporating agricultural and food-processing by-products (such as grains silage, citrus pulp, and oilseed meals) into ruminant diets not only valorizes waste streams but also reduces feed costs and environmental burden, optimize nutrient recycling, and diminish reliance on conventional diet (Ravindran and Jaiswal, 2016; Greenwood, 2021; Pfau et al., 2023).

Understanding the rumen microbiome is essential for optimizing feed efficiency and mitigating environmental impacts. However, the majority of rumen microbial species remain uncultivable. Advances in sequencing technologies have enabled the application of approaches such as metagenomics and metatranscriptomics, allowing for the exploration of both microbial diversity and functional activity (Shabat et al., 2016; Li and Guan, 2017;

Gruninger et al., 2019). Previous studies have linked microbial composition to feed efficiency (Guan et al., 2008; Hernandez-Sanabria et al., 2010; Carberry et al., 2012; Conteville et al., 2023, 2024), but most of these investigations focused on taxonomic profiles, limiting our understanding of the functional basis of these relationships. The integration of metagenomic and metatranscriptomic data enables the identification of actively expressed genes in response to dietary inputs, unveiling metabolic pathways related to fiber degradation, methane production, and phenotypic variation (Li et al., 2019). Although previous studies have investigated the influence of diet on microbiome activity in *Bos taurus* (Li and Guan, 2017; Mann et al., 2018; Nguyen et al., 2023), the impact of diet on rumen microbial activity in *Bos indicus* remains largely unexplored.

Furthermore, the interaction between the host and its microbiota can be understood in the concepts of “holobiont” and “hologenome” (Margulis and Fester, 1991; Rosenberg et al., 2007), which considers the set of genes of the animal and its microorganisms as a functional unit. Within this context, microRNAs (miRNAs) play a key role in mediating the complex interplay between ruminant hosts and their gut microbiota, including the rumen (Liang et al., 2014). These small non-coding RNA molecules function as post-transcriptional regulators of gene expression and are involved in a range of host cellular processes that may, in turn, influence microbial activity (Ricci et al., 2022). Emerging evidence suggests that miRNAs contribute to host–microbe interactions by modulating nutrient absorption, metabolism, and immune responses in the ruminant digestive system (Liang et al., 2014; Ricci et al., 2022; Ojo and Kreuzer-Redmer, 2023). Additionally, host-derived miRNAs are capable of modulating bacterial gene expression at the post-transcriptional level, potentially altering the structure of the microbial community (Cuinat et al., 2025). They may also be internalized by bacterial cells through endocytosis, where they selectively regulate gene transcripts and impact bacterial proliferation (Datta et al., 2023). While this suggests a potential regulatory role of the host on its microbiota, emerging evidence highlights that this communication is bidirectional. Some studies have shown that bacteria can actively modulate host miRNA expression to favor their own survival or function (Das et al., 2016; Aguilar et al., 2019), suggesting a complex cross-talk between host and microbes in the rumen ecosystem. Despite this, no studies to date have explored these mechanisms of host–microbiome interaction in *Bos indicus* cattle.

To address these knowledge gaps, our study was the first to evaluate the rumen microbiome of *Bos indicus* (Nelore) cattle and its functional responses to dietary interventions, particularly the incorporation of by-products, using metatranscriptomics. We also generated the first Nelore Ruminal Prokaryotic Microbiome Genes (NRPMG) catalog from metagenomic data derived from ruminal content. By integrating these data with

metatranscriptomic profiles, we identified its transcriptionally active subset, termed the active-NRPMG (aNRPMG) catalog. This pioneering effort enabled an unprecedented characterization of the active ruminal microbiome in Nelore cattle, allowing us to pinpoint specific microbial taxa and functional pathways associated with methane emissions and feed efficiency. To further explore host–microbiome interactions, we incorporated ruminal wall miRNA profiles and constructed coexpression networks linking host miRNAs, microbial taxa, and microbial functions.

1.1.1 Nelore breed (*Bos indicus*)

The Nelore breed (*Bos indicus*) represents Brazil's predominant beef cattle breed, constituting approximately 80% of the national cattle population, according to the Brazilian Zebu Breeders Association (ABCZ, http://www.abcz.com.br). Originally known as Ongole in India, Nelore cattle were imported to Brazil during the last century through the 1970s (Peripolli et al., 2018). This Zebu breed has gained prominence primarily due to its exceptional adaptation to tropical climates and has become the cornerstone of Brazilian beef production systems (Chan et al., 2010; Antunes De Lemos et al., 2018). The importance of Nelore cattle extends beyond national borders, positioning Brazil as one of the world's largest beef exporters. Significant growth projections show beef consumption expected to increase from 60 to 130 million tons by 2050, with approximately 70% of this growth anticipated from tropical and subtropical production systems (Cooke et al., 2020). *Bos indicus* is the predominant cattle breed in tropical regions, yet it is often managed using practices developed for *Bos taurus* breeds adapted to temperate climates (Cooke et al., 2020), overlooking the genetic, physiological, and adaptive particularities of Nelore cattle that directly influence the production. Thus, to meet the growing global demand for beef, it is essential to develop management strategies tailored to *B. indicus*, considering the biological and behavioral divergences between these subspecies that stem from distinct processes of selection and domestication (Cooke et al., 2020).

1.1.2 The importance of the microbiome in the ruminal environment of beef cattle

Ruminants do not produce cellulolytic or hemicellulolytic enzymes and instead rely on the collaborative activity of diverse microorganisms in the rumen to break down complex plant polysaccharides (Badhan et al., 2025). This complex community, composed of bacteria, archaea, protozoa, and fungi, enables ruminants to convert otherwise indigestible plant material into absorbable nutrients, supporting both animal health and productivity (Perez et al., 2024). Bacteria are the most abundant microorganisms in the rumen and play

a central role in the breakdown of cellulose, hemicellulose, starch, proteins, and lipids (Perez et al., 2024).

Plant-derived carbohydrates are hydrolyzed into simple sugars and, through microbial fermentation, metabolized via glycolysis to pyruvate (Sanjorjo et al., 2023; Perez et al., 2024) (Sanjorjo et al., 2023; Perez et al., 2024). Fermentation process produces VFAs which can supply up to 80% of the ruminant's energy requirements (Sanjorjo et al., 2023), along with hydrogen (H_2), carbon dioxide (CO_2), and other metabolites (Perez et al., 2024). The incomplete fermentation of pyruvate results in the production of VFAs and the primary metabolic pathways involved include: (a) acetate formation from acetyl-CoA, (b) propionate production via the succinate and acrylate pathways, and (c) butyrate synthesis through the condensation of two acetyl-CoA molecules (Ungerfeld, 2020). Acetate is typically the most abundant, followed by propionate and butyrate (Liu et al., 2022). Each VFA plays a distinct metabolic role: acetate serves as a key precursor for lipid synthesis (Hanson and Ballard, 1967); propionate is gluconeogenic, contributing to hepatic glucose synthesis (Wang et al., 2023a); and butyrate provides energy for ruminal epithelial cells (Zhuang et al., 2024). The relative proportions of VFAs are strongly influenced by diet composition.

High-fiber diets (*e.g.*, forage-based) favor a higher acetate-to-propionate ratio, while grain-rich (starch-based) diets tend to increase the production of propionate and butyrate (Wang et al., 2020; Liu et al., 2022). These shifts reflect changes in the rumen microbial community and the physicochemical conditions promoted by different substrates, such as pH and substrate availability. In this context, cellulolytic bacteria degrade fibrous polymers through the action of cellulases, whereas amylolytic and pectinolytic bacteria hydrolyze non-structural carbohydrates, including starch, pectin, and soluble sugars, using amylases and pectinases. (Wang et al., 2020; Silva et al., 2024). The excess hydrogen generated during fermentation is consumed by methanogenic archaea, which reduce CO_2 to methane (CH_4) as a means of generating ATP, thereby maintaining low H_2 concentrations and enabling the continued efficiency of microbial fermentation. Although they represent only 1–4% of the microbial community (Neves et al., 2017; Conteville et al., 2023), methanogenic archaea play a crucial role. They consume H_2 and CO_2 (via the hydrogenotrophic pathway) or methylated compounds (via the methylotrophic pathway) to produce methane (CH_4), thereby maintaining a low partial pressure of hydrogen, an essential condition for sustained bacterial fermentation (McAllister et al., 2025). The composition and activity of the rumen microbiota are influenced by factors such as diet, host genetics and environmental conditions, and are central to the modulation of key phenotypes, including feed efficiency and enteric methane emission (Badhan et al., 2025).

1.1.3 Feed Efficiency

Feed represents up to 75% of the direct costs in beef production (Nielsen et al., 2013; Kenny et al., 2018). Improving feed efficiency therefore not only increases profitability but also shortens production cycles, reduces competition with land for human food crops, and lowers the use of natural resources and greenhouse gas emissions (Basarab et al., 2013; Sell-Kubiak et al., 2017). Feed efficiency is a complex trait influenced by multiple biological processes, including digestive, metabolic, and behavioral mechanisms (Kenny et al., 2018). It is estimated that 70 to 75% of the nutrients ingested by cattle are used for body maintenance, highlighting the importance of optimizing the utilization of consumed feed (Ojo et al., 2024). As mentioned before, the rumen and its microbiota play a central role in this process, producing VFAs, which serve as the animal's main energy source. Therefore, efficient rumen function has a direct impact on feed efficiency.

Feed efficiency can be defined as the animal's ability to convert ingested feed into useful products, such as meat, milk, or fiber, with minimal waste of energy and nutrients (Badhan et al., 2025). Among the various metrics used to assess feed efficiency, Residual Feed Intake (RFI) has emerged as one of the most relevant and widely adopted (Kenny et al., 2018; Ojo et al., 2024; Badhan et al., 2025). RFI is defined as the difference between an animal's actual feed intake and the expected intake based on its metabolic weight and growth rate (Kock et al., 1963; Martin et al., 2021; Badhan et al., 2025). Because RFI is derived after adjusting body weight and average daily gain, it provides a measure of feed efficiency that is independent of these conventional productive traits (Ojo et al., 2024). Animals with low or negative RFI values are considered more efficient, as they consume less feed than expected for their level of performance. In contrast, animals with high or positive RFI values are less efficient, as they consume more feed than necessary to sustain their production (Elolimy et al., 2018).

Historically, the selection of more feed-efficient animals has focused primarily on host genomics. For instance, genome-wide association studies (GWAS) have used single nucleotide polymorphism (SNP) markers to identify genomic regions associated with feed efficiency (De Oliveira et al., 2014). In another study, several candidate genes have been identified through these studies, including *GHR* (Growth Hormone Receptor), *CAST* (Calpastatin), and *CACNA1G*, all linked to RFI (Jiang et al., 2024).

With the advancement of omics sciences, particularly metagenomics and metatranscriptomics, growing evidence indicates that the rumen microbiome also plays a significant role in determining feed efficiency in ruminants. Recent studies have shown that variations in both the composition and functional activity of the ruminal microbial community are directly associated with feed efficiency. For example, animals with lower microbial

diversity have been linked to higher feed efficiency (Martinez Boggio et al., 2024). In beef cattle, efficient animals were found to have a higher relative abundance of *Bacteroidetes* and *Prevotella* (Delgado et al., 2019). Beyond composition, the functional capacity of the microbiome has also proven to be a critical factor. Metatranscriptomic analyses have revealed differences in metabolic pathway expression between efficient and inefficient *Bos taurus*, suggesting that the rumen microbiomes of inefficient cattle exhibit more diverse metabolic activities, which may reflect differences in host feed efficiency (Li and Guan, 2017).

1.1.4 Methane emission

Methane (CH_4) production from enteric fermentation is a global concern due to its significant contribution to the accumulation of greenhouse gases (GHGs) in the atmosphere and the energy loss it represents for the animals. It is estimated that between 2% and 12% of the gross energy intake of ruminants is lost as methane (Hook et al., 2010). This gas has a global warming potential 25 times greater than that of carbon dioxide (CO_2) and an atmospheric lifespan of approximately 12 years, making it the second most significant anthropogenic greenhouse gas, surpassed only by CO_2. (Hook et al., 2010; European Commission. Joint Research Centre., 2021). Agriculture accounts for approximately 50–60% of global methane emissions, with ruminants contributing around 16% of total CH_4 emissions. Of these, 35% are attributed to beef production and 30% to dairy production (Hook et al., 2010; Tseten et al., 2022).

Methane is primarily produced in the rumen of ruminants such as cattle, sheep, and goats by a specialized group of archaea known as methanogens, which belong to the phylum *Euryarchaeota* (Balch et al., 1979; Hook et al., 2010). These microorganisms utilize fermentation-derived compounds such as hydrogen (H_2), formic acid, and methylamines to reduce CO_2 to CH_4 through metabolic pathways including hydrogenotrophic, acetoclastic, and methylotrophic methanogenesis (Ungerfeld, 2020). The majority of methane emitted by ruminants is produced in the rumen and expelled through the mouth and nose (Murray et al., 1976). It is estimated that domesticated ruminants produce approximately 86 million metric tons (Tg) of methane annually, with 55.9 Tg originating from beef cattle (McMichael et al., 2007). The ruminal fermentation process is sustained by the dynamic flow of reducing equivalents, particularly hydrogen (H_2), mediated by microbial species (Badhan et al., 2025). The concentration of H_2 directly influences the fate of these equivalents through different metabolic pathways, thereby affecting methane production and the molar proportions of short-chain fatty acids (SCFAs) (Ungerfeld, 2020). Propionate formation, for instance, competes with methanogenesis for [H] utilization, whereas the formation of acetate and

butyrate releases [H], thus favoring CH_4 production (Janssen, 2010; Wang et al., 2023b). Most bacterial and archaeal genomes in the rumen encode [FeFe], [NiFe], or [Fe] hydrogenases, which catalyze the production or consumption of H_2 depending on the metabolic pathway involved (Greening et al., 2019). The diversity and functionality of the ruminal microbiome play essential roles in feed conversion efficiency and methane production. More efficient animals tend to harbor specialized and metabolically optimized microbial communities for energy extraction, which may be associated with lower levels of methanogenesis (Martínez-Álvaro et al., 2022; Sasson et al., 2022; Martinez Boggio et al., 2024).

In light of global efforts to limit temperature rise to 1.5°C by 2050 (European Commission. Joint Research Centre., 2021), strategies to reduce enteric methane emissions have gained prominence. Among these, dietary manipulation stands out as the most cost-effective and impactful approach, with the potential to reduce emissions by up to 60% (Tseten et al., 2022). This reduction is largely linked to the modulation of the rumen microbiome, as changes in forage quality and the forage-to-concentrate ratio directly influence microbial composition and activity (Tseten et al., 2022). Various feed additives, both organic and inorganic, have also shown promise by shifting microbial populations or directly inhibiting methanogens. Compounds such as 3-nitrooxypropanol (3-NOP), ionophores, and halogenated substances can suppress methane production by targeting methanogenic archaea or enhancing the growth of competing microbes (Tseten et al., 2022; Badhan et al., 2025). There is also growing interest in biological additives, such as essential oils, macroalgae, biochar, and plant metabolites, due to their ability to modulate microbial pathways in a more natural and potentially safer manner (Tseten et al., 2022). Also, probiotics further represent a promising strategy to favorably reshape the rumen microbiota (Tseten et al., 2022; Badhan et al., 2025). Overall, targeting the rumen microbiome offers a powerful avenue to both mitigate methane emissions and improve the energetic efficiency of livestock production systems.

1.1.5 16S rRNA, metagenomic and metatranscriptomic approaches in the ruminal microbiome

Understanding the ruminal microbiome requires integrating different sequencing strategies, each offering unique insights into microbial structure and function. The most commonly used approaches include 16S rRNA gene sequencing, metagenomics, and metatranscriptomics. The 16S rRNA gene sequencing targets conserved regions of the ribosomal gene in bacteria and archaea, allowing for taxonomic identification and relative quantification of microbial taxa (Denman et al., 2018). Although considered a low-cost and simple approach, 16S has some limitations, such as not providing information on microbial

metabolic functions, as it does not target functional genes (Peterson et al., 2021).

Metagenomics, based on shotgun sequencing of all DNA extracted from the rumen, overcomes this limitation by capturing the entire microbial genetic repertoire, including organisms not amplified by 16S (Peterson et al., 2021). This approach enables the reconstruction of metagenome-assembled genomes (MAGs) and the identification of functional genes (Peterson et al., 2021; Yang et al., 2021). Metatranscriptomics sequences total RNA, with a focus on microbial mRNAs, providing a real-time snapshot of the genes actively transcribed by the community (Li et al., 2019).

In summary, these approaches are complementary: 16S rRNA sequencing reveals microbial composition, metagenomics uncovers functional potential, and metatranscriptomics captures active metabolic processes. Within this context, our research group has been actively investigating the microbiome of Nelore cattle, particularly its relationship with production phenotypes under different dietary treatments. Using both 16S rRNA gene sequencing (Andrade et al., 2022) and shotgun metagenomics (Conteville et al., 2023), we have identified significant differences in microbial diversity and detected specific genera associated with traits such as feed efficiency and methane emissions. Additionally, a comprehensive dataset of microbial genomes recovered from the rumen and feces of Brazilian Nelore bulls has provided a valuable resource for exploring the functional potential of the Nelore microbiome and its variation across different environments and management systems (Conteville et al., 2024). While these studies have significantly advanced our understanding of microbial composition and host–microbiome interactions, there remains a critical gap regarding the actual metabolic activity of these microbial communities. Thus, metatranscriptomic analyses are still needed to uncover the active functional profiles of the rumen microbiome and to elucidate how these functions are modulated by host and dietary factors.

1.1.6 Host–Microbiome interactions mediated by bovine microRNAs

The interaction between the host and its microbiota can be understood in the concepts of “holobiont” and “hologenome” (Margulis and Fester, 1991; Rosenberg et al., 2007), which considers the set of genes of the animal and its microorganisms as a functional unit. Thus the bovine hologenome encompasses both bovine genes and the genetic capabilities of rumen microbes. Because host and microbes co-evolve, selection on cattle can indirectly alter microbial traits. Indeed, heritability of rumen microbial taxa has been estimated (h^2 ~0.05–0.40) and host genome-wide association studies have begun to identify bovine *loci* influencing key microbial groups (Gonzalez-Recio et al., 2023). In this context, recent research suggests that host microRNAs (miRNAs), small regulatory RNAs expressed by bovine cells, may help mediate cross-talk between the cow and its microbiome (Liang et

al., 2014; Ricci et al., 2022; Ojo and Kreuzer-Redmer, 2023). MiRNAs are ~22 nucleotide RNAs that post-transcriptionally regulate host genes, but there is growing evidence they can also affect microbial communities (Liang et al., 2014). Importantly, this cross-talk is bidirectional. While the host can regulate microbial communities through miRNAs, bacteria can also influence the host through small RNAs (sRNAs) (Koeppen et al., 2016).

In cattle, miRNAs produced by rumen epithelial cells can be secreted into rumen fluid (*e.g.* via exosomes) and be internalized in the microbes (Ricci et al., 2022). Ricci et al. (2022) were the first to identify hundreds of host-derived miRNAs in the rumen of Holstein cows, suggesting a host–microbiota cross-talk mediated by these molecules. They reported associations between specific miRNAs and microbial taxa or functions, for example, the bta-miR-487b was correlated with *Ruminococcus* and with methane metabolism, indicating that host-derived miRNAs may play an active role in shaping ruminal microbial composition and function and modulate the expression of microbiome genes involved in important metabolic pathways, such as those related to methanogenesis. Also, a study in dairy calves revealed temporal and regional changes in miRNA expression and a correlation between miRNA expression and microbial population in the gastrointestinal tract during early life (Liang et al., 2014), which provides further evidence for a mechanism by which the gut microbiota may influence host gene regulation, specifically through the modulation of miRNA expression during gut development.

Although there are relevant studies on the interaction between the genome and microbiome in model organisms (Dalmasso et al., 2011; Liu et al., 2016) and *Bos taurus* (Li et al., 2012; Liang et al., 2014; Ricci et al., 2022), to date, no studies have been conducted on *Bos indicus*, particularly the Nelore breed, which is widely used in Brazilian livestock production. Given its unique physiological and adaptive traits, it is essential to investigate the Nelore hologenome specifically. Advances in this field enable an integrative approach combining host genome and microbiome data, including metagenomics and metatranscriptomics, to enhance productivity, sustainability, and animal health.

1.2 Justification

Beef production systems in tropical regions face increasing challenges to improve feed efficiency while reducing environmental impacts. Despite the widespread use of Nelore cattle (*Bos indicus*) in Brazil, studies investigating the functional rumen microbiome from an integrated hologenomic perspective remain limited. Understanding how the active microbiota responds to dietary interventions and interacts with the host is essential to identify microbial pathways and mechanisms that influence feed efficiency and methane emissions. This study addresses this gap by applying metatranscriptomic approaches and integrating

metagenomics, metatranscriptomics and host-derived ruminal wall miRNA data, providing a comprehensive view of microbiome–host interactions in *Bos indicus*.

1.3 Objectives

1.3.1 Main Objective

To unravel the functional dynamics of the ruminal microbiota in Nelore (*Bos indicus*) bulls, exploring microbial activity in association with diet, feed efficiency and methane emission, as well as its interactions with host regulatory mechanisms.

1.3.2 Specific Objectives

- Characterize the functional landscape and transcriptional activity of the ruminal microbiome in 50 Nelore bulls subjected to different nutritional interventions (conventional and by-product-based diets), investigating how diet shapes microbial functions and their contribution to methane emissions.
- Integrate metatranscriptomic and metagenomic data from the ruminal microbiome to build complementary gene catalogs, distinguishing the functional potential from the expressed activity, and identify active microorganisms and enzyme-coding transcripts associated with methane emissions and feed efficiency.
- Investigate the host–microbiota relationship by integrating ruminal metatranscriptomic data with ruminal wall microRNA expression profiles from the ruminal wall, aiming to elucidate cross-regulatory mechanisms.

1.4 References

Aguilar, C., Mano, M., and Eulalio, A. (2019). Multifaceted Roles of microRNAs in Host-Bacterial Pathogen Interaction. *Microbiol. Spectr.* 7, 7.3.13. doi: 10.1128/microbiolspec.BAI-0002-2019

Andrade, B. G. N., Bressani, F. A., Cuadrat, R. R. C., Cardoso, T. F., Malheiros, J. M., De Oliveira, P. S. N., et al. (2022). Stool and Ruminal Microbiome Components Associated With Methane Emission and Feed Efficiency in Nelore Beef Cattle. *Front. Genet.* 13, 812828. doi: 10.3389/fgene.2022.812828

Antunes De Lemos, M. V., Berton, M. P., Ferreira De Camargo, G. M., Peripolli, E., De Oliveira Silva, R. M., Ferreira Olivieri, B., et al. (2018). Copy number variation regions in Nellore cattle: Evidences of environment adaptation. *Livest. Sci.* 207, 51–58. doi: 10.1016/j.livsci.2017.11.008

Badhan, A., Wang, Y., Terry, S., Gruninger, R., Guan, L. L., and McAllister, T. A. (2025). Invited review: Interplay of rumen microbiome and the cattle host in modulating feed efficiency and methane emissions. *J. Dairy Sci.* 108, 5489–5501. doi: 10.3168/jds.2024-26063

Balch, W. E., Fox, G. E., Magrum, L. J., Woese, C. R., and Wolfe, R. S. (1979).

Methanogens: reevaluation of a unique biological group. *Microbiol. Rev.* 43, 260–296. doi: 10.1128/mr.43.2.260-296.1979

Barbosa, B. R. P., Santos, S. A., Abreu, U. G. P. D., Egito, A. A., Comastri Filho, J. A., Juliano, R. S., et al. (2014). Tolerância ao calor em bovinos das raças Nelore branco, Nelore vermelho e Pantaneira. *Rev. Bras. Saúde E Produção Anim.* 15, 854–865. doi: 10.1590/S1519-99402014000400010

Basarab, J. A., Beauchemin, K. A., Baron, V. S., Ominski, K. H., Guan, L. L., Miller, S. P., et al. (2013). Reducing GHG emissions through genetic improvement for feed efficiency: effects on economically important traits and enteric methane production. *Animal* 7, 303–315. doi: 10.1017/S1751731113000888

Carberry, C. A., Kenny, D. A., Han, S., McCabe, M. S., and Waters, S. M. (2012). Effect of Phenotypic Residual Feed Intake and Dietary Forage Content on the Rumen Microbial Community of Beef Cattle. *Appl. Environ. Microbiol.* 78, 4949–4958. doi: 10.1128/AEM.07759-11

Chan, E. K. F., Nagaraj, S. H., and Reverter, A. (2010). The evolution of tropical adaptation: comparing taurine and zebu cattle. *Anim. Genet.* 41, 467–477. doi: 10.1111/j.1365-2052.2010.02053.x

Cole, M. B., Augustin, M. A., Robertson, M. J., and Manners, J. M. (2018). The science of food security. *Npj Sci. Food* 2, 14. doi: 10.1038/s41538-018-0021-9

Conteville, L. C., Silva, J. V., Andrade, B. G. N., Cardoso, T. F., Bruscadin, J. J., Oliveira, P. S. N., et al. (2023). Rumen and fecal microbiomes are related to diet and production traits in Bos indicus beef cattle. *Front. Microbiol.* doi: https://doi.org/10.3389/fmicb.2023.1282851

Conteville, L. C., Silva, J. V. D., Andrade, B. G. N., Coutinho, L. L., Palhares, J. C. P., and Regitano, L. C. D. A. (2024). Recovery of metagenome-assembled genomes from the rumen and fecal microbiomes of Bos indicus beef cattle. *Sci. Data* 11, 1385. doi: 10.1038/s41597-024-04271-3

Cooke, R. F., Daigle, C. L., Moriel, P., Smith, S. B., Tedeschi, L. O., and Vendramini, J. M. B. (2020). Cattle adapted to tropical and subtropical environments: social, nutritional, and carcass quality considerations. *J. Anim. Sci.* 98, skaa014. doi: 10.1093/jas/skaa014

Cuinat, C., Pan, J., and Comelli, E. M. (2025). Host-dependent alteration of the gut microbiota: the role of luminal microRNAs. *Microbiome Res. Rep.* 4. doi: 10.20517/mrr.2024.46

Da Silva, W. A. L., Da Costa E Silva, E. V., Ferreira, M. G. C. R., Gheller, J. M., Poehland, R., and Melo-Sterza, F. D. A. (2023). Effect of shading on the physiological and reproductive parameters in Nelore cows. *Trop. Anim. Health Prod.* 55, 374. doi: 10.1007/s11250-023-03774-2

Dalmasso, G., Nguyen, H. T. T., Yan, Y., Laroui, H., Charania, M. A., Ayyadurai, S., et al. (2011). Microbiota Modulate Host Gene Expression via MicroRNAs. *PLoS ONE* 6, e19293. doi: 10.1371/journal.pone.0019293

Das, K., Garnica, O., and Dhandayuthapani, S. (2016). Modulation of Host miRNAs by Intracellular Bacterial Pathogens. *Front. Cell. Infect. Microbiol.* 6. doi:

10.3389/fcimb.2016.00079

Datta, N., Johnson, C., Kao, D., Gurnani, P., Alexander, C., Polytarchou, C., et al. (2023). MicroRNA-based therapeutics for inflammatory disorders of the microbiota-gut-brain axis. *Pharmacol. Res.* 194, 106870. doi: 10.1016/j.phrs.2023.106870

De Oliveira, P. S., Cesar, A. S., Do Nascimento, M. L., Chaves, A. S., Tizioto, P. C., Tullio, R. R., et al. (2014). Identification of genomic regions associated with feed efficiency in Nelore cattle. *BMC Genet.* 15. doi: 10.1186/s12863-014-0100-0

Delgado, B., Bach, A., Guasch, I., González, C., Elcoso, G., Pryce, J. E., et al. (2019). Whole rumen metagenome sequencing allows classifying and predicting feed efficiency and intake levels in cattle. *Sci. Rep.* 9. doi: 10.1038/s41598-018-36673-w

Denman, S. E., Morgavi, D. P., and McSweeney, C. S. (2018). Review: The application of omics to rumen microbiota function. *Animal* 12, s233–s245. doi: 10.1017/S175173111800229X

Elolimy, A. A., Arroyo, J. M., Batistel, F., Iakiviak, M. A., and Loor, J. J. (2018). Association of residual feed intake with abundance of ruminal bacteria and biopolymer hydrolyzing enzyme activities during the peripartal period and early lactation in Holstein dairy cows. *J. Anim. Sci. Biotechnol.* 9. doi: 10.1186/s40104-018-0258-9

European Commission. Joint Research Centre. (2021). *GHG emissions of all world: 2021 report.* LU: Publications Office. Available at: https://data.europa.eu/doi/10.2760/173513 (Accessed July 9, 2025).

Gonzalez-Recio, O., Scrobota, N., López-Paredes, J., Saborío-Montero, A., Fernández, A., López De Maturana, E., et al. (2023). Review: Diving into the cow hologenome to reduce methane emissions and increase sustainability. *animal* 17, 100780. doi: 10.1016/j.animal.2023.100780

Greening, C., Geier, R., Wang, C., Woods, L. C., Morales, S. E., McDonald, M. J., et al. (2019). Diverse hydrogen production and consumption pathways influence methane production in ruminants. *ISME J.* 13, 2617–2632. doi: 10.1038/s41396-019-0464-2

Greenwood, P. L. (2021). Review: An overview of beef production from pasture and feedlot globally, as demand for beef and the need for sustainable practices increase. *Animal* 15, 100295. doi: 10.1016/j.animal.2021.100295

Gruninger, R. J., Ribeiro, G. O., Cameron, A., and McAllister, T. A. (2019). Invited review: Application of meta-omics to understand the dynamic nature of the rumen microbiome and how it responds to diet in ruminants. *Animal* 13, 1843–1854. doi: 10.1017/S1751731119000752

Guan, L. L., Nkrumah, J. D., Basarab, J. A., and Moore, S. S. (2008). Linkage of microbial ecology to phenotype: correlation of rumen microbial ecology to cattle's feed efficiency. *FEMS Microbiol. Lett.* 288, 85–91. doi: 10.1111/j.1574-6968.2008.01343.x

Hanson, R. W., and Ballard, F. J. (1967). The relative significance of acetate and glucose as precursors for lipid synthesis in liver and adipose tissue from ruminants. *Biochem. J.* 105, 529–536. doi: 10.1042/bj1050529

Henchion, M., Moloney, A. P., Hyland, J., Zimmermann, J., and McCarthy, S. (2021). Review: Trends for meat, milk and egg consumption for the next decades and the role played

by livestock systems in the global production of proteins. *Animal* 15, 100287. doi: 10.1016/j.animal.2021.100287

Henderson, G., Cox, F., Ganesh, S., Jonker, A., Young, W., Global Rumen Census Collaborators, et al. (2015). Rumen microbial community composition varies with diet and host, but a core microbiome is found across a wide geographical range. *Sci. Rep.* 5, 14567. doi: 10.1038/srep14567

Hernandez-Sanabria, E., Guan, L. L., Goonewardene, L. A., Li, M., Mujibi, D. F., Stothard, P., et al. (2010). Correlation of Particular Bacterial PCR-Denaturing Gradient Gel Electrophoresis Patterns with Bovine Ruminal Fermentation Parameters and Feed Efficiency Traits. *Appl. Environ. Microbiol.* 76, 6338–6350. doi: 10.1128/AEM.01052-10

Hook, S. E., Wright, A.-D. G., and McBride, B. W. (2010). Methanogens: Methane Producers of the Rumen and Mitigation Strategies. *Archaea* 2010, 1–11. doi: 10.1155/2010/945785

Janssen, P. H. (2010). Influence of hydrogen on rumen methane formation and fermentation balances through microbial growth kinetics and fermentation thermodynamics. *Anim. Feed Sci. Technol.* 160, 1–22. doi: 10.1016/j.anifeedsci.2010.07.002

Jiang, W., Mooney, M. H., and Shirali, M. (2024). Unveiling the Genetic Landscape of Feed Efficiency in Holstein Dairy Cows: Insights into Heritability, Genetic Markers, and Pathways via Meta-Analysis. *J. Anim. Sci.* 102. doi: 10.1093/jas/skae040

Kenny, D. A., Fitzsimons, C., Waters, S. M., and McGee, M. (2018). Invited review: Improving feed efficiency of beef cattle – the current state of the art and future challenges. *Animal* 12, 1815–1826. doi: 10.1017/s1751731118000976

Kock, R. M., Swiger, L. A., Chamber, D., and Gregory, K. E. (1963). EFFICIENCY OF FEED USE IN BEEF CATTLE. doi: https://doi.org/10.2527/jas1963.222486x

Koeppen, K., Hampton, T. H., Jarek, M., Scharfe, M., Gerber, S. A., Mielcarz, D. W., et al. (2016). A Novel Mechanism of Host-Pathogen Interaction through sRNA in Bacterial Outer Membrane Vesicles. *PLOS Pathog.* 12, e1005672. doi: 10.1371/journal.ppat.1005672

Li, F., and Guan, L. L. (2017). Metatranscriptomic Profiling Reveals Linkages between the Active Rumen Microbiome and Feed Efficiency in Beef Cattle. *Appl. Environ. Microbiol.* 83, e00061-17. doi: 10.1128/AEM.00061-17

Li, F., Hitch, T. C. A., Chen, Y., Creevey, C. J., and Guan, L. L. (2019). Comparative metagenomic and metatranscriptomic analyses reveal the breed effect on the rumen microbiome and its associations with feed efficiency in beef cattle. *Microbiome* 7, 6. doi: 10.1186/s40168-019-0618-5

Li, L., Huang, J., Zhang, X., Ju, Z., Qi, C., Zhang, Y., et al. (2012). One SNP in the 3′-UTR of HMGB1 gene affects the binding of target bta-miR-223 and is involved in mastitis in dairy cattle. *Immunogenetics* 64, 817–824. doi: 10.1007/s00251-012-0641-1

Liang, G., Malmuthuge, N., McFadden, T. B., Bao, H., Griebel, P. J., Stothard, P., et al. (2014). Potential Regulatory Role of MicroRNAs in the Development of Bovine Gastrointestinal Tract during Early Life. *PLoS ONE* 9, e92592. doi: 10.1371/journal.pone.0092592

Liu, J., Bai, Y., Liu, F., Kohn, R. A., Tadesse, D. A., Sarria, S., et al. (2022). Rumen Microbial Predictors for Short-Chain Fatty Acid Levels and the Grass-Fed Regimen in Angus Cattle. *Animals* 12, 2995. doi: 10.3390/ani12212995

Liu, S., da Cunha, A. P., Rezende, R. M., Cialic, R., Wei, Z., Bry, L., et al. (2016). The Host Shapes the Gut Microbiota via Fecal MicroRNA. *Cell Host Microbe* 19, 32–43. doi: 10.1016/j.chom.2015.12.005

Malmuthuge, N., Liang, G., and Guan, L. L. (2019). Regulation of rumen development in neonatal ruminants through microbial metagenomes and host transcriptomes. *Genome Biol.* 20, 172. doi: 10.1186/s13059-019-1786-0

Mann, E., Wetzels, S. U., Wagner, M., Zebeli, Q., and Schmitz-Esser, S. (2018). Metatranscriptome Sequencing Reveals Insights into the Gene Expression and Functional Potential of Rumen Wall Bacteria. *Front. Microbiol.* 9, 43. doi: 10.3389/fmicb.2018.00043

Margulis, L., and Fester, R. (1991). *Symbiosis as a Source of Evolutionary Innovation*. Cambrigde: The MIT Press.

Martin, M. J., Dórea, J. R. R., Borchers, M. R., Wallace, R. L., Bertics, S. J., DeNise, S. K., et al. (2021). Comparison of methods to predict feed intake and residual feed intake using behavioral and metabolite data in addition to classical performance variables. *J. Dairy Sci.* 104, 8765–8782. doi: 10.3168/jds.2020-20051

Martinez Boggio, G., Monteiro, H. F., Lima, F. S., Figueiredo, C. C., Bisinotto, R. S., Santos, J. E. P., et al. (2024). Host and rumen microbiome contributions to feed efficiency traits in Holstein cows. *J. Dairy Sci.* 107, 3090–3103. doi: 10.3168/jds.2023-23869

Martínez-Álvaro, M., Auffret, M. D., Duthie, C.-A., Dewhurst, R. J., Cleveland, M. A., Watson, M., et al. (2022). Bovine host genome acts on rumen microbiome function linked to methane emissions. *Commun. Biol.* 5, 350. doi: 10.1038/s42003-022-03293-0

McAllister, T. A., Thomas, K. D., Gruninger, R. J., Elshahed, M., Li, Y., and Cheng, Y. (2025). International Symposium on Ruminant Physiology: Rumen fungi, archaea, and their interactions. *J. Dairy Sci.* 108, 7545–7566. doi: 10.3168/jds.2024-25713

McMichael, A. J., Powles, J. W., Butler, C. D., and Uauy, R. (2007). Food, livestock production, energy, climate change, and health. *The Lancet* 370, 1253–1263. doi: 10.1016/s0140-6736(07)61256-2

Murray, R. M., Bryant, A. M., and Leng, R. A. (1976). Rates of production of methane in the rumen and large intestine of sheep. *Br. J. Nutr.* 36, 1–14. doi: 10.1079/bjn19760053

Neves, A. L. A., Li, F., Ghoshal, B., McAllister, T., and Guan, L. L. (2017). Enhancing the Resolution of Rumen Microbial Classification from Metatranscriptomic Data Using Kraken and Mothur. *Front. Microbiol.* 8, 2445. doi: 10.3389/fmicb.2017.02445

Nguyen, T. T. M., Badhan, A. K., Reid, I. D., Ribeiro, G., Gruninger, R., Tsang, A., et al. (2023). Comparative analysis of functional diversity of rumen microbiome in bison and beef heifers. *Appl. Environ. Microbiol.* 89, e01320-23. doi: 10.1128/aem.01320-23

Nielsen, M. K., MacNeil, M. D., Dekkers, J. C. M., Crews, D. H., Rathje, T. A., Enns, R. M., et al. (2013). Review: Life-cycle, total-industry genetic improvement of feed efficiency in

beef cattle: Blueprint for the Beef Improvement Federation11The development of this commentary was supported by the Beef Improvement Federation. *Prof. Anim. Sci.* 29, 559–565. doi: 10.15232/s1080-7446(15)30285-0

Ojo, A. O., Mulim, H. A., Campos, G. S., Junqueira, V. S., Lemenager, R. P., Schoonmaker, J. P., et al. (2024). Exploring Feed Efficiency in Beef Cattle: From Data Collection to Genetic and Nutritional Modeling. *Animals* 14, 3633. doi: 10.3390/ani14243633

Ojo, O. E., and Kreuzer-Redmer, S. (2023). MicroRNAs in Ruminants and Their Potential Role in Nutrition and Physiology. *Vet. Sci.* 10, 57. doi: 10.3390/vetsci10010057

Perez, H. G., Stevenson, C. K., Lourenco, J. M., and Callaway, T. R. (2024). Understanding Rumen Microbiology: An Overview. *Encyclopedia* 4, 148–157. doi: 10.3390/encyclopedia4010013

Peripolli, E., Metzger, J., De Lemos, M. V. A., Stafuzza, N. B., Kluska, S., Olivieri, B. F., et al. (2018). Autozygosity islands and ROH patterns in Nellore lineages: evidence of selection for functionally important traits. *BMC Genomics* 19, 680. doi: 10.1186/s12864-018-5060-8

Peterson, D., Bonham, K. S., Rowland, S., Pattanayak, C. W., RESONANCE Consortium, and Klepac-Ceraj, V. (2021). Comparative Analysis of 16S rRNA Gene and Metagenome Sequencing in Pediatric Gut Microbiomes. *Front. Microbiol.* 12, 670336. doi: 10.3389/fmicb.2021.670336

Pfau, A. P., Shepherd, E. A., Martin, M. G., Ascolese, S., Mason, K. M., Egert-McLean, A. M., et al. (2023). Beta-Adrenergic Agonists, Dietary Protein, and Rumen Bacterial Community Interactions in Beef Cattle: A Review. *Vet. Sci.* 10, 579. doi: 10.3390/vetsci10090579

Ravindran, R., and Jaiswal, A. K. (2016). Exploitation of Food Industry Waste for High-Value Products. *Trends Biotechnol.* 34, 58–69. doi: 10.1016/j.tibtech.2015.10.008

Ricci, S., Petri, R. M., Pacífico, C., Castillo-Lopez, E., Rivera-Chacon, R., Sener-Aydemir, A., et al. (2022). Characterization of presence and activity of microRNAs in the rumen of cattle hints at possible host-microbiota cross-talk mechanism. *Sci. Rep.* 12. doi: 10.1038/s41598-022-17445-z

Rosenberg, E., Koren, O., Reshef, L., Efrony, R., and Zilber-Rosenberg, I. (2007). The role of microorganisms in coral health, disease and evolution. *Nat. Rev. Microbiol.* 5, 355–362. doi: 10.1038/nrmicro1635

Sanjorjo, R. A., Tseten, T., Kang, M.-K., Kwon, M., and Kim, S.-W. (2023). In Pursuit of Understanding the Rumen Microbiome. *Fermentation* 9, 114. doi: 10.3390/fermentation9020114

Sasson, G., Moraïs, S., Kokou, F., Plate, K., Trautwein-Schult, A., Jami, E., et al. (2022). Metaproteome plasticity sheds light on the ecology of the rumen microbiome and its connection to host traits. *ISME J.* 16, 2610–2621. doi: 10.1038/s41396-022-01295-8

Sell-Kubiak, E., Wimmers, K., Reyer, H., and Szwaczkowski, T. (2017). Genetic aspects of feed efficiency and reduction of environmental footprint in broilers: a review. *J. Appl. Genet.* 58, 487–498. doi: 10.1007/s13353-017-0392-7

Shabat, S. K. B., Sasson, G., Doron-Faigenboim, A., Durman, T., Yaacoby, S., Berg Miller,

M. E., et al. (2016). Specific microbiome-dependent mechanisms underlie the energy harvest efficiency of ruminants. *ISME J.* 10, 2958–2972. doi: 10.1038/ismej.2016.62

Silva, É. B. R. D., Silva, J. A. R. D., Silva, W. C. D., Belo, T. S., Sousa, C. E. L., Santos, M. R. P. D., et al. (2024). A Review of the Rumen Microbiota and the Different Molecular Techniques Used to Identify Microorganisms Found in the Rumen Fluid of Ruminants. *Animals* 14, 1448. doi: 10.3390/ani14101448

Tseten, T., Sanjorjo, R. A., Kwon, M., and Kim, S.-W. (2022). Strategies to Mitigate Enteric Methane Emissions from Ruminant Animals. *J. Microbiol. Biotechnol.* 32, 269–277. doi: 10.4014/jmb.2202.02019

Ungerfeld, E. M. (2020). Metabolic Hydrogen Flows in Rumen Fermentation: Principles and Possibilities of Interventions. *Front. Microbiol.* 11, 589. doi: 10.3389/fmicb.2020.00589

Wang, G. Y., Qin, S. L., Zheng, Y. N., Geng, H. J., Chen, L., Yao, J. H., et al. (2023a). Propionate promotes gluconeogenesis by regulating mechanistic target of rapamycin (mTOR) pathway in calf hepatocytes. *Anim. Nutr.* 15, 88–98. doi: 10.1016/j.aninu.2023.07.001

Wang, K., Xiong, B., and Zhao, X. (2023b). Could propionate formation be used to reduce enteric methane emission in ruminants? *Sci. Total Environ.* 855, 158867. doi: 10.1016/j.scitotenv.2022.158867

Wang, L., Zhang, G., Li, Y., and Zhang, Y. (2020). Effects of High Forage/Concentrate Diet on Volatile Fatty Acid Production and the Microorganisms Involved in VFA Production in Cow Rumen. *Animals* 10, 223. doi: 10.3390/ani10020223

Yang, C., Chowdhury, D., Zhang, Z., Cheung, W. K., Lu, A., Bian, Z., et al. (2021). A review of computational tools for generating metagenome-assembled genomes from metagenomic sequencing data. *Comput. Struct. Biotechnol. J.* 19, 6301–6314. doi: 10.1016/j.csbj.2021.11.028

Zhuang, Y., Abdelsattar, M. M., Fu, Y., Zhang, N., and Chai, J. (2024). Butyrate metabolism in rumen epithelium affected by host and diet regime through regulating microbiota in a goat model. *Anim. Nutr.* 19, 41–55. doi: 10.1016/j.aninu.2024.04.027

2 Dietary modulation of the rumen microbiome drives the expression of metabolic and methanogenic pathways in *Bos indicus*

In this chapter, we explored how diet influences the taxonomy and activity of the Nelore cattle (*Bos indicus*) gastrointestinal microbiota. Using a metatranscriptomic approach, we examine how different diets shape microbial gene expression and its association with residual methane emissions. While taxonomic composition remained relatively stable between dietary groups, functional analysis revealed distinct metabolic profiles, including unique pathways and gene families enriched under each diet. These results were published in the journal *mSphere* on October 9, 2025.

Silva, J. V., Conteville, L. C., Bruscadin, J. J., Cardoso, T. F., Porto, T., Oliveira, P. S. N., Zerlotini, A., Medeiros, S. R., Mourão, G. B., Coutinho, L. L., Palhares, J. C. P., Berndt, A., Guan, L., Andrade, B. G. N., & Regitano, L. C. A. (2025). Dietary modulation of the rumen microbiome drives the expression of metabolic and methanogenic pathways in *Bos indicus*. mSphere. https://doi.org/10.1128/msphere.00535-25

2.1 Abstract

Diet influences ruminal methane emissions by modulating the composition and activity of the rumen microbiome. However, how diet shapes the functional capacity of the rumen microbiome in Nelore cattle (*Bos indicus*), a key tropical beef breed, remains unclear. This study used metatranscriptomics to investigate how dietary supplementation with agro-industrial by-products affects the active rumen microbiome and its association with residual methane emissions. Rumen samples from 50 Nelore cattle fed either a conventional or by-product-based diet revealed that the active microbiome was dominated by Bacteria (88.4% ± 3.16%) and Archaea (11.6% ± 3.16%), with no significant taxonomic differences between diets. Despite this, functional profiling identified genes from 193 pathways and 3,512 gene families, with distinct metabolic signatures between diets. Specifically, six pathways and 87 gene families were unique to the conventional diet, while seven pathways and 210 gene families were unique to the by-product diet. The associations between gene families enriched under each diet with residual methane emission revealed that the expression of two gene families exhibited negative correlations, while four were positively correlated with methane emission under conventional diet. In the by-product diet, we identified four gene families positively associated with methane emissions and 11 negatively associated. These results demonstrate that diet alters rumen microbial functions with methane mitigation potential, without affecting taxonomic composition.

Importance Understanding how diet modulates the functional activity of the rumen microbiome is essential for developing strategies to mitigate methane emissions in cattle. This study provides novel insights into how feeding agro-industrial by-products to Nelore cattle (*Bos indicus*), a key tropical beef breed, reshapes the functional profile of the rumen microbiome. Although no taxonomic shifts were detected, animals fed the by-product diet exhibited a greater number of microbial functions associated with lower methane production potential. These findings suggest that diet-driven modulation of microbial metabolism could contribute to strategies aimed at reducing methane emissions. Moreover, the use of by-products supports circular economy principles, enhancing the sustainability and economic resilience of tropical livestock systems. This work emphasizes the importance of examining the active microbiome through RNA, rather than solely profiling taxonomic composition without considering microbial activity. It also contributes to unveiling microbial functions to support future methane mitigation and sustainable feeding strategies.

Keywords Beef cattle, Citrus pulp, Diet-induced changes, Greenhouse gas, Metatranscriptome, Microbiome gene expression, Peanut meal, Residual Methane Emission, Ruminal fermentation

2.2 Introduction

With the global population projected to exceed 9 billion by 2050, there is growing pressure to adopt more sustainable and efficient production practices capable of maximizing the nutritional utilization of forage ingredients while mitigating environmental impacts (1). Ruminants, particularly the Nelore breed (*Bos indicus*), accounting for approximately 80 % of Brazil's cattle herd, play a pivotal role in underpinning the country's status as one of the world's leading beef producers and exporters (2, 3). It's efficient use of tropical forages highlights its potential to drive more efficient and sustainable cattle production systems in tropical regions.

In beef cattle, around 70% of feed energy is used for maintenance, while only 20% is converted into beef (4–6). This emphasizes the importance of optimizing feed utilization, as it plays a central role in energy and nutrient absorption (5). Rumen microbiota is essential for digestion, yielding volatile fatty acids and microbial protein that are indispensable to the bovine nutrition and growth. Additionally, it modulates methane emissions, which may represent a loss of up to 12 % of the ingested energy (7). Alterations in feed composition can drive corresponding shifts in the microbiome's structure and function (8). For example, high-fiber diets promote cellulolytic and fibrolytic bacteria that efficiently degrade cellulose and hemicellulose, however, this intensive fiber fermentation generates excess hydrogen, thereby stimulating methanogenesis (9). Conversely, grain-rich diets favor amylolytic

bacteria that rapidly metabolize soluble carbohydrates, producing predominantly lactic and propionic acids, which lower ruminal pH and consequently suppress methane production (10).

Recent advances in high-throughput omics technologies, such as metagenomics and metatranscriptomics, have enabled a comprehensive exploration of the microbiome and its interactions with the host physiology. These approaches have allowed studies to assess both the associations between microbiota composition and production traits (11–15) and the impact of diet on the microbiome (9, 16, 17). However, there are few studies relating dietary interventions to Nelore microbiomes (18, 19). Our research group has previously investigated the role of microbiome components and production phenotypes in Nelore cattle under different dietary treatments based both on 16 S ribosomal RNA gene sequencing (18) and on shotgun metagenomic sequencing (19), and revealed significant differences in microbiome diversity and identified several genera associated with phenotypes, such as feed efficiency and methane emission (19). Although both approaches have greatly improved our understanding of microbial population composition and host-microbiome associations, they have inherent limitations. The 16S rRNA gene sequencing offers limited taxonomic resolution and no functional information (18), while shotgun metagenomics cannot differentiate between active and inactive microbes/genes (19). Therefore, investigating the active fraction of the microbiome, through approaches such as metatranscriptomics, provides a more accurate understanding of microbial functions under different dietary conditions and their influence on host performance.

Although previous studies have investigated the influence of diet on microbiome activity in beef cattle (13, 14, 20), to date, the influence of diet on rumen microbial activity in *Bos indicus* is yet to be explored. To address this gap, our study pioneers the evaluation of rumen microbiome and its functions in response to dietary interventions in Nelore cattle using metatranscriptomics, including the incorporation of by-products in the diet. Incorporating agricultural and food-processing by-products (such as grains silage, citrus pulp, and oilseed meals) into ruminant diets not only valorizes waste streams but also reduces feed costs and environmental burden, optimize nutrient recycling, and diminish reliance on conventional diet (5, 21, 22). In particular, we focused on microbial functions associated with methane emissions, with the goal of identifying gene families that may contribute to lower environmental impact through dietary modulation.

2.3 Materials and methods

2.3.1 Animal study and sample collection

All the experimental procedures followed the Animal Welfare and Humane Slaughter guidelines and were approved by the Embrapa Southeastern Livestock Science Ethics Committee on Animal Experimentation, São Carlos, São Paulo, Brazil (Protocol No. 09/2016).

The experiment was conducted in the feedlot facilities of Embrapa Southeastern Livestock, involving 52 non castrated Nelore males born in 2014 and slaughtered in 2016. These animals were descendants of 28 commercial Nelore bulls, with an average of 1.78 offspring per bull. Due to initial body weight heterogeneity, animals were assigned to two weight classes (heavy: 323 ± 17.2 kg; light: 272.3 ± 35.8 kg). Heavier and lighter animals were evenly allocated within each diet group. The feedlot experiment lasted for 90 or 121 days, depending on the initial body weight. This included 10 days for animal adaptation to the feedlot, 29 days for heavy animals and 55 days for light animals in the growing phase, and an additional 51 days for heavy animals and 56 days for light animals in the finishing phase.

Also, the study included two nutritional interventions, a conventional and a by-products based diet, during all the feedlot. Specifically in the finishing phase, when biological samples were collected, the first group (Conventional group, n = 26) received a mainstream diet, containing corn silage (46.5%), soybean meal (6.1%), corn grains (41.6%), protected fat (2.5%), urea (1.3%) and a mineral mixture (Confinatto N235 Agroceres Multimix®; 2.0%). The second group (By-products group, n = 26) received a diet rich in by-products, containing corn silage (30.0%), peanut meal (7.5%), germ corn oil meal (35.9%), citrus pulp (24.0%), urea (0.5%) and the same mineral mixture (Confinatto N235 Agroceres Multimix®; 2.1%). The composition and nutritional levels of both dietary treatments are available in Supplementary Table S1. Both treatment groups received mineral supplements, active dry yeast, virginiamycin, and monensin. The animals were slaughtered at 23–24 months of age after fasting from food and water for 16 hours, according to the current Brazilian Ministry of Agriculture, Livestock, and Food Supply (MAPA) regulations, (conventional, 448.97 ± 20.3 kg, and by-products, 442.61 ± 43.2 kg). Approximately 50 mL of ruminal content was collected from each animal immediately after slaughter, snap frozen in liquid nitrogen and stored at −80°C before RNA extraction. All animal data used in this study are available in Supplementary Table S2 and an overview diagram of the method used is presented in Supplementary Figure 1.

2.3.2 Phenotype data collection

Enteric methane emissions were measured during the finishing period in the feedlot using the GreenFeed automated system (C-lock Inc., Rapid City, SD, United States). The calculation of RME (residual methane emission) used the following equation:

$$MEi = \beta_0 + \beta_1 (DMIi) + RMEi$$

Where MEi is the methane emission observed for animal i; $DMIi$ is the dry matter intake predicted for animal *i* (calculated as described in (18, 19)); β_0 is the regression intercept; β_1 is the partial regression coefficient of DMI; and $RMEi$ of animal *i* is the residual methane emission as proposed by (23) and (24), where it is referred to as RMP_R.

The RME was further corrected for experimental effects. The model considered the 26 animals on each diet separately and corrected for the contemporary group (CG), which was defined as the weighing groups (heavy-weight and light-weight animals) and slaughter groups (groups of animals slaughtered on different days). These corrections were implemented by the MIXED procedure of the SAS statistical program (SAS Institute, Cary, NC, United States, 2011), including the weighing group as fixed effect. For this model, β_0 = 215,72 and β_1 = −3,2782 considering the conventional diet and β_0 = 162,17 and β_1 = −0,3083 considering the by-products diet. Detailed information on the RME values corrected for individual animals is provided in Supplementary Table S2.

2.3.3 RNA extraction and metatranscriptomic sequencing

Total RNA was extracted using TRIzol (Invitrogen, Carlsbad, CA, USA) according to the manufacturer's instructions. Specifically, for ~200 mg of rumen content sample, 1.5 ml of TRIzol reagent, 0.4 ml of chloroform, 0.3 ml of isopropanol, and 0.3 ml of high salt solution (1.2 M sodium acetate, 0.8 M NaCl) were used. RNA quality and quantity were determined with an Agilent 2100 Bioanalyzer (Agilent Technologies, Santa Clara, CA, USA) and a Nanodrop 1000 spectrophotometer (Thermo Fisher Scientific), respectively. RNA samples with an RNA integrity number (RIN) greater than 7.0 (25) were used for downstream analysis. One sample from each diet group was excluded due to low RNA quality, resulting in 25 samples per group (conventional, n = 25; by-products, n = 25).

Total RNA sequencing libraries were prepared using an Illumina Stranded Total RNA Prep with Ribo-Zero Plus (Illumina, San Diego, CA, USA) according to the manufacturer's instructions. The purified libraries were sequenced on two Illumina NextSeq sequencing runs (ESALQ Genomics Center, Piracicaba, SP, Brazil) using a NextSeq P3 flow cell with 200

cycles (Illumina) (paired-end 2 × 100 bp). An overview diagram of the method used is presented in Supplementary Figure 1.

2.3.4 Metatranscriptomics pre-processing and functional annotation

The quality of the raw reads and adaptor contamination were checked with FastQC v0.11.5. Low-quality sequences and adapter sequences were removed in a trimming step by using Cutadapt v3.7 (26) with parameter '*-q 10*'. To eliminate rRNA and cattle host contaminants, trimmed reads were mapped against the SILVA (27) and RFAM (28) databases using SortMeRNA v.2.1b (29) with default parameters and subsequently, against the reference cattle genome assembly ARS-UCD1.2 (RefSeq assembly accession: GCF_002263795.1) using BBmap v34.08 with the option '*-outu*' to save the unmapped paired reads. An overview diagram of the method used is presented in Supplementary Figure 1.

2.3.5 Assessment of the active rumen microbiota using metatranscriptomics

The taxonomic classification of the metatranscriptomic reads was performed using Kraken2 (30) with the options "--paired --gzip-compressed --threads 24 --use-names --use-mpa-style," and using the complete set of bacterial and archaeal in NCBI RefSeq database as reference. Taxonomic profiles were aggregated at the phylum, family, and genus levels for both bacteria and archaea. Next, the taxonomic abundances were corrected to account for variation associated with contemporary groups (defined by weighing and slaughter groups) using the batch correction model (adjust_batch) implemented in MMUPHin (Meta-Analysis Methods with a Uniform Pipeline for Heterogeneity in microbiome studies) (31), with default parameters. Subsequently, linear discriminant analysis (LDA) was performed using LEfSe (32) to identify taxonomic features associated with different dietary groups. For LEfSe analysis, a Kruskal–Wallis test with a significance threshold of $p \leq 0.05$ and a LDA score >2.0 were used as selection criteria. The methodological workflow was illustrated in Supplementary Figure 2.

Microbial community diversity was assessed at both alpha and beta diversity levels. Alpha-diversity was estimated for each metatranscriptome using the Shannon and Simpson indices. The Shannon index captures both species richness and evenness, being particularly sensitive to rare taxa. In contrast, the inverse Simpson index (InvSimpson) gives more weight to dominant species and reflects the effective number of equally abundant species. While Shannon emphasizes diversity from a richness perspective, inverse Simpson highlights community evenness and dominance structure. To evaluate statistical differences in alpha diversity between dietary groups, pairwise Wilcoxon rank-sum tests were applied.

Beta diversity measures the differences in microbial community composition between samples. We evaluated beta diversity using Bray–Curtis dissimilarity, a metric that quantifies differences based on the relative abundances of taxa shared between samples. Ordination was performed using Principal Coordinate Analysis (PCoA) to visualize these differences.

2.3.6 Estimation of functional activities from rumen metatranscriptomes

Functional annotation of the metatranscriptomic reads was performed using HUMAnN3.0 (33). We used the taxonomic profile obtained from the ruminal metagenomic data of the same animals (19), as additional input to HUMAnN3.0 via the *--taxonomic-profile* flag to optimize the accuracy and robustness of the analysis. For functional annotation, HUMANn3 uses the DIAMOND aligner to map reads to the UniRef90 and MetaCyc databases (34), enabling the identification of UniRef protein families and microbial pathways. The identified gene families were regrouped (using the '*humann_regroup_table module*') based on a reference set of four databases: level 4 enzyme classes (ECs) (35), KEGG Orthology (KOs) (36), MetaCyc reactions (RXNs) (34) and Clusters of Orthologous Groups (COGs) (37). Subsequently, we renamed the identified gene families based on the four databases using the humann_rename_table with options '*--names ec, --names kegg-orthology, --names metacyc-rxn and --names eggnog'*. Metatranscriptomic abundances derived from HUMAnN3 were normalized to account for differences in sequencing depth across samples. After obtaining the default RPK values from HUMAnN3, we used the *humann_renorm_table* utility with the *--units relab* option to perform sum-normalization and convert gene families and pathway abundances to relative abundance units. This normalization yields comparable proportions across samples and was used as the input for downstream statistical analyses. Following this aggregation, functional profiles were corrected to account for variation associated with contemporary groups (defined by weighing and slaughter groups) using the batch correction model (adjust_batch) implemented in MMUPHin (Meta-Analysis Methods with a Uniform Pipeline for Heterogeneity in microbiome studies) (31), with default parameters. The files were filtered to only include gene families and metabolic pathways present in more than 20% of the animals (15). The methodological workflow was illustrated in Supplementary Figure 2.

2.3.7 Impact of diet on gene expression of the rumen microbiome of Nelore

To evaluate the impact of diet on ruminal microbial activity, we performed a Principal Coordinate Analysis (PCoA) based on Bray–Curtis dissimilarity distances. Moreover, a Venn diagram analysis was generated to identify both the common and exclusive metabolic pathways and gene families expressed in response to two different dietary treatments. For

the exclusive functions in each dietary group, a barplot was generated to understand the most expressed gene families and metabolic pathways specific to each diet.

Regarding common functions shared between the two diets, the Wilcoxon rank-sum test was performed, as described in (14, 15) to determine ECs, KOs, RXNs, COGs and MetaCyc pathways that were differentially expressed between the dietary groups. To control the false discovery rate (FDR), we employed Benjamini-Hochberg adjusted p-values *(Padj)* for each database (38). Statistical significance was defined as $Padj < 0.05$ (14, 15). We calculated the $\log_2$ fold change to estimate the direction and intensity of these differential patterns between diets, where positive values are associated with the conventional diet and negative values with the by-products diet (15). A $\log_2$ fold change threshold of 1 in magnitude was applied. The methodological workflow was illustrated in Supplementary Figure 2.

Additionally, the functions were classified and clustered according to their respective metabolic categories. Functions related to the metabolism of inorganic ions and xenobiotics were grouped under the category "Other".

2.3.8 Associations between microbiome gene families and RME

To investigate the impact of diet on the expression of genes associated with methane emission, gene families that were either differentially expressed or exclusive to each diet were selected for the following analysis. The expression levels of these gene families were correlated with residual methane emission (RME) using the PCIT (Partial Correlation with Information Theory) method (39), which enables the identification of significant relationships between gene families expression and phenotypic traits. Associations with an absolute correlation value ($|r| \geq 0.2$) were considered relevant. Based on these correlations, a diet-specific interaction heatmap was constructed, highlighting gene families potentially involved in the regulation of methane emission. The methodological workflow was illustrated in Supplementary Figure 2.

2.4 Results

2.4.1 Metatranscriptomic data

A total of 4.49 billion reads were generated from 50 rumen samples, with an average yield of approximately 98.48 ± 6.93 million reads per metatranscriptome (mean ± standard deviation; Supplementary Table S2). Following the preprocessing step, that involved the removal of rRNA and host contaminants, around 1.80 billion high-quality reads (36.59 ± 4.78 million reads per metatranscriptome) were retained for downstream analysis.

2.4.2 Active rumen bacterial and archaeal communities of Nelore

To explore the diversity of bacterial and archaeal microbiomes between the two dietary groups, we conducted alpha and beta-diversity analyses based on the genera identified by Kraken (Supplementary Table S3). Alpha diversity demonstrated that no significant differences were observed between the dietary groups (FDR-corrected Wilcoxon test: $p > 0.05$; Figure 1a), regarding both bacterial and archaeal diversities. Additionally, Bray–Curtis dissimilarity analysis followed by Principal Coordinate Analysis (PCoA) revealed no clear segregation in microbiome composition between the dietary groups (Figure 1b).

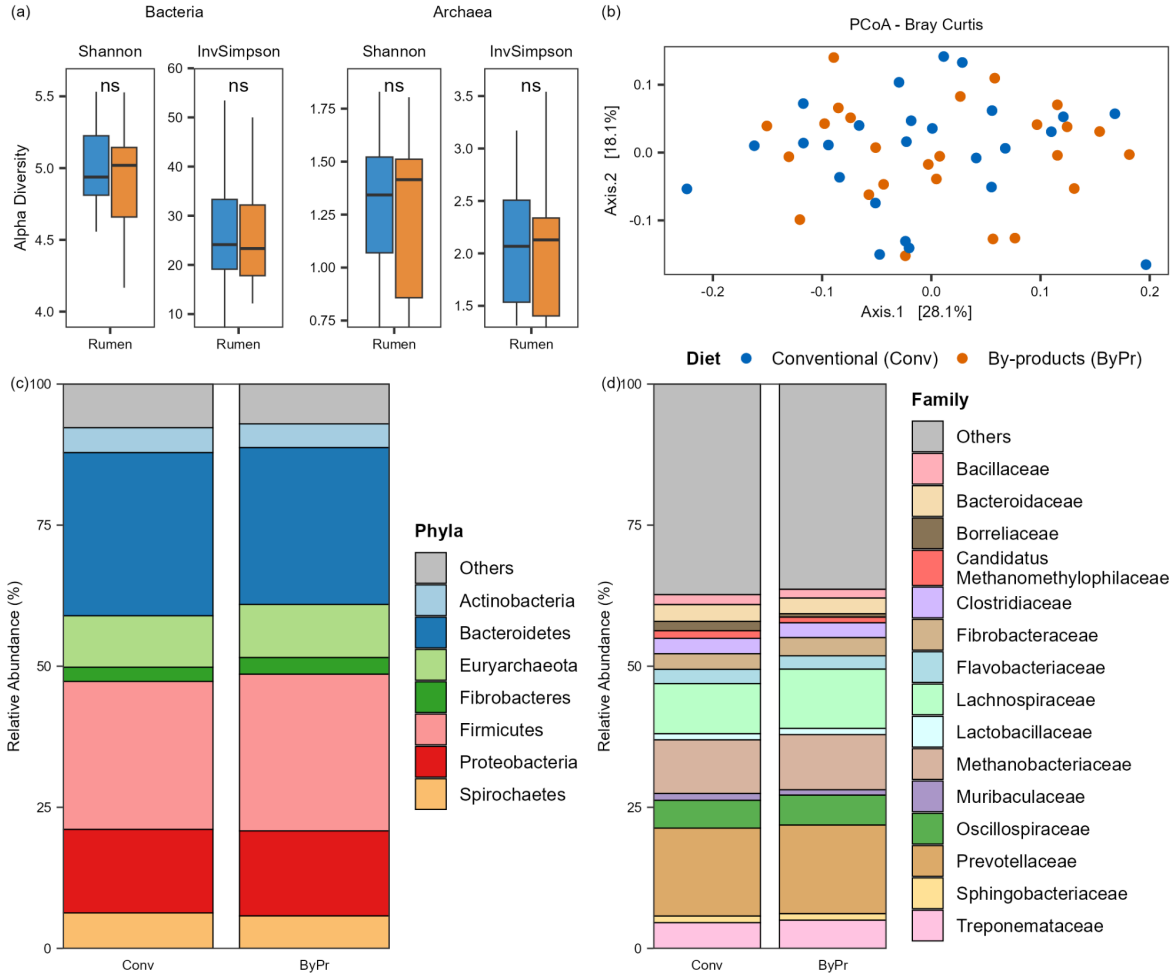

Figure 1: Taxonomic diversity and composition of the Nelore ruminal microbiomes. (a) Alpha diversity of the Nelore microbiomes were calculated using Shannon and inverse Simpson indices at the genus level. ns, not significant (FDR-corrected Wilcoxon test) when comparing the two dietary groups. (b) Principal coordinate analysis (PCoA) generated with Bray–Curtis dissimilarity distances of microbial genera identified in the metatranscriptome. (c) Relative abundance of the main phyla (whose mean abundance is greater than 1%) in the ruminal microbiomes of the two treatment groups. (d) Relative abundance of the main families

(whose mean abundance is greater than 1%) in the ruminal microbiomes of the two treatment groups.

The active taxonomic composition of the Brazilian Nelore rumen microbiome was found to be predominantly composed of Bacteria, accounting for an average of 88.4% (± 3.16%). This bacterial dominance was accompanied by a smaller fraction of reads corresponding to Archaea, which represented, on average, 11.6% (± 3.16%) of the total reads. The microbiomes were compared at both the phylum and family levels to identify which bacterial and archaeal taxa differentiate between the dietary groups (FDR-corrected Wilcoxon test: $p < 0.05$). However, no significant differences in relative abundance profiles were observed. The most abundant phyla were *Bacteroidetes*, *Firmicutes*, *Proteobacteria*, and *Euryarchaeota*, followed by *Spirochaetes*, *Actinobacteria*, and *Fibrobacteres* (Figure 1c). At the family level (Figure 1d), within the bacterial domain, *Prevotellaceae*, *Lachnospiraceae*, *Oscillospiraceae*, *Treponemataceae*, *Fibrobacteraceae*, and *Bacteroidaceae* were the most prominent. Within the archaeal domain, the predominant families were *Methanobacteriaceae* and *Candidatus Methanomethylophilaceae*.

Additionally, linear discriminant analysis (LDA) performed with LEfSe ($p \leq 0.05$, LDA score >2.0) did not reveal any significantly differentially abundant genera between the dietary groups in the rumen.

2.4.3 Active pathways and functions in the rumen microbiome of Nelore cattle

Further functional analysis based on HUMAnN3 revealed the metabolic pathways and gene families of the rumen microbiome. After excluding results with low prevalence (*prevalence < 20%*) and selecting functions related to metabolism, we retrieved 193 MetaCyc pathways and 660 ECs, 1,507 RXN, 630 KOs and 715 COGs, totaling 3,512 active gene families. The expression of active pathways and gene families on the ruminal microbiome of Nelore cattle are available in Supplementary Table S4 and Supplementary Table S5 respectively. Additionally, Bray–Curtis dissimilarity analysis followed by Principal Coordinate Analysis (PCoA) revealed no clear segregation in microbiome metabolic pathways between the dietary groups (Figure 2a).

Using the first level of the MetaCyc database, we explored the abundances of active metabolic pathways in the rumen microbiome of Nelore cattle (Figure 2b). Most of the identified pathways were associated with biosynthesis (130 instances), followed by degradation, utilization, and assimilation (38 instances), generation of precursor metabolites and energy (24 instances), and macromolecule modification (1 instance). Abundances of metabolic pathways based on the second level of the MetaCyc database were illustrated in

Figure 2c. Biosynthetic pathways were prominently represented, with amino acid, nucleoside and nucleotide, carbohydrate, and cofactor, carrier, and vitamin biosynthesis standing out. Additionally, the degradation, utilization, and assimilation pathways reveal a metabolic profile related to degradation of the nucleoside and nucleotide, carboxylate, carbohydrate, and amino acid degradation and C1 compound utilization. Furthermore, considering the generation of precursor metabolites and energy category, pathways involved in fermentation and glycolysis stood out.

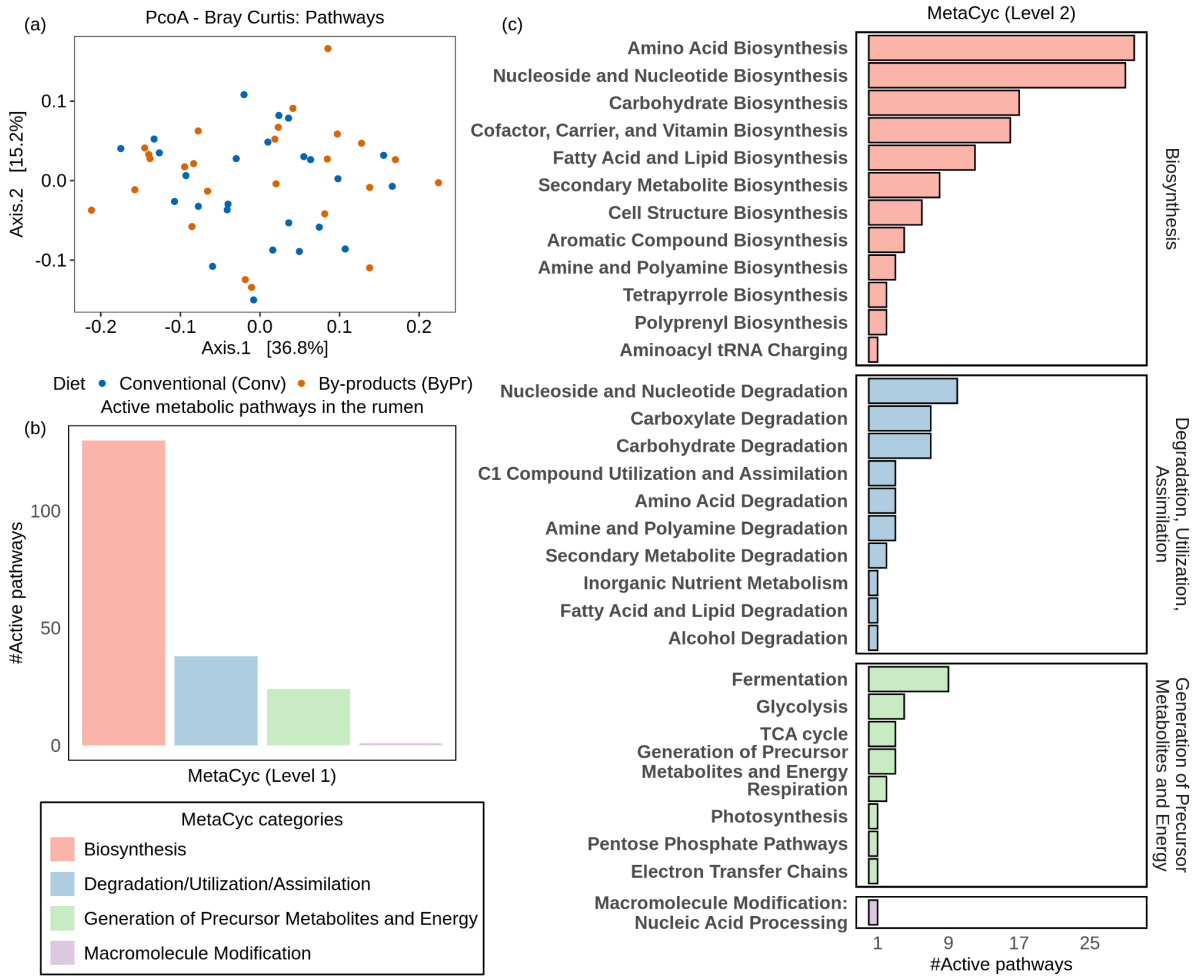

Figure 2: Profiles of active metabolic pathways in the rumen microbiome of Nelore cattle based on MetaCyc pathway database. (a) Principal coordinate analysis (PCoA) generated with Bray–Curtis dissimilarity distances of microbial metabolic pathways identified in the metatranscriptome. (b) Abundances of metabolic pathways based on the first level MetaCyc database. (c) Abundances of metabolic pathways based on the second level of the MetaCyc database.

Considering the active gene families in the rumen microbiome of Nelore cattle, the Bray–Curtis dissimilarity analysis followed by Principal Coordinate Analysis (PCoA) revealed no clear segregation between the dietary groups (Figure 3a). Regarding the functional

categories, the main were carbohydrate, amino acid and energy metabolism, based on COG and KEGG annotations (Figure 3b). Carbohydrate metabolism emerged as the most prevalent functional category, with 467 occurrences, followed by amino acid metabolism, with 396 instances, and energy metabolism, with 364 instances. Categories such as coenzyme, cofactor, and vitamins and nucleotides also showed notable activity, while metabolism of lipids, inorganic ions and xenobiotics (grouped as "Others"), secondary metabolites and glycan represented the least active category.

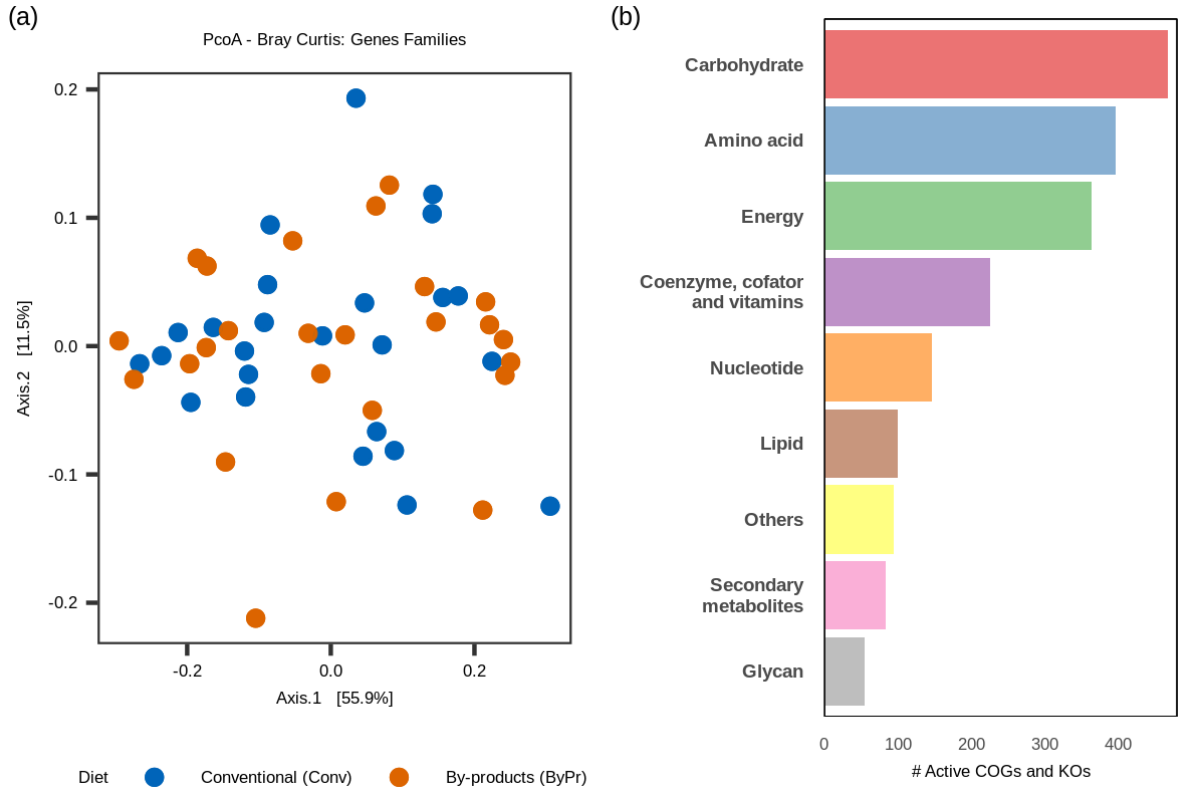

Figure 3: Profiles of active gene families in the rumen microbiome of Nelore cattle. (a) Principal coordinate analysis (PCoA) generated with Bray–Curtis dissimilarity distances of microbial genes families identified in the metatranscriptome. (b) Abundances of microbial metabolic functions based on COG categories and the KEGG hierarchy.

2.4.4 Effect of diet on the microbial activity in the rumen of Nelore cattle

To investigate the impact of diet on ruminal microbial activity, we compared the metabolic pathways expressed in animals fed the conventional and the by-product diet. This analysis identified both common and exclusive metabolic pathways between the two groups (Figure 4a). The six metabolic pathways uniquely associated with the conventional diet were related to carbohydrate metabolism (starch biosynthesis and glycogen degradation I), amino acid degradation (4-aminobutanoate degradation V) and the production of short-chain fatty acids (hexitol fermentation to lactate, formate, ethanol, and acetate and 4-aminobutanoate

degradation V). Moreover, the identification of the pathway CDP-archaeol biosynthesis indicates the activity of methanogenic archaeas in the rumen (Figure 4b). In contrast, the seven metabolic pathways uniquely associated with the by-product diet were primarily related to lipid, terpenoid, polyamine, and nucleotide metabolism. These included geranylgeranyl diphosphate biosynthesis II and all-trans-farnesol biosynthesis (both related to terpenoid metabolism), (5Z)-dodecenoate biosynthesis II and all-trans-farnesol (both related to lipid metabolism), the superpathway of arginine and polyamine biosynthesis and the superpathway of polyamine biosynthesis I (both involved in polyamine metabolism), and the superpathway of pyrimidine deoxyribonucleotides de novo biosynthesis (E. coli) (nucleotide metabolism) (Figure 4b).

Differential expression analysis of the 180 functions shared between both dietary groups (Figure 4a) revealed no significantly differentially expressed metabolic pathway between the two dietary groups (*Padj* < 0.05; $\log_2$ fold change > |1|), as shown in Figure 4c. The complete list of common and unique metabolic pathways among diets is provided in Supplementary Table S6.

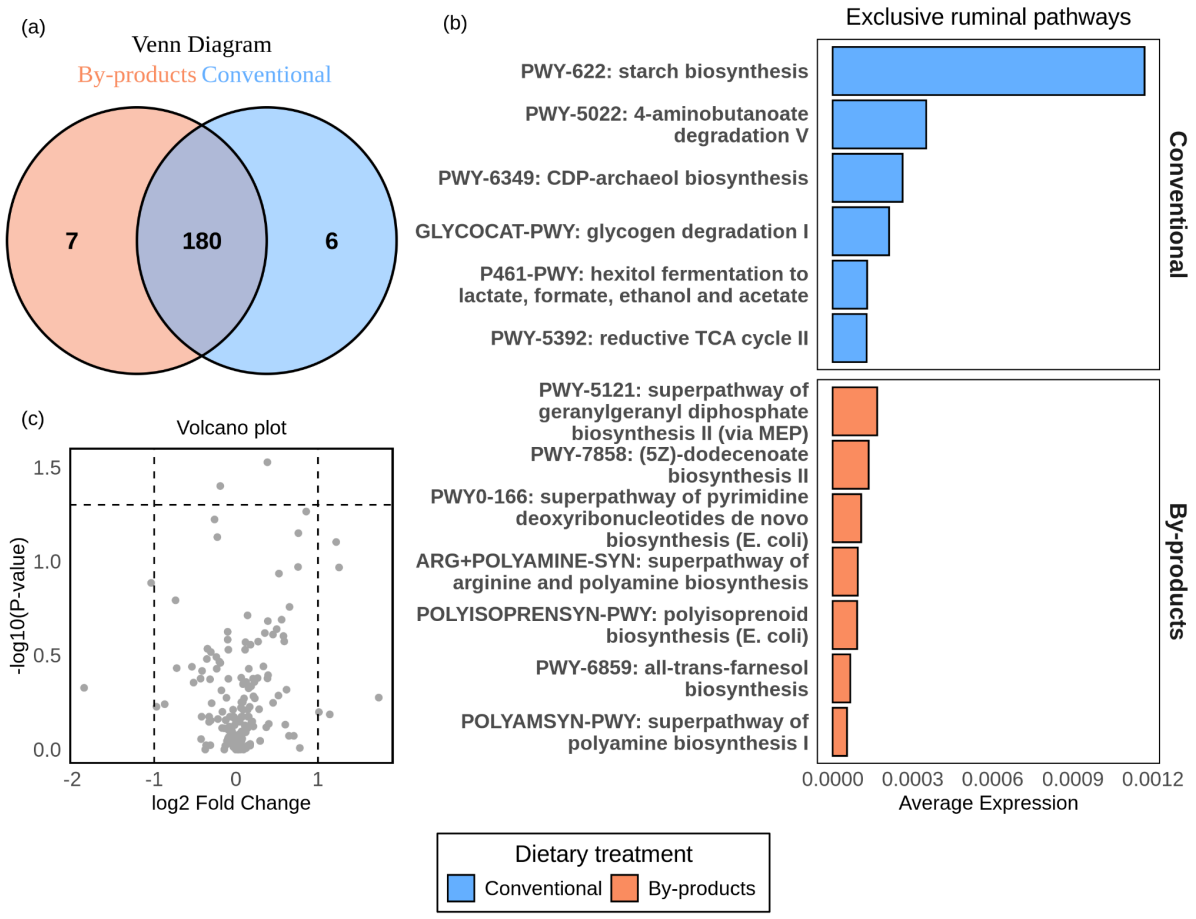

Figure 4: Effect of diet on the expression of microbial metabolic pathways in the rumen of Nelore cattle. (a) Venn diagram showing the metabolic pathways unique and common to each diet. The blue circle represents the conventional diet and the orange circle represents

the by-products. The purple intersection region represents the common pathways between the two diets. (b) Ruminal metabolic pathways unique to the conventional diet (in blue) and the by-product diet (in orange). (c) Volcano plot showing the relationship between log_2 fold change (X-axis) and adjusted p-value (-log10(p-value), Y-axis). The p-value threshold was 0.05 and the log_2 fold change threshold was |1|. Metabolic pathways in gray do not show significant differences between dietary groups for the thresholds analyzed.

Regarding gene families profiles in the rumen of Nelore, a total of 3,215 functions were shared between the two dietary groups (Figure 5a). Statistical analysis using the Wilcoxon test and log2 fold change revealed that eight gene functions were differentially expressed (Padj < 0.05; log2 fold change > |1|) between the dietary groups (Figure 5b), with four showing higher activity in the conventional diet and four in the by-product diet (Figure 5c).

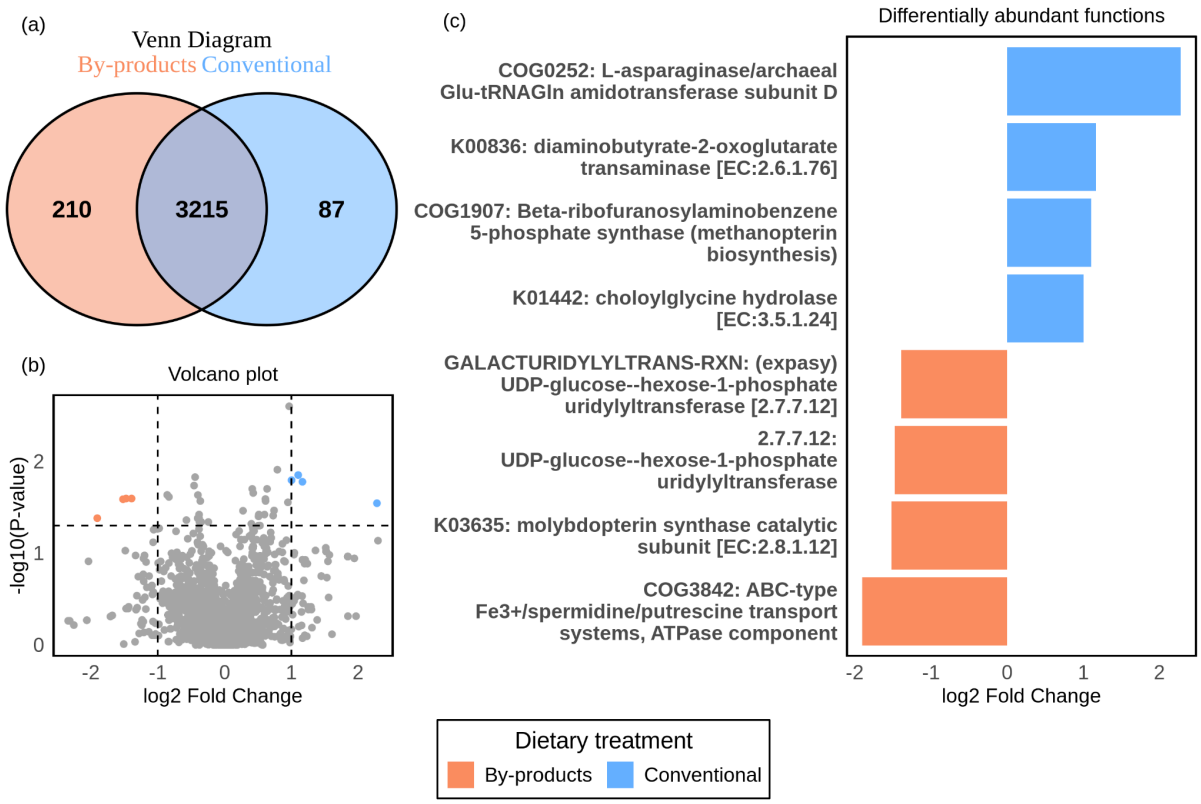

Figure 5: Effect of diet on the expression of microbial gene families in the rumen of Nelore cattle. (a) Venn diagram showing the gene families unique and common to each diet. The blue circle represents the conventional diet and the orange circle represents the byproducts. The purple intersection region represents the common functions between the two diets. (b) Volcano plot showing the relationship between log2 fold change (X-axis) and adjusted p-value (-log10(p-value), Y-axis). The p-value threshold was 0.05 and the log2 fold change threshold was |1|. Functions more expressed in the conventional diet are highlighted in blue, while those associated with the by-product diet are shown in orange. Functions in gray do

not show significant differences between dietary groups for the thresholds analyzed. (c) Gene families that showed statistical differences in expression levels between diets. In blue, functions most expressed in the conventional diet. In orange, functions most expressed in the by-product diet.

Regarding the exclusive functions, the conventional diet exhibited 87 unique functions, while the by-product diet contained 210 unique active functions (Figure 5a). The complete list of common and unique gene families among diets is provided in Supplementary Table S7. By selecting the 15 most active functions that were exclusive to the conventional group (Figure 6a) and the by-products group (Figure 6b), we observed that the metabolic focus of the Nelore ruminal microbiome varied according to the diet.

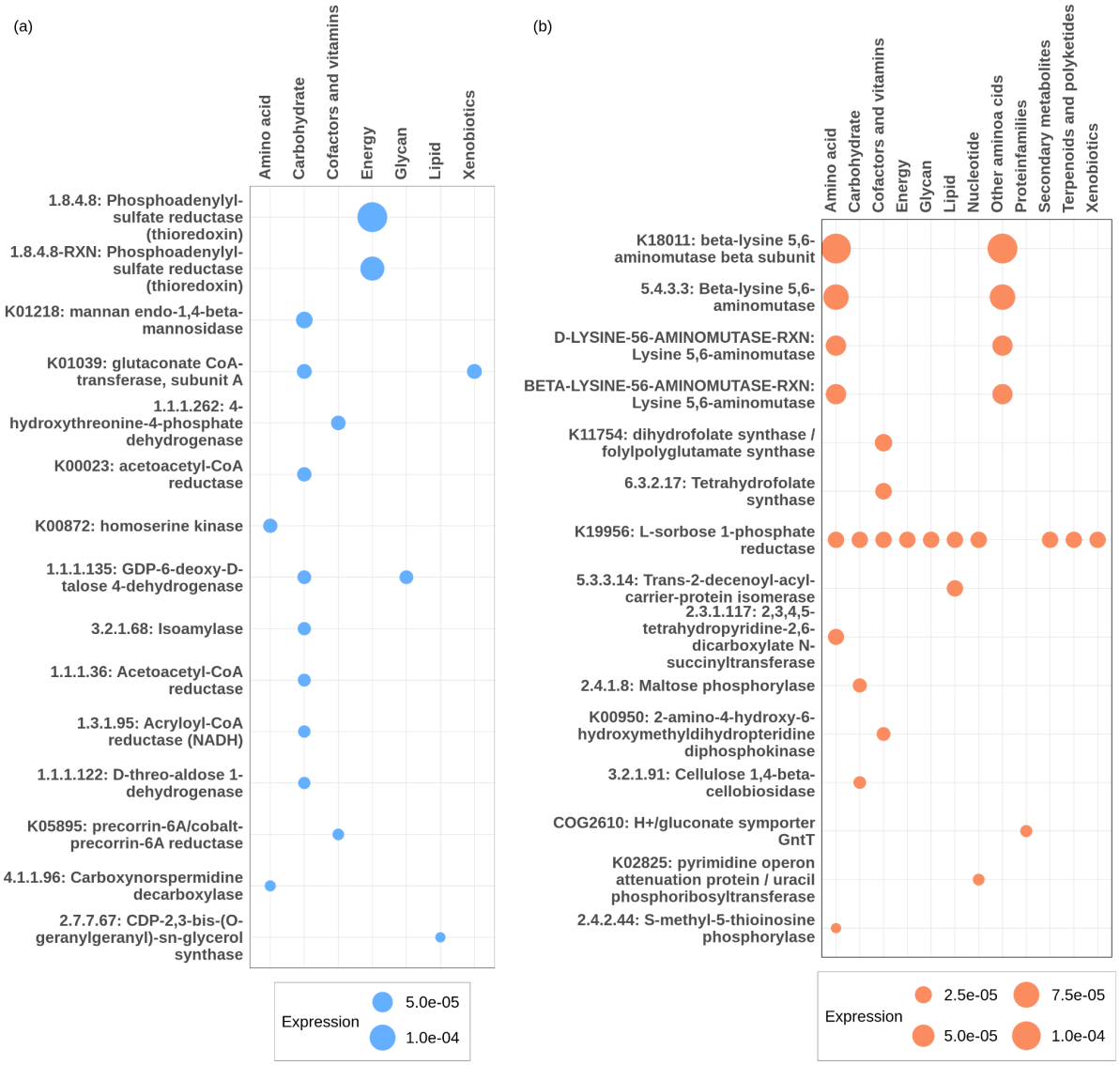

Figure 6: Most expressed functions are exclusively expressed in the rumen of cattle fed conventional diets (blue bubbles) or by-product diets (orange bubbles), grouped along the x-axis by functional class, with bubble diameter representing average gene expression

intensity. (a) Represents the functions related to the conventional diet. (b) Represents the functions associated with the by-product diet.

In the conventional group, most of the functions expressed by the microbiome were related with carbohydrates and reflected a fermentation process of easily fermentable carbohydrates, for example starch and mannose (mannan endo-1,4-beta-mannosidase). In contrast, in the by-product group, the microbial activities observed belonged to metabolic pathways related with breakdown of complex carbohydrates such as cellulose. In respect to amino acids metabolism, the conventional diet stimulated the expression of gene families such as L-asparaginase/archaeal Glu-tRNAGln amidotransferase and diaminobutyrate-2-oxoglutarate transaminase that are related to metabolism of aspartate and asparagine and glycine, serine and threonine metabolism. In the by-product group, the microbial activities were found focusing on lysine, arginine, and tryptophan metabolism. Lipid metabolism also exhibited a different profile between the two dietary groups. In the conventional group, the ruminal microbiome of Nelore was mainly focused on the synthesis and processing of fatty acids. In the by-product group, the ruminal microbiome appeared to be more specialized in the modification and adaptation of lipid compounds.

Regarding the metabolism of cofactors and vitamins, our results showed that animals fed the conventional diet had a microbiome activity focused on the metabolism of thiamine (vitamin B1). While those fed the by-product diet had a prevalence of gene families related to folate (vitamin B9) metabolism. Furthermore, the conventional diet had a greater expression of functions related to the biosynthesis of cofactors, such as methanopterin.

2.4.5 Impact of diet on the expression of genes associated to residual methane emission

The correlation analysis between gene family expression and RME, using the PCIT method, revealed eight enzymes significantly correlated with RME in animals fed the conventional diet (Figure 7a) and 19 in animals under the by-product diet (Figure 7b). Notably, although both diets included expression of enzymes associated with increased methane emissions, the by-product group had a greater number of enzymes correlated with reduced methane emissions.

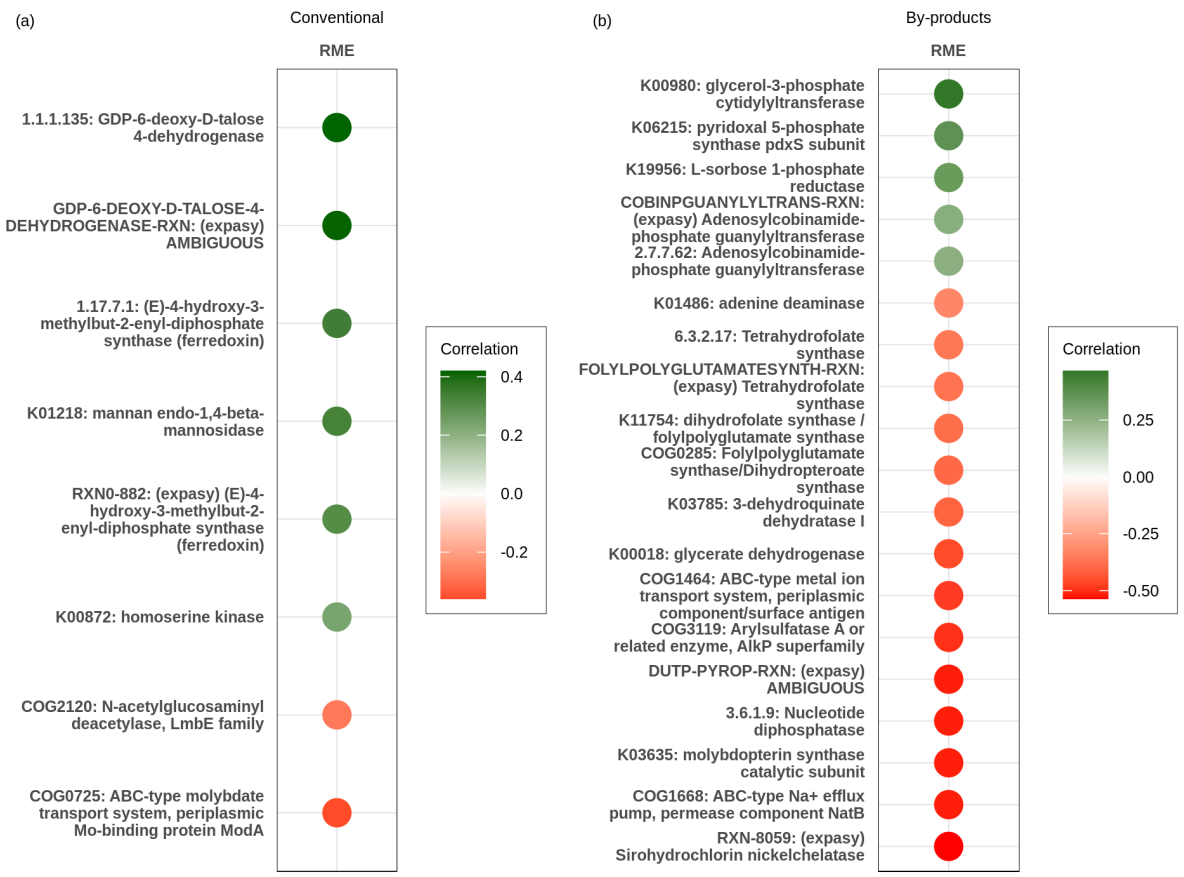

Figure 7: Gene families significantly associated with Residual Methane Emission (RME). The values displayed in the heatmap represent significant correlations identified by the PCIT method. Color gradients range from green (positive correlation) to red (negative correlation), with color intensity indicating the strength of the correlation. (a) Represents gene families associated with RME in the conventional diet. (b) Represents gene families associated with RME in the by-products diet.

Regarding the conventional diet, our results showed that expression of two enzymes, ABC-type molybdate transport system (COG0725) and N-acetylglucosaminyl deacetylase (COG2120), exhibited negative correlations with RME (Figure 7a). In contrast, six gene families, which correspond to four different enzymes, had their expression positively correlated with RME (Figure 7a): GDP-6-deoxy-D-talose 4-dehydrogenase, (E)-4-hydroxy-3-methylbut-2-enyl-diphosphate synthase, homoserine kinase, and mannan endo-1,4-beta-mannosidase.

In the by-product diet, we identified five gene families, which corresponded to four different enzymes, whose expressions were positively associated with residual methane emissions (Figure 7b): adenosylcobinamide-phosphate guanylyltransferase, glycerol-3-phosphate cytidylyltransferase, pyridoxal 5-phosphate synthase, and L-sorbose 1-phosphate reductase. Additionally, 11 enzymes (14 genes families) were negatively

associated with residual methane emissions (Figure 7b): ABC-type metal ion transport system, ABC-type Na^+ efflux pump, arylsulfatase A, nucleotide diphosphatase, tetrahydrofolate synthase, glycerate dehydrogenase, adenine deaminase, 3-dehydroquinate dehydratase I, dihydrofolate synthase/folylpolyglutamate synthase, sirohydrochlorin nickel chelatase, and molybdopterin synthase catalytic subunit.

2.5 Discussion

In this study, we used metatranscriptomics to investigate how two different diets (conventional or by-product-based diet) affect the rumen microbiome of Nelore cattle. Unlike taxonomic or gene-content approaches, metatranscriptomics captures active gene expression, revealing functional microbial responses to diet (14, 17). Our analysis uncovered diet-associated shifts in both microbial composition and function, including associations between specific gene families and methane emissions. To our knowledge, this is the first metatranscriptomic study of the rumen in Nelore cattle.

Taxonomic profiling revealed no significant differences in diversity or taxonomic profiles between diets, suggesting that dietary interventions did not substantially alter the active ruminal microbiome composition of Nelore cattle. This contrasts with previous metagenomic findings from the same cohort, where the total microbiota of animals fed the by-product diet showed increased archaeal diversity and higher abundance of *Fibrobacteres,* with higher *Actinobacteria* and *Euryarchaeota* in animals fed the conventional diet (19). In the context of functional annotation, the main active functions in the ruminal microbiome of Nelore cattle were carbohydrate, amino acid, and energy metabolism, central to nutrient conversion and host energy supply (20, 40, 41).

In this study, we highlight the main diet-driven shifts in microbial activity and their implications for ruminal fermentation and methane emissions. In the conventional diet, soybean meal (6.01% DM), a source of β-mannan (42), likely contributed to the exclusive expression of endo-β-mannanase. The higher starch content (37.73% vs. 19.91% DM) also supported the expression of isoamylase and other starch-related enzymes (e.g., acetoacetyl-CoA reductase, acryloyl-CoA reductase), involved in acetyl-CoA conversion to short-chain fatty acids such as butyrate and propionate (43–47). Also, the higher expression of choloylglycine hydrolase suggests modulation of bile acid metabolism in the rumen in response to high-starch conditions, echoing plasma-based findings in other studies (48, 49). In contrast, the by-product diet enhanced microbial activity toward the degradation of complex fibers such as cellulose, hemicellulose, and pectin. This diet contained ~20% more hemicellulose than the conventional diet, primarily from corn silage, peanut meal, and citrus pulp (50–55). Pectin metabolism was also evident through the higher expression of

UDP-glucose--hexose-1-phosphate uridylyltransferase, involved in galactose utilization (56, 57), indicating greater microbial use of pectin-derived sugars.

Concerning amino acids, the conventional group exhibited higher expression of enzymes and pathways related to threonine, lysine, and glutamate metabolism. While corn is low in lysine and threonine (58), soybean meal supplies lysine, glutamate, and other amino acids (59–61). Glutamate, a precursor of gamma-aminobutyric acid (GABA) via glutamate decarboxylase (62–64), detected in soybean and corn fermentations (65), can affect fermentation and methanogenesis (66). The expression of enzymes such as carboxynorspermidine decarboxylase and glutaconate CoA-transferase supports glutamate fermentation, polyamine synthesis, and H_2 production (67), consistent with methanogenic activity, further confirmed by the archaeal-specific CDP-archaeol pathway (68). In contrast, the by-product diet was more associated with nitrogen-related pathways, notably lysine and arginine metabolism. Peanut meal (7.54% DM) is protein-rich and high in arginine (50, 69), supporting nitrogen metabolism and the synthesis of nitric oxide, polyamines, and urea (70, 71). Exclusive expression of arginine and polyamine pathways, including ABC-type Fe^{3+}/spermidine/putrescine transporters, suggests enhanced polyamine metabolism, linked to oxidative stress control and host physiology (72–75). However, peanut meal is low in methionine, cysteine, and lysine (50, 69, 76), which may explain the elevated expression of lysine-related gene families (e.g., beta-lysine 5,6-aminomutase) and lower ruminal urea levels in this group. We hypothesize that under nitrogen-limited conditions, ruminal microbes may activate lysine-utilization pathways to scavenge available nitrogen, a potential adaptive strategy.

Animals fed the by-product diet showed higher activity in pathways related to lipid modification and biohydrogenation. Ingredients such as corn germ meal, rich in polyunsaturated fatty acids (PUFA), may have stimulated microbial responses that reduce hydrogen availability for methanogenesis, but can also stress gram-positive bacteria and alter fermentation efficiency (75, 77).

Vitamin-related pathways also diverged between diets. The conventional diet promoted expression linked to thiamine (B1), pyridoxine (B6), and cobalamin (B12), reflecting the high corn and soybean meal content (78). Although corn and soybean are low in B12 (79), increased expression of cobalamin biosynthetic genes suggests microbial compensation (80, 81). In the by-product group, microbial activity was enriched in pantothenic acid (B5) and folate (B9) metabolism, consistent with the high content of peanut meal (76, 78, 82). These vitamins support fatty acid biosynthesis and one-carbon metabolism (83, 84). Additionally, gene families related to L-sorbose metabolism were uniquely detected in animals fed citrus pulp, suggesting this ingredient may contribute to glycolysis and microbial energy metabolism (85).

Cattle farming contributes to greenhouse gas emissions, notably methane, which also represents energy loss for ruminants (86, 87). In our study, both diets showed transcripts encoding enzymes linked to methane production. At the same time, gross methane production was lower in the by-product group (88), but due to differences in DMI, RME did not differ between diets (19). Functional profiling revealed changes in microbial pathways, supported by metabolomic data showing increased ruminal propionate in the by-product group (Conv: 3.59 mM; ByPr: 4.97 mM) (88). The lower ruminal pH and higher dietary fat content (7.62%, mostly from corn germ) likely favored propionate production and inhibited methanogenesis (89, 90), even with high effective NDF mitigating a more severe pH drop (Conv: 22.46%; ByPr: 18.23%).

In the by-product group, methane emissions were positively associated with genes supporting methanogenesis. Cobalamin biosynthesis genes, such as adenosylcobinamide-phosphate guanylyltransferase, likely enhance methyl transfer in methanogens (91). Pyridoxal 5′-phosphate synthase, while known to inhibit coenzyme M (92), contributes to tryptophan metabolism and glycolysis (93, 94), pathways that can increase methane production (95). Genes involved in bacterial growth and fermentation, including glycerol-3-phosphate cytidylyltransferase and L-sorbose 1-phosphate reductase, further support hydrogen and acetate production (68, 85), fueling methanogenesis.

However, several enzymes showed negative correlations with methane under the by-product diet. Tetrahydrofolate synthase, a key enzyme in the reductive acetogenesis pathway (96), that may redirect H_2 and CO_2 to acetate rather than methane, while folylpolyglutamate synthase/dihydropteroate synthase, likely reflects methionine limitation (88) and may reduce the availability of substrates for methanogens that rely on tetrahydromethanopterin (H_4MPT) (97, 98). Glycerate dehydrogenase reroutes carbon from acetate and hydrogen production (99–101), thereby limiting methanogenesis, while arylsulfatase A and molybdopterin synthase support sulfate or nitrate metabolism that competes with methanogenesis (96, 102–105). ABC-type metal ion transporters, particularly for iron, cobalt, and nickel, may reduce methane (106) by favoring iron-reducing bacteria that compete for electrons (107–110), a process reinforced by the high iron content of the by-product diet (Conv: 114.27%; ByPr: 180.62%). Finally, Na^+ efflux pumps, crucial for ionic balance and energy metabolism, are involved in propionate-producing pathways (111), which aligns with the observed increase in propionate levels in the same animals (88).

In the conventional diet, several enzymes were positively correlated with RME. GDP-6-deoxy-D-talose 4-dehydrogenase and mannan endo-1,4-β-mannanase, involved in mannose metabolism, release hydrogen through pyruvate and acetate formation, supporting methanogenesis (41, 112). Accordingly, acetate levels were higher in animals fed the conventional diet (88). Similarly, (E)-4-hydroxy-3-methylbut-2-enyl-diphosphate synthase,

part of the methylerythritol phosphate pathway, suggests enhanced ferredoxin-dependent redox activity favoring methane (113), while homoserine kinase likely supports methanopterin, key cofactors in methanogenesis (114–116). Conversely, two enzymes were negatively correlated with RME: the ABC-type molybdate transport system, which facilitates nitrate reduction by competing for hydrogen (102, 103), and N-acetylglucosaminyl deacetylase, which produces acetate without hydrogen release (117). Both findings suggest alternative pathways that divert substrates away from methane production.

An important methodological limitation of this study involves sample collection post-slaughter, following a 16-hour pre-slaughter fasting period, as required by Brazilian regulations. Similar fasting-related conditions were also observed in other rumen metatranscriptomic studies with beef cattle, where sampling occurred prior to feeding and therefore under fasting status (118, 119). This fasting is not trivial, since feed withdrawal is known to substantially reduce ruminal substrate availability, thereby decreasing volatile fatty acid concentrations and H_2 availability, altering microbial activity, shifting the proportion of VFAs in favor of acetate, and favoring taxa adapted to nutrient scarcity or opportunistic pathogens (120–122). Thus, we recognize that these changes may have attenuated diet-driven differences by homogenizing microbial activity and methane production across treatments, or conversely amplifying responses of taxa more resilient to nutrient limitation. Reports of microbial restructuring after fasting (122–124) highlight that our results should be interpreted in light of these potential biases. Future studies should consider sampling before fasting (e.g., via rumen cannulation or stomach tubing) to more accurately capture the ruminal microbial activity under normal feeding conditions.

2.6 Conclusion

Using a metatranscriptomic approach, this study assessed how diet influences the composition and functionality of the active rumen microbiome in Nelore cattle and its association with methane emissions. Although taxonomic composition remained stable between dietary groups, clear functional differences emerged. Overall, the inclusion of agro-industrial by-products based on citrus pulp and peanut meal altered ruminal microbial metabolism, expanded gene family expression, and favored pathways that compete with methanogenesis. These findings highlight the potential of by-product-based diets to reduce enteric methane emissions, decrease feed costs, and support more sustainable livestock production systems.

2.7 Data availability

The data presented in the study are deposited in the National Center for Biotechnology Information repository, accession number PRJNA1131826.

2.8 Supplementary Figure

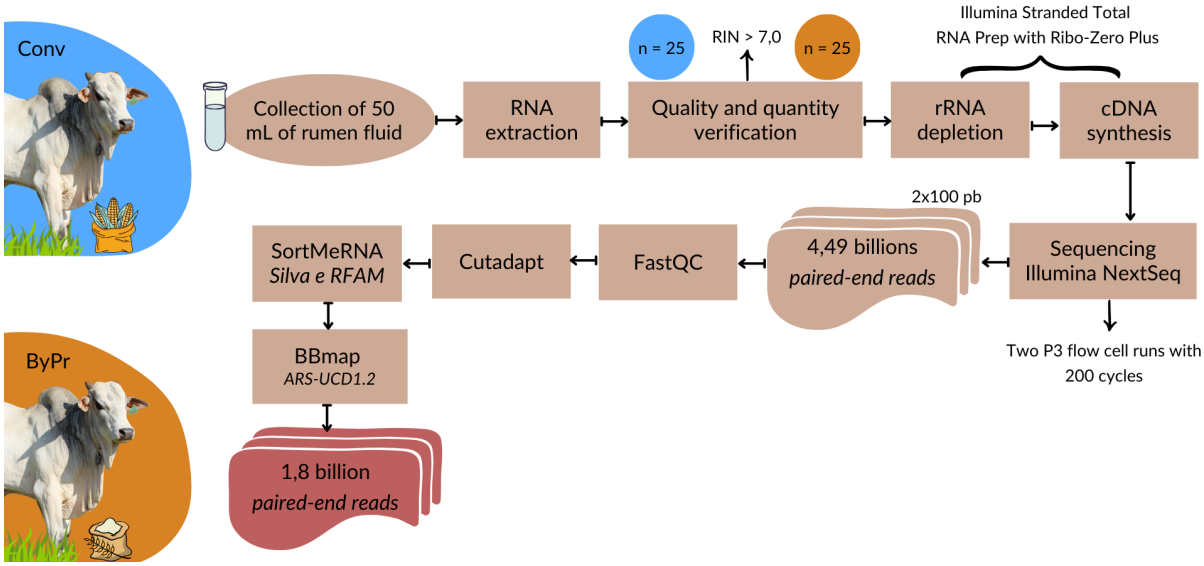

Supplementary Figure 1. Overview of the workflow comprising sample collection, RNA extraction, sequencing, and preprocessing of rumen microbiome RNA reads from Nelore cattle.

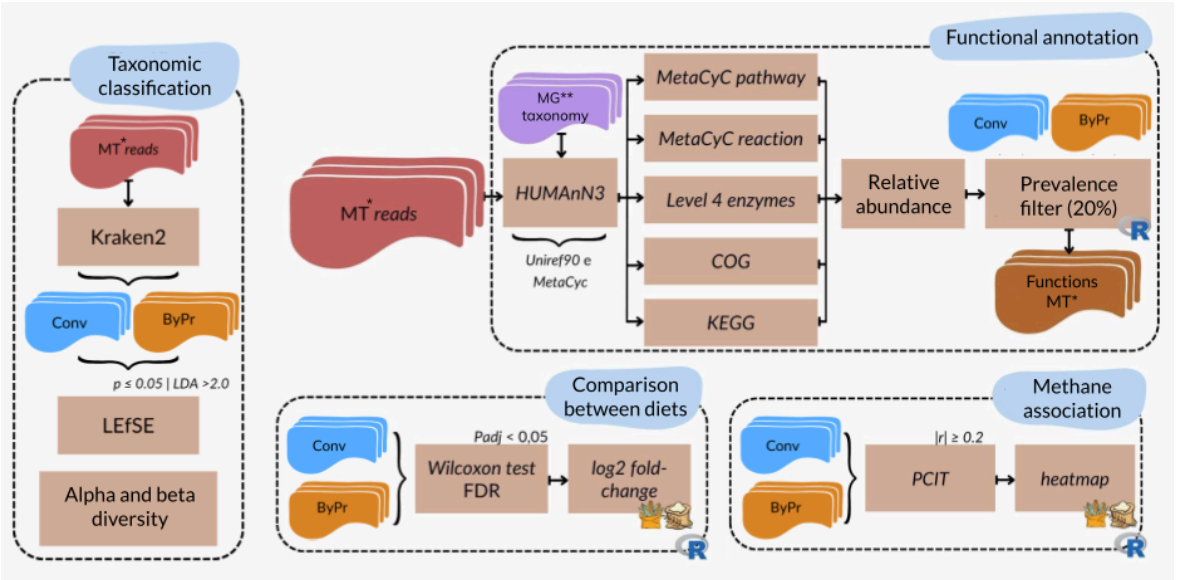

Supplementary Figure 2. Overview of taxonomic classification, functional annotation, dietary impact evaluation, and associations with methane emissions. Abbreviations: MT*, metatranscriptome; MG**, metagenome.

2.9 References

1. Cole MB, Augustin MA, Robertson MJ, Manners JM. 2018. The science of food security. Npj Sci Food 2:14.

2. Barbosa BRP, Santos SA, Abreu UGPD, Egito AA, Comastri Filho JA, Juliano RS, Paiva SR, McManus C. 2014. Tolerância ao calor em bovinos das raças Nelore branco, Nelore vermelho e Pantaneira. Rev Bras Saúde E Produção Anim 15:854–865.

3. Da Silva WAL, Da Costa E Silva EV, Ferreira MGCR, Gheller JM, Poehland R, Melo-Sterza FDA. 2023. Effect of shading on the physiological and reproductive parameters in Nelore cows. 6. Trop Anim Health Prod 55:374.

4. Del Pilar Solar Diaz I, Bezerra LAF, Lôbo RB, De Araújo Neto FR, De Camargo GMF, Da Cruz VAR, Costa RB, De Oliveira HN. 2022. Selection effect for growth traits on energy requirements in beef Nelore steers. Trop Anim Health Prod 54:213.

5. Greenwood PL. 2021. Review: An overview of beef production from pasture and feedlot globally, as demand for beef and the need for sustainable practices increase. Animal 15:100295.

6. Walmsley BJ, Lee SJ, Parnell PF, Pitchford WS. 2016. A review of factors influencing key biological components of maternal productivity in temperate beef cattle. 1. Anim Prod Sci 58:1.

7. Johnson KA, Johnson DE. 1995. Methane emissions from cattle. 8. J Anim Sci 73:2483–2492.

8. Lin L, Lai Z, Zhang J, Zhu W, Mao S. 2023. The gastrointestinal microbiome in dairy cattle is constrained by the deterministic driver of the region and the modified effect of diet. Microbiome 11:10.

9. Miller GA, Auffret MD, Roehe R, Nisbet H, Martinez-Alvaro M. 2023. Different microbial genera drive methane emissions in beef cattle fed with two extreme diets. Differ Microb Genera Drive Methane Emiss Beef Cattle Fed Two Extreme Diets https://doi.org/10.3389/fmicb.2023.1102400 Abstract.

10. Matthews C, Crispie F, Lewis E, Reid M, O'Toole PW, Cotter PD. 2019. The rumen microbiome: a crucial consideration when optimising milk and meat production and nitrogen utilisation efficiency. Gut Microbes 10:115–132.

11. Mizoguchi Y, Guan LL. 2024. — Invited Review — Translational gut microbiome research for strategies to improve beef cattle production sustainability and meat quality. Anim Biosci 37:346–359.

12. Congiu M, Lourenco J, Cesarani A, Lamichhane U, Macciotta NPP, Dimauro C. 2024. Predicting feed efficiency of Angus steers using the gastrointestinal microbiome. animal 18:101102.

13. Nguyen TTM, Badhan AK, Reid ID, Ribeiro G, Gruninger R, Tsang A, Guan LL, McAllister T. 2023. Comparative analysis of functional diversity of rumen microbiome in bison and beef heifers. Appl Environ Microbiol 89:e01320-23.

14. Li F, Guan LL. 2017. Metatranscriptomic Profiling Reveals Linkages between the Active Rumen Microbiome and Feed Efficiency in Beef Cattle. Appl Environ Microbiol 83:e00061-17.

15. Xue M-Y, Xie Y-Y, Zhong Y, Ma X-J, Sun H-Z, Liu J-X. 2022. Integrated meta-omics reveals new ruminal microbial features associated with feed efficiency in dairy cattle. Microbiome 10:32.

16. Badhan A, Wang Y, Terry S, Gruninger R, Guan LL, McAllister TA. 2025. Interplay of rumen microbiome and the cattle host in modulating feed efficiency and methane emissions. J Dairy Sci S0022030225002164.

17. Malik PK, Trivedi S, Kolte AP, Mohapatra A, Biswas S, Bhattar AVK, Bhatta R, Rahman H. 2023. Comparative analysis of rumen metagenome, metatranscriptome, fermentation and methane yield in cattle and buffaloes fed on the same diet. Front Microbiol 14:1266025.

18. Andrade BGN, Bressani FA, Cuadrat RRC, Cardoso TF, Malheiros JM, De Oliveira PSN, Petrini J, Mourão GB, Coutinho LL, Reecy JM, Koltes JE, Neto AZ, R. De Medeiros S, Berndt A, Palhares JCP, Afli H, Regitano LCA. 2022. Stool and Ruminal Microbiome Components Associated With Methane Emission and Feed Efficiency in Nelore Beef Cattle. Front Genet 13:812828.

19. Conteville LC, Silva JV, Andrade BGN, Cardoso TF, Bruscadin JJ, Oliveira PSN, Mourão GB, Coutinho LL, Palhares JCP, Berndt A, de Medeiros SR, Regitano LC de A. 2023. Rumen and fecal microbiomes are related to diet and production traits in Bos indicus beef cattle. Front Microbiol https://doi.org/10.3389/fmicb.2023.1282851.

20. Mann E, Wetzels SU, Wagner M, Zebeli Q, Schmitz-Esser S. 2018. Metatranscriptome Sequencing Reveals Insights into the Gene Expression and Functional Potential of Rumen Wall Bacteria. Front Microbiol 9:43.

21. Pfau AP, Shepherd EA, Martin MG, Ascolese S, Mason KM, Egert-McLean AM, Voy BH, Myer PR. 2023. Beta-Adrenergic Agonists, Dietary Protein, and Rumen Bacterial Community Interactions in Beef Cattle: A Review. 9. Vet Sci 10:579.

22. Ravindran R, Jaiswal AK. 2016. Exploitation of Food Industry Waste for High-Value Products. 1. Trends Biotechnol 34:58–69.

23. Herd RM, Arthur PF, Donoghue KA, Bird SH, Bird-Gardiner T, Hegarty RS. 2014. Measures of methane production and their phenotypic relationships with dry matter intake, growth, and body composition traits in beef cattle1,2. J Anim Sci 92:5267–5274.

24. Donoghue KA, Bird-Gardiner T, Arthur PF, Herd RM, Hegarty RF. 2016. Genetic and phenotypic variance and covariance components for methane emission and postweaning traits in Angus cattle12. J Anim Sci 94:1438–1445.

25. Li F, Henderson G, Sun X, Cox F, Janssen PH, Guan LL. 2016. Taxonomic Assessment of Rumen Microbiota Using Total RNA and Targeted Amplicon Sequencing Approaches. Front Microbiol 7.

26. Martin M. 2011. Cutadapt Removes Adapter Sequences From High-Throughput Sequencing Reads. Cutadapt Removes Adapt Seq High-Throughput Seq Reads 1:10–12.

27. Quast C, Pruesse E, Yilmaz P, Gerken J, Schweer T, Yarza P, Peplies J, Glöckner FO. 2012. The SILVA ribosomal RNA gene database project: improved data processing and web-based tools. Nucleic Acids Res 41:D590–D596.

28. Griffiths-Jones S. 2003. Rfam: an RNA family database. Nucleic Acids Res 31:439–441.

29. Kopylova E, Noé L, Touzet H. 2012. SortMeRNA: fast and accurate filtering of ribosomal RNAs in metatranscriptomic data. Bioinformatics 28:3211–3217.

30. Wood DE, Lu J, Langmead B. 2019. Improved metagenomic analysis with Kraken 2. 1. Genome Biol 20:257.

31. Ma S, Shungin D, Mallick H, Schirmer M, Nguyen LH, Kolde R, Franzosa E, Vlamakis H, Xavier R, Huttenhower C. 2022. Population structure discovery in meta-analyzed microbial communities and inflammatory bowel disease using MMUPHin. 1. Genome Biol 23:208.

32. Segata N, Izard J, Waldron L, Gevers D, Miropolsky L, Garrett WS, Huttenhower C. 2011. Metagenomic biomarker discovery and explanation. Genome Biol 12:R60.

33. Beghini F, McIver LJ, Blanco-Míguez A, Dubois L, Asnicar F, Maharjan S, Mailyan A, Manghi P, Scholz M, Thomas AM, Valles-Colomer M, Weingart G, Zhang Y, Zolfo M, Huttenhower C, Franzosa EA, Segata N. 2021. Integrating taxonomic, functional, and strain-level profiling of diverse microbial communities with bioBakery 3. eLife 10:e65088.

34. Karp PD. 2002. The MetaCyc Database. Nucleic Acids Res 30:59–61.

35. Qian W, Wang X, Kang Y, Pan P, Hou T, Hsieh C-Y. 2024. A general model for predicting enzyme functions based on enzymatic reactions. J Cheminformatics 16:38.

36. Kanehisa M, Goto S. 2000. KEGG: Kyoto Encyclopedia of Genes and Genomes. Nucleic Acids Res https://doi.org/10.1093/nar/28.1.27.

37. Tatusov RL, Koonin EV, Lipman DJ. 1997. A Genomic Perspective on Protein Families. Science 278:631–637.

38. Benjamini Y, Hochberg Y. 1995. Controlling the False Discovery Rate: A Practical and Powerful Approach to Multiple Testing. J R Stat Soc Ser B Stat Methodol 57:289–300.

39. Watson-Haigh NS, Kadarmideen HN, Reverter A. 2010. PCIT: an R package for weighted gene co-expression networks based on partial correlation and information theory approaches. Bioinformatics 26:411–413.

40. Na SW, Guan LL. 2022. Understanding the role of rumen epithelial host-microbe interactions in cattle feed efficiency. Anim Nutr 10:41–53.

41. Iqbal S, Zebeli Q, Mazzolari A, Bertoni G, Dunn SM, Yang WZ, Ametaj BN. 2009. Feeding barley grain steeped in lactic acid modulates rumen fermentation patterns and increases milk fat content in dairy cows. 12. J Dairy Sci 92:6023–6032.

42. Lin J, Pantalone VR, Li G, Chen F. 2011. Molecular Cloning and Biochemical Characterization of an Endo-β-mannanase Gene from Soybean for Soybean Meal

Improvement. 9. J Agric Food Chem 59:4622–4628.

43. Asao M, Alber BE. 2013. Acrylyl-Coenzyme A Reductase, an Enzyme Involved in the Assimilation of 3-Hydroxypropionate by Rhodobacter sphaeroides. 20. J Bacteriol 195:4716–4725.

44. Beauchemin KA, Ungerfeld E, Gruninger R. 2022. Control of Methanogenesis in Dairy Animals, p. 65–78. *In* Encyclopedia of Dairy Sciences. Elsevier.

45. Olavarria K, Carnet A, Van Renselaar J, Quakkelaar C, Cabrera R, Guedes Da Silva L, Smids AL, Villalobos PA, Van Loosdrecht MCM, Wahl SA. 2021. An NADH preferring acetoacetyl-CoA reductase is engaged in poly-3-hydroxybutyrate accumulation in Escherichia coli. J Biotechnol 325:207–216.

46. Zhao Y, Xue F, Hua D, Wang Y, Pan X, Nan X, Sun F, Jiang L, Xiong B. 2020. Metagenomic Insights into Effects of Thiamine Supplementation on Carbohydrate-Active Enzymes' Profile in Dairy Cows Fed High-Concentrate Diets. 2. Animals 10:304.

47. Hua D, Hendriks WH, Xiong B, Pellikaan WF. 2022. Starch and Cellulose Degradation in the Rumen and Applications of Metagenomics on Ruminal Microorganisms. 21. Animals 12:3020.

48. Zheng L, Shen J, Han X, Jin C, Chen X, Yao J. 2023. High rumen degradable starch diet induced blood bile acids profile changes and hepatic inflammatory response in dairy goats. Anim Nutr 14:121–129.

49. Zheng L, Wu S, Shen J, Han X, Jin C, Chen X, Zhao S, Cao Y, Yao J. 2020. High rumen degradable starch decreased goat milk fat via trans-10, cis-12 conjugated linoleic acid-mediated downregulation of lipogenesis genes, particularly, INSIG1. 1. J Anim Sci Biotechnol 11:30.

50. Zhao T, Ying P, Zhang Y, Chen H, Yang X. 2023. Research Advances in the High-Value Utilization of Peanut Meal Resources and Its Hydrolysates: A Review. 19. Molecules 28:6862.

51. Toomer OT. 2018. Nutritional chemistry of the peanut (*Arachis hypogaea)*. Crit Rev Food Sci Nutr 58:3042–3053.

52. Bampidis VA, Robinson PH. 2006. Citrus by-products as ruminant feeds: A review.

3–4. Anim Feed Sci Technol 128:175–217.

53. Santos GT, Lima LS, Schogor ALB, Romero JV, De Marchi FE, Grande PA, Santos NW, Santos FS, Kazama R. 2014. Citrus Pulp as a Dietary Source of Antioxidants for Lactating Holstein Cows Fed Highly Polyunsaturated Fatty Acid Diets. 8. Asian-Australas J Anim Sci 27:1104–1113.

54. Shibanuma K, Takamine K, Maseda S, Osaki S, Abet J, Hizukuri S. 1999. Partial Acid Hydrolysis of Corn Fiber for the Production of L-Arabinose. 3. J Appl Glycosci 46:249–256.

55. Zhao Z, Xian M, Liu M, Zhao G. 2020. Biochemical routes for uptake and conversion of xylose by microorganisms. 1. Biotechnol Biofuels 13:21.

56. Li J, Peng C, Mao A, Zhong M, Hu Z. 2024. An overview of microbial enzymatic approaches for pectin degradation. Int J Biol Macromol 254:127804.

57. Bonnin E, Garnier C, Ralet M-C. 2014. Pectin-modifying enzymes and pectin-derived materials: applications and impacts. 2. Appl Microbiol Biotechnol 98:519–532.

58. Lewis AJ, Barnes MB, Grosbach DA, Peo ER. 1982. Sequence in Which the Amino Acids of Corn (Zea mays) Become Limiting for Growing Rats. 4. J Nutr 112:782–788.

59. Miranda MS, Arcaro JRP, Saran Netto A, Silva SL, Pinheiro MG, Leme PR. 2019. Effects of partial replacement of soybean meal with other protein sources in diets of lactating cows. 7. Animal 13:1403–1411.

60. Qin P, Wang T, Luo Y. 2022. A review on plant-based proteins from soybean: Health benefits and soy product development. J Agric Food Res 7:100265.

61. Tian Y, Zhang X, Huang R, Yu P. 2019. Protein molecular structure, degradation and availability of canola, rapeseed and soybean meals in dairy cattle diets. Asian-Australas J Anim Sci 32:1381–1388.

62. Yoshida C, Maekawa M, Bannai M, Yamamoto T. 2016. Glutamate promotes nucleotide synthesis in the gut and improves availability of soybean meal feed in rainbow trout. 1. SpringerPlus 5:1021.

63. Ku BS, Mamuad LL, Kim S-H, Jeong CD, Soriano AP, Lee H-I, Nam K-C, Ha JK, Lee SS. 2013. Effect of γ-Aminobutyric Acid (GABA) Producing Bacteria on In vitro Rumen Fermentation, Biogenic Amine Production and Anti-oxidation Using Corn Meal as

Substrate. 6. Asian-Australas J Anim Sci 26:804–811.

64. Wang Y-L, Zhang Z-H, Wang W-K, Wu Q-C, Zhang F, Li W-J, Li S-L, Wang W, Cao Z-J, Yang H-J. 2023. The Effect of γ-Aminobutyric Acid Addition on In Vitro Ruminal Fermentation Characteristics and Methane Production of Diets Differing in Forage-to-Concentrate Ratio. 2. Fermentation 9:105.

65. Asun AC, Lin S-T, Ng HS, Lan JC-W. 2022. Production of gamma-aminobutyric acid (GABA) by Bacillus subtilis BBEL02 fermentation using nitrogen-rich industrial wastes as crude feedstocks. Biochem Eng J 187:108654.

66. Wang Y-L, Zhang Z-H, Wang W-K, Wu Q-C, Zhang F, Li W-J, Li S-L, Wang W, Cao Z-J, Yang H-J. 2023. The Effect of γ-Aminobutyric Acid Addition on In Vitro Ruminal Fermentation Characteristics and Methane Production of Diets Differing in Forage-to-Concentrate Ratio. Fermentation 9:105.

67. Mack M, Buckel W. 1997. Conversion of glutaconate CoA-transferase from *Acidaminococcus fermentans* into an acyl-CoA hydrolase by site-directed mutagenesis. FEBS Lett 405:209–212.

68. Jain S, Caforio A, Fodran P, Lolkema JS, Minnaard AJ, Driessen AJM. 2014. Identification of CDP-Archaeol Synthase, a Missing Link of Ether Lipid Biosynthesis in Archaea. Chem Biol 21:1392–1401.

69. Batal A, Dale N, Café M. 2005. Nutrient Composition of Peanut Meal. 2. J Appl Poult Res 14:254–257.

70. Morris SM. 2016. Arginine Metabolism Revisited. 12. J Nutr 146:2579S-2586S.

71. Si H, Han Y, Liu H, Lou Y, Li Z. 2021. Effects of rumen-protected arginine supplementation on the plasma amino acids and gut microbiota of sika deer (Cervus nippon). Anim Feed Sci Technol 273:114828.

72. Lenis YY, Elmetwally MA, Maldonado-Estrada JG, Bazer FW. 2017. Physiological importance of polyamines. 3. Zygote 25:244–255.

73. Laube G, Bernstein H-G. 2017. Agmatine: multifunctional arginine metabolite and magic bullet in clinical neuroscience? 15. Biochem J 474:2619–2640.

74. Holbert CE, Dunworth M, Foley JR, Dunston TT, Stewart TM, Casero RA. 2020. Autophagy induction by exogenous polyamines is an artifact of bovine serum amine

oxidase activity in culture serum. 27. J Biol Chem 295:9061–9068.

75. Xuan M, Gu X, Li J, Huang D, Xue C, He Y. 2023. Polyamines: their significance for maintaining health and contributing to diseases. 1. Cell Commun Signal 21:348.

76. Bonku R, Yu J. 2020. Health aspects of peanuts as an outcome of its chemical composition. 1. Food Sci Hum Wellness 9:21–30.

77. Vargas JE, Andrés S, López-Ferreras L, López S. 2020. Effects of supplemental plant oils on rumen bacterial community profile and digesta fatty acid composition in a continuous culture system (RUSITEC). Anaerobe 61:102143.

78. Chen YF, Huang CF, Liu L, Lai CH, Wang FL. 2019. Concentration of vitamins in the 13 feed ingredients commonly used in pig diets. Anim Feed Sci Technol 247:1–8.

79. Sherwood DH, Sloan HJ. 1954. Vitamin B12 and Choline in Corn-Soy Rations for Starting Poults ,. 5. Poult Sci 33:1015–1021.

80. A. Roessner C, B. Spencer J, J. Stolowich N, Wang J, Parmesh Nayar G, J. Santander P, Pichon C, Min C, T. Holderman M, Ian Scott A. 1994. Genetically engineered synthesis of precorrin-6x and the complete corrinoid, hydrogenobyrinic acid, an advanced precursor of vitamin B12. 2. Chem Biol 1:119–124.

81. Fang H, Kang J, Zhang D. 2017. Microbial production of vitamin B12: a review and future perspectives. 1. Microb Cell Factories 16:15.

82. Zhao T, Ying P, Zhang Y, Chen H, Yang X. 2023. Research Advances in the High-Value Utilization of Peanut Meal Resources and Its Hydrolysates: A Review. Molecules 28:6862.

83. Maia MRG, Chaudhary LC, Figueres L, Wallace RJ. 2007. Metabolism of polyunsaturated fatty acids and their toxicity to the microflora of the rumen. 4. Antonie Van Leeuwenhoek 91:303–314.

84. Ragaller V, Hüther L, Lebzien P. 2008. Folic acid in ruminant nutrition: a review. 2. Br J Nutr 101:153–164.

85. Sprenger GA, Lengeler JW. 1984. L-Sorbose metabolism in Klebsiella pneumoniae and Sor+ derivatives of Escherichia coli K-12 and chemotaxis toward sorbose. J Bacteriol 157:39–45.

86. Ungerfeld EM. 2020. Metabolic Hydrogen Flows in Rumen Fermentation: Principles and Possibilities of Interventions. Front Microbiol 11:589.

87. Kamke J, Kittelmann S, Soni P, Li Y, Tavendale M, Ganesh S, Janssen PH, Shi W, Froula J, Rubin EM, Attwood GT. 2016. Rumen metagenome and metatranscriptome analyses of low methane yield sheep reveals a Sharpea-enriched microbiome characterised by lactic acid formation and utilisation. Microbiome 4:56.

88. Malheiros JM, Correia BSB, Ceribeli C, Bruscadin JJ, Diniz WJS, Banerjee P, Da Silva Vieira D, Cardoso TF, Andrade BGN, Petrini J, Cardoso DR, Colnago LA, Bogusz Junior S, Mourão GB, Coutinho LL, Palhares JCP, De Medeiros SR, Berndt A, De Almeida Regitano LC. 2023. Ruminal and feces metabolites associated with feed efficiency, water intake and methane emission in Nelore bulls. Sci Rep 13:18001.

89. Nuray N. 2015. Do fats reduce methane emission by ruminants? - a review. Fats Reduce Methane Emiss Rumin - Rev 33:305–321.

90. Bionaz M, Vargas-Bello-Pérez E, Busato S. 2020. Advances in fatty acids nutrition in dairy cows: from gut to cells and effects on performance. J Anim Sci Biotechnol 11:110.

91. Tavares NK, Zayas CL, Escalante-Semerena JC. 2018. The *Methanosarcina mazei* MM2060 Gene Encodes a Bifunctional Kinase/Decarboxylase Enzyme Involved in Cobamide Biosynthesis. Biochemistry 57:4478–4495.

92. Liu R, Shen Y, Ma H, Li Y, Lambo MT, Dai B, Shen W, Qu Y, Zhang Y. 2023. Silibinin reduces in vitro methane production by regulating the rumen microbiome and metabolites. Front Microbiol 14:1225643.

93. Cellini B, Zelante T, Dindo M, Bellet MM, Renga G, Romani L, Costantini C. 2020. Pyridoxal 5′-Phosphate-Dependent Enzymes at the Crossroads of Host–Microbe Tryptophan Metabolism. Int J Mol Sci 21:5823.

94. Yi S, Dai D, Wu H, Chai S, Liu S, Meng Q, Zhou Z. 2022. Dietary Concentrate-to-Forage Ratio Affects Rumen Bacterial Community Composition and Metabolome of Yaks. Front Nutr 9:927206.

95. De Jesús JAC, Elghandour MMMY, Adegbeye MJ, Aguirre DL, Roque-Jimenez JA, Lackner M, Salem AZM. 2024. Nano-encapsulation of essential amino acids: ruminal methane, carbon monoxide, hydrogen sulfide and fermentation. AMB Express 14:109.

96. Denman SE, Martinez Fernandez G, Shinkai T, Mitsumori M, McSweeney CS. 2015. Metagenomic analysis of the rumen microbial community following inhibition of methane formation by a halogenated methane analog. Front Microbiol 6.

97. Buchenau B, Thauer RK. 2004. Tetrahydrofolate-specific enzymes in Methanosarcina barkeri and growth dependence of this methanogenic archaeon on folic acid or p-aminobenzoic acid. Arch Microbiol 182:313–325.

98. Maden BEH. 2000. Tetrahydrofolate and tetrahydromethanopterin compared : functionally distinct carriers in C1 metabolism.

99. Goldberg JD, Yoshida T, Brick P. 1994. Crystal structure of a NAD-dependent d-glycerate dehydrogenase at 2·4 Å resolution. J Mol Biol 236:1123–1140.

100. Locasale JW. 2013. Serine, glycine and one-carbon units: cancer metabolism in full circle. Nat Rev Cancer 13:572–583.

101. Newman AC, Maddocks ODK. 2017. One-carbon metabolism in cancer. Br J Cancer 116:1499–1504.

102. Yang C, Rooke JA, Cabeza I, Wallace RJ. 2016. Nitrate and Inhibition of Ruminal Methanogenesis: Microbial Ecology, Obstacles, and Opportunities for Lowering Methane Emissions from Ruminant Livestock. Front Microbiol 7.

103. Ringel P, Krausze J, Van Den Heuvel J, Curth U, Pierik AJ, Herzog S, Mendel RR, Kruse T. 2013. Biochemical Characterization of Molybdenum Cofactor-free Nitrate Reductase from Neurospora crassa. J Biol Chem 288:14657–14671.

104. Christl SU, Gibson GR, Cummings JH. 1992. Role of dietary sulphate in the regulation of methanogenesis in the human large intestine. Gut 33:1234–1238.

105. Kunito T, Kurita H, Kumori M, Sakaguchi K, Nishizawa S, Fujita K, Moro H, Sawada K, Miyabara Y, Toda H, Nagaoka K, Ishikawa Y. 2022. Microbial synthesis of arylsulfatase depends on the soluble and adsorbed sulfate concentration in soils. Eur J Soil Biol 111:103418.

106. Martínez-Álvaro M, Auffret MD, Duthie C-A, Dewhurst RJ, Cleveland MA, Watson M, Roehe R. 2022. Bovine host genome acts on rumen microbiome function linked to methane emissions. Commun Biol 5:350.

107. Sousa FL, Thiergart T, Landan G, Nelson-Sathi S, Pereira IAC, Allen JF, Lane N,

Martin WF. 2013. Early bioenergetic evolution. Philos Trans R Soc B Biol Sci 368:20130088.

108. Braymer JJ, Freibert SA, Rakwalska-Bange M, Lill R. 2021. Mechanistic concepts of iron-sulfur protein biogenesis in Biology. Biochim Biophys Acta BBA - Mol Cell Res 1868:118863.

109. Baek G. 2019. A review of the effects of iron compounds on methanogenesis in anaerobic environments.

110. Clemmons BA, Schneider LG, Melchior EA, Lindholm-Perry AK, Hales KE, Wells E, Freetly HC, Hansen SL, Drewnoski ME, Hartman SJ, Myer PR. The effects of feeding ferric citrate on ruminal bacteria, methanogenic archaea and methane production in growing beef steers https://doi.org/10.1099/acmi.0.000180.

111. Reichardt N, Duncan SH, Young P, Belenguer A, McWilliam Leitch C, Scott KP, Flint HJ, Louis P. 2014. Phylogenetic distribution of three pathways for propionate production within the human gut microbiota. ISME J 8:1323–1335.

112. Pressman EM, Kebreab E. 2024. A review of key microbial and nutritional elements for mechanistic modeling of rumen fermentation in cattle under methane-inhibition. Front Microbiol 15:1488370.

113. Stepanchenko N, Stefenoni H, Hennessy M, Nagaraju I, Wasson DE, Cueva SF, Räisänen SE, Dechow CD, Pitta DW, Hristov AN. 2023. Microbial composition, rumen fermentation parameters, enteric methane emissions, and lactational performance of phenotypically high and low methane-emitting dairy cows. 9. J Dairy Sci 106:6146–6170.

114. Wang Y, Xu H, Jones MK, White RH. 2015. Identification of the Final Two Genes Functioning in Methanofuran Biosynthesis in Methanocaldococcus jannaschii. 17. J Bacteriol 197:2850–2858.

115. Dumitru R, Palencia H, Schroeder SD, DeMontigny BA, Takacs JM, Rasche ME, Miner JL, Ragsdale SW. 2003. Targeting Methanopterin Biosynthesis ToInhibitMethanogenesis. 12. Appl Environ Microbiol 69:7236–7241.

116. White RH. 1990. Biosynthesis of Methanopterid.

117. Roseman S. 1957. GLUCOSAMINE METABOLISM. J Biol Chem 226:115–124.

118. Zhang Y, Li F, Chen Y, Wu H, Meng Q, Guan LL. 2020. Metatranscriptomic Profiling Reveals the Effect of Breed on Active Rumen Eukaryotic Composition in Beef Cattle With Varied Feed Efficiency. Front Microbiol 11.

119. Liu Y, Wu H, Chen W, Liu C, Meng Q, Zhou Z. 2022. Rumen Microbiome and Metabolome of High and Low Residual Feed Intake Angus Heifers. Front Vet Sci 9.

120. Welch CB, Lourenco JM, Seidel DS, Krause TR, Rothrock MJ, Pringle TD, Callaway TR. 2021. The Impact of Pre-Slaughter Fasting on the Ruminal Microbial Population of Commercial Angus Steers. Microorganisms 9:2625.

121. Kim JN, Song J, Kim EJ, Chang J, Kim C-H, Seo S, Chang MB, Bae G-S. 2019. Effects of short-term fasting on in vivo rumen microbiota and in vitro rumen fermentation characteristics. Asian-Australas J Anim Sci 32:776–782.

122. Stumm CK, Gijzen HJ, Vogels GD. 1982. Association of methanogenic bacteria with ovine rumen ciliates. Br J Nutr 47:95–99.

123. Lam S, Munro JC, Zhou M, Guan LL, Schenkel FS, Steele MA, Miller SP, Montanholi YR. 2018. Associations of rumen parameters with feed efficiency and sampling routine in beef cattle. Animal 12:1442–1450.

124. Galyean ML, Lee RW, Hubbert ME. 1981. Influence of Fasting and Transit on Ruminal and Blood Metabolites in Beef Steers2. J Anim Sci 53:7–18.

3 Integrating metagenomics and metatranscriptomics to uncover microbial and enzyme determinants of methane emissions and feed efficiency in *Bos indicus*

In this chapter, we investigated the active ruminal microbiome (metatranscriptome) of *Bos indicus* (Nelore breed) cattle, comparing it to the total metagenomic catalog. By focusing on the functionally active fraction of the microbiota, we identified microorganisms and enzymes directly linked to methane emissions and feed efficiency. The results revealed that microbial gene expression, rather than mere microbial presence, is a key determinant of fermentative processes in the rumen, offering new perspectives for methane mitigation strategies and improved feed efficiency in tropical production systems. This section contains transcriptions from the manuscript “Catalog of active prokaryotic genes from the ruminal microbiome of *Bos indicus* cattle: insights into methane emission and feed efficiency”, which has been submitted to the journal *Microbiome*.

Title: Catalog of active prokaryotic genes from the ruminal microbiome of *Bos indicus* cattle: insights into methane emission and feed efficiency

Juliana Virginio da Silva, Liliane Costa Conteville, Gabriel Alexander Colmenarez Pena, Aline Teixeira do Brasil Morais, Gerson Barreto Mourão, Luiz Lehmann Coutinho, Adhemar Zerlotini, Julio Cesar Palhares, Alexandre Berndt, Sergio Raposo de Medeiros, Bruno Gabriel Nascimento Andrade, LeLuo Guan, Luciana Correia de Almeida Regitano

3.1 Abstract

The rumen microbiome plays a critical role in ruminant nutrition and greenhouse gas emissions. Yet widely investigated, most studies have focused on *Bos taurus*, leaving a gap in knowledge regarding *Bos indicus*, predominant in tropical systems. Here, we constructed the Nelore Ruminal Prokaryotic Microbiome Gene Catalog (NRPMG) using metagenomic data collected from 52 Nelore bulls, and identified the actively expressed genes (aNRPMG) through metatranscriptomic profiling of the same rumen microbiome. In addition, we used sparse Partial Least Squares (sPLS) analysis to identify microbial genera and expressed enzymes-coding transcripts associated with residual methane emissions (RME) and residual feed intake (RFI). Functional and taxonomic characterization revealed a metabolically active microbiome dominated by *Bacteroidetes*, *Firmicutes*, and *Methanobacteriaceae* with gene expression enriched in pathways related to carbohydrate, energy, and amino acid metabolism. The active gene catalog showed high prevalence of CAZymes targeting plant cell wall polysaccharides, especially hemicelluloses. Complex enzymes–microbial networks linked to these traits modulate fermentation pathways and redox balance. Enzymes CE20,

GH51, GH105, GH2, and K00355, along with genera Monoglobus, Halosimplex, and Microcystis, emerged as potential indicators or modulators of host performance traits. This study provides a comprehensive and functionally informed resource for understanding the rumen microbiome of *Bos indicus*, underpinning targeted strategies to improve feed efficiency and reduce methane emissions in tropical cattle production.

Keywords
Feed efficiency, Metagenomics, Metatranscriptomics, Methane emission, Nelore, Rumen microbiome

3.2 Introduction

The rumen is a highly specialized microbial ecosystem that plays a pivotal role in the digestion of plant polysaccharides and the production of volatile fatty acids (VFAs), which can supply up to 80% of the energy requirements of ruminants (Sanjorjo et al., 2023). This complex community, mainly composed of bacteria and archaea, enables ruminants to convert otherwise indigestible fibers into absorbable nutrients, supporting both animal health and food production (Perez et al., 2024).

Within this community, bacteria dominate and play a central role in the breakdown of cellulose, hemicellulose, starch, proteins, and lipids and subsequently production of VFAs mainly acetate, propionate, and butyrate through microbial fermentation (Cammack et al., 2018). However, this fermentation process also generates gases such as hydrogen (H_2) and carbon dioxide (CO_2), which accumulate as a result of anaerobic metabolism (Cammack et al., 2018; Perez et al., 2024). Although methanogenic archaea represent only 1-4% of the microbial community (Neves et al., 2017; Conteville et al., 2023), they play a crucial role in consuming H_2 and CO_2 via the hydrogenotrophic pathway, or methylated compounds via the methylotrophic pathway to produce methane (CH_4). This activity helps to maintain a low partial pressure of hydrogen, an essential condition for sustained bacterial fermentation (McAllister et al., 2025).

The composition and activity of the rumen microbiome are influenced by many factors such as diet, host genetics and environmental conditions, and are central to the modulation of important host phenotypes including feed efficiency and enteric methane emission (Badhan et al., 2025). Feed efficiency reflects the animal's capacity to convert consumed feed into growth. A usual measure of feed efficiency is residual feed intake (RFI). Cattle with low-RFI are considered more efficient, as they consume less feed while achieving similar weight gains compared to their high-RFI counterparts (Basarab et al., 2013). Enteric methane, a potent greenhouse gas, is a byproduct of ruminal fermentation and accounts for 2-12% of gross energy intake loss (Hook et al., 2010). Globally, 40% of the anthropogenic

methane emissions originate from the agricultural sector (Saunois et al., 2025), with ruminants as the major contributors (Costa Jr et al., 2021; Saunois et al., 2025). Therefore, strategies targeting feed intake modulation and microbiome interactions are essential for production sustainability (Zhao et al., 2024). Nonetheless, the relationship between feed efficiency and methane emission intensity is multifactorial, shaped not only by feed intake but also by rumen microbiome composition and host physiology (Badhan et al., 2025).

Therefore, characterizing the composition, diversity, and metabolic functions of the microbial communities is essential to understand the mechanisms underlying the impact of the rumen microbiome on cattle phenotypes. However, information on the rumen microbiome of *Bos indicus*, particularly the Nelore breed that predominates in tropical beef production systems, remains limited, despite its physiological and metabolic particularities that may influence both microbial composition and function (Latham et al., 2018).

Our previous study has identified significant microbial taxa associated with diet and production phenotypes based on 16S rRNA gene (Andrade et al., 2022) and shotgun metagenomics profile (Conteville et al., 2023). Although these approaches have advanced our knowledge of microbial composition and functional potential, they cannot differentiate active from inactive microbes. In contrast, metatranscriptomics provides a dynamic perspective of the functional microbiota, capturing real-time gene expression and allowing the linkage of microbial activities with host traits such as methane emission and feed efficiency (Li et al., 2019). A prior study from our group characterized the Nelore rumen metatranscriptome profile relating diet and methane emission (Silva et al., 2025). However, integrative analyses combining metagenomic and metatranscriptomic data are crucial to connect genes and transcripts with phenotypic variation.

Here, we construct a gene catalog named Nelore Ruminal Prokaryotic Microbiome Genes (NRPMG) using metagenomic data from the ruminal content of Nelore bulls. In addition, to identify the expressed genes (active genes) within the NRPMG catalog referred to as the active NRPMG (aNRPMG) catalog, we conducted an integrative analysis with metatranscriptomic data from the ruminal content of the same animals. Our goals were to characterize the active ruminal microbiome of Nelore cattle, to identify microbial taxa, and metabolic functions associated with important traits for a sustainable livestock production. Together, this approach enhances our understanding of the functional ruminal microbiome and its role in shaping environmentally relevant traits.

3.3 Materials and methods

3.3.1 Animals and sample collection

All experimental procedures followed the Animal Welfare and Humane Slaughter guidelines and were approved by EMBRAPA Livestock Science Ethics Committee on Animal Experimentation, São Carlos, São Paulo, Brazil (Protocol No. 09/2016). The experiment was conducted in the confinement facilities of Embrapa Pecuária Sudeste, involving 52 non-castrated Nelore breed males born in 2014 and slaughtered in 2016. These animals were descendants of 28 commercial Nelore bulls, with an average of 1.78 offspring per bull.

Due to initial body weight heterogeneity, heavier and lighter animals were evenly allocated within each dietary group (conventional and by-product). The feedlot experiment lasted for 90 or 121 days, depending on the initial body weight. This included 10 days for animal adaptation to the feedlot, 29 days for heavy animals and 55 days for light animals in the growing phase, 51 days for heavy animals and 56 days for light animals in the finishing phase. The animals were sent to slaughter at 23-24 months of age after fasting from food and water for 16 hours, according to the current Brazilian Ministry of Agriculture, Livestock, and Food Supply (MAPA) regulations. Approximately 50 mL of ruminal content was collected immediately after slaughter and frozen in liquid nitrogen, and then stored at −80 °C until DNA and RNA extraction.

3.3.2 Phenotype data collection

Automatic feeding data were collected using GrowSafe Systems Ltd. (Airdrie, Alberta, Canada), and enteric methane emissions were recorded during the finishing period with the GreenFeed system (C-Lock Inc., Rapid City, SD, USA). Animals were weighed at the start and end of the feedlot period after a 16-hour fast, and every 28 days without fasting to monitor live weight gain. Dry Matter Intake (DMI, kg/d) was automatically recorded via GrowSafe System. Average Daily Gain (ADG, kg/d) was estimated by linear regression of body weight over time, as described previously by Andrade et al. (2022). Residual Feed Intake (RFI, kg/d) was calculated as the residuals from the regression of DMI on mid-test metabolic body weight ($BW^{0.75}$) and ADG (Kock et al., 1963). Residual Methane Emissions (RME, kg/d) were estimated from the regression of methane emissions on DMI (Herd et al., 2014; Donoghue et al., 2016), as described previously by Conteville et al. (2023). Correction models were applied to RFI and RME, including all animals, adjusting for contemporary groups (CG), which accounted for animal weight class (light vs. heavy) and slaughter date, as well as dietary group (conventional vs. by-product). Detailed information on the RME and RFI values corrected for individual animals is provided in Supplementary Table S1.

3.3.3 Metagenomics and Metatranscriptomics data

The metagenomic and metatranscriptomic data used in this study were obtained from rumen content collected from 52 animals, Nelore steers (*Bos indicus*). Both data were previously published by our group (Conteville et al., 2023; Silva et al., 2025) Additional methodological details are available in the respective publications. The metagenomes are available under BioProject ID PRJNA987743, and the metatranscriptomes under PRJNA1131826.

For the metagenomes, total DNA was extracted using the Quick-DNA™ Fecal/Soil Microbe Miniprep Kit (ZYMO Research Corp., Irvine, CA). Metagenomic libraries were constructed using the Illumina DNA Prep Kit and sequenced on an Illumina NextSeq platform (ESALQ Genomics Center, Piracicaba, SP, Brazil) using the NextSeq P3 flowcell for 300 cycles. Sequencing reads underwent trimming, quality filtering, and mapping to the host genome to remove contaminant sequences. In total, this process yielded approximately 2.67 billion high-quality metagenomic reads, across all samples.

For the metatranscriptomes, total RNA were extracted from the same rumen content samples using TRIzol reagent (Invitrogen, Carlsbad, CA, USA). Only RNA samples with an RNA Integrity Number (RIN) greater than 7.0 were retained for downstream analysis, resulting in the exclusion of two samples and a final dataset comprising 50 animals. Metatranscriptomic libraries were prepared using the Illumina Stranded Total RNA Prep with Ribo-Zero Plus Kit, which includes rRNA depletion, and sequenced on the Illumina NextSeq platform using two NextSeq P3 flowcells for 200 cycles. Reads were processed by trimming, filtering, host genome mapping, and removal of rRNA sequences. In total, this generated around 1.80 billion high-quality reads.

3.3.4 Generation of the gene catalog based on metagenomic data

The construction of the gene catalog was achieved by *de novo* assembly of shotgun metagenomic data. Each metagenome was independently assembled using MEGAHIT v1.2.9 (Li et al., 2015) with default parameters. Contigs shorter than 500 bp were filtered out using SeqKit v. 2.8.2 (Shen et al., 2024), via the seq subcommand designed for sequence transformation. To maximize the usage of sequencing reads and identify rare genes, metagenomic reads of all samples were mapped back to the assembled contigs with Bowtie 2 v2.3.4.1 (Langmead and Salzberg, 2012). Unassembled sequence reads were extracted using SAMtools v1.18 (Li et al., 2009) and BEDtools v2.31.0 (Quinlan and Hall, 2010). These reads were pooled and co-assembled with MEGAHIT v1.2.90 (Li et al., 2015) with default parameters. The host or other eukaryotes sequences were removed with Tiara v1.0.2 (Karlicki et al., 2022).

The resulting non-eukaryotic contigs were subsequently used for gene prediction with Prodigal v2.6.3 (Hyatt et al., 2010). Only complete genes, defined as those containing both start and stop codons, were retained for downstream analyses. CD-HIT v4.8.1 (Li and Godzik, 2006) was employed to cluster complete genes at the protein level minimizing redundancy. Genes were clustered at 100%, 95%, 90%, and 50% protein identity to align with the UniRef clustering model and generate the C100, C95, C90, and C50 clusters, respectively (Li et al., 2020; Chen et al., 2021; Lin et al., 2023). All gene clusters were aligned to the Uniprot TrEMBL database (https://www.uniprot.org/statistics/TrEMBL) to determine the number of known proteins (Chen et al., 2021). A summary of the methodological workflow can be found in Supplementary Figure 1.

3.3.5 Identification of active genes using metatranscriptomic data

Metatranscriptomic reads were aligned to the C95 cluster, designated Nelore Ruminal Prokaryotic Microbiome Genes (NRPMG), using BWA mem v0.7.17 (Li, 2013) with the parameters -a -M -Y -t 32. The alignments were filtered to retain only primary alignments (samtools view -ubh -F 0x900) with a minimum identity of 90%, following the pipeline available by New et al. (2022). Genes with less than 80% coverage of their length were excluded. Abundance normalization of each gene was performed using a modified reads per kilobase million (RPKM) method, which accounted for the total number of sequenced reads per sample rather than only the mapped reads, a more appropriate approach for microbiome studies (New et al., 2022). This process aimed to identify the active genes, constructing the active Nelore Ruminal Prokaryotic Microbiome Genes (aNRPMG). A summary of the methodological workflow can be found in Supplementary Figure 1.

Additionally, a prevalence analysis of the active genes was performed to identify those consistently present across the samples. Genes detected in at least 20% of the samples were retained to generate a subcatalog. Expression rates of the aNRPMG subcatalog were corrected using MMUPHin v. 1.22.0 (Meta-Analysis Methods with a Uniform Pipeline for Heterogeneity in microbiome studies) (Ma et al., 2022), to mitigate potential biases and technical variability introduced by confounding factors, contemporary group effects (weighing and slaughter groups) and dietary influences. The batch correction was performed using the adjust_batch model with default parameters. The methodological workflow was illustrated in Supplementary Figure 2.

The subcatalog was used for subsequent analysis, such as functional annotation and investigation of associations with traits of interest in livestock and environmental contexts, such as RME and RFI.

3.3.6 Taxonomic classification

The taxonomic classification of the NRPMG and aNRPMG was performed using Kraken2 v. 2.1.2 (Wood et al., 2019) with the options --paired --gzip-compressed --threads 24 --use-names --use-mpa-style and using the complete set of bacterial and archaeal in NCBI RefSeq database as reference. Taxonomic profiles were aggregated at the phylum, family, and genus levels for both bacteria and archaea.

In the aNRPMG subcatalog, genus expression levels were calculated as RPKMs based on the alignment of metatranscriptomic reads to the NRPMG catalog, by summing the expression of their constituent taxa. Active genera with relative abundance below 1% across all samples were removed using a custom R script. The methodological workflow was illustrated in Supplementary Figure 2.

3.3.7 Functional annotation

The putative amino acid sequences translated from the NRPMG catalog using Prodigal v2.6.3 (Hyatt et al., 2010) were aligned against proteins and domains in the eggNOG databases through eggnog-mapper v2.1.12 (Cantalapiedra et al., 2021). The output from eggNOG was further analyzed, and two functional categories were selected: COGs (Clusters of Orthologous Groups) and KOs (KEGG Orthologies). The protein sequences were also used for CAZymes (Carbohydrate-Active enZymes) annotation (Lombard et al., 2014) with the run_dbcan3 (Zheng et al., 2023), using as parameter --tools all. Additionally, CAZymes and their predicted substrates were identified through the --cgc_substrate option. Only CAZyme predictions supported by at least two out of the three methods were retained for downstream analysis, increasing confidence of the model. The method overview is shown in Supplementary Figure 2.

For each functional category, a hierarchical exploration was performed to better understand the activity of the ruminal microbiome. KOs were analyzed across multiple hierarchical levels, from broad functional classes (*e.g.,* metabolism, environmental information processing) to specific pathways and modules. Additionally, COGs were interpreted based on their single-level functional categories, such as energy production and conversion or carbohydrate transport and metabolism. CAZymes were segregated by families, including glycoside hydrolases (GHs), glycosyltransferases (GTs), polysaccharide lyases (PLs), carbohydrate esterases (CEs), auxiliary activities (AAs), and carbohydrate-binding modules (CBMs) (Lombard et al., 2025).

Regarding the aNRPMG subcatalog, the expression levels of COGs, KOs, and CAZymes were determined by calculating RPKM values based on the alignment of metatranscriptomic reads to the NRPMG catalog (Xie et al., 2021). RPKM values were first calculated for each contig. During the functional annotation step, contigs were assigned to a

functional identifier (COG, KO, or CAZymes). Then, the expression levels of each functional identifier were calculated by summing the RPKM values of all associated contigs (Li et al., 2014).

3.3.8 Association of biological datasets with methane emission and feed efficiency

Sparse Partial Least Squares (sPLS), implemented in the mixOmics R package v6.24.0 (Rohart et al., 2017), enables simultaneous variable selection across two datasets by applying LASSO penalization (Cao et al., 2008). In this exploratory analysis, original variables are projected onto latent components, each representing a weighted combination of selected variables, and correlations are approximated by the inner product of these components (Cao et al., 2008).

We used sPLS to link enzyme profiles and genus-level microbial dataset with phenotypic traits (RME and RFI). For enzyme data, sPLS1 evaluated associations between each trait separately, using absolute correlation thresholds of $|r| \geq 0.35$ for RME and $|r| \geq 0.20$ for RFI. For sPLS2, which assessed associations with both traits simultaneously, a single threshold of $|r| \geq 0.20$ was applied to identify enzymes-coding transcripts with joint effects. For genus-level microbial data, sPLS1 was applied separately to bacterial and archaeal datasets, using absolute correlation thresholds of $|r| \geq 0.2$ for RME and for RFI. Similarly, sPLS2 was applied separately to each dataset, using a single threshold of $|r| \geq 0.45$ to select genera associated with both traits. An overview diagram of the method used is presented in Supplementary Figure 2.

After selecting variables with sPLS1 and sPLS2 for enzyme and microbial genera, we performed Multiblock Partial Least Squares (MB-PLS) analyses separately for bacterial and archaeal datasets, using absolute correlation thresholds of $|r| \geq 0.60$ for bacteria, and $|r| \geq 0.50$ for archaea. MB-PLS integrates multiple datasets by projecting each block into latent components, allowing the identification of variables that jointly explain variation across datasets (Westerhuis et al., 1998). The resulting networks were visualized using the ggraph package v2.2.1 in R, and centrality measures (degree, betweenness, closeness, and eigenvector) were computed to identify key elements.

3.3.9 Validation between complete genes and active consensus sequences

The active consensus sequences were validated via subsampling approach using Cochran's sample size formula, adjusting for a finite population (Woolson et al., 1986). This formula accounts for population size and margin of error, providing a reliable estimate of the sample size needed. We applied Cochran's sample size formula using the following

parameters: a total of 71,217 genes, a 95% confidence level (Z = 1.96), with a margin of error of 5% (E = 0.05), and a proportion of 0.5 to represent the most conservative scenario. After adjusting for a finite number of genes, the required sample size was calculated as approximately 382 genes. Annotations from the eggNOG database were used to filter complete genes containing both Enzyme Commission (EC) numbers and KEGG Orthology (KO) identifiers, for well-characterized genes. From this filtered set, 400 genes were randomly selected to ensure comprehensive representation. For each selected gene, consensus sequences were generated. The gathered data was subsequently re-annotated using eggNOG to assess the consistency of functional assignments, with a particular emphasis on seed orthologs, EC numbers, and KO and COG identifiers. Finally, a confusion matrix was constructed to assess agreement between the annotations of complete genes (reference) and their corresponding consensus sequences (predicted) and the accuracy rate was calculated.

3.4 Results

3.4.1 Nelore Ruminal Prokaryotic Microbiome Genes (NRPMG)

From the 52 metagenomes derived from the ruminal content of Nelore cattle, approximately 16.34 million contigs were obtained from the single assembly, while the co-assembly of unassembled reads generated approximately 7.74 million contigs. A total of 11.23 million complete genes (46.79%) were retained for downstream analyses following the removal of sequences attributed to the host, other eukaryotes, and incomplete genes.

These complete genes were clustered at the protein level at 100%, 95%, 90%, and 50% protein identity, generating 7,513,072 (C100), 5,226,749 (C95), 4,532,296 (C90), and 1,737,222 (C50) clustered non-redundant sequences, respectively (Supplementary Figure 1). The numbers of known proteins and taxa to each catalog gene were 2,528,155 and 1,794,284 (C100), 2,411,269 and 1,108,586 (C95), 2,309,931 and 896,421 (C90), and 654,273 and 207,323 (C50), respectively (Supplementary Figure 1). Although the non-redundant protein sequence numbers in C95 and C90 were lower than C100 (69.6% and 60.3%, respectively), the reduction in known proteins and taxa was less pronounced (95.4% and 91.4% for protein, 61.8% and 59% for taxa). Therefore, C95 was used for downstream comparison and annotation analysis, resulting in the construction of the catalog of Nelore Ruminal Prokaryotic Microbiome Genes (NRPMG).

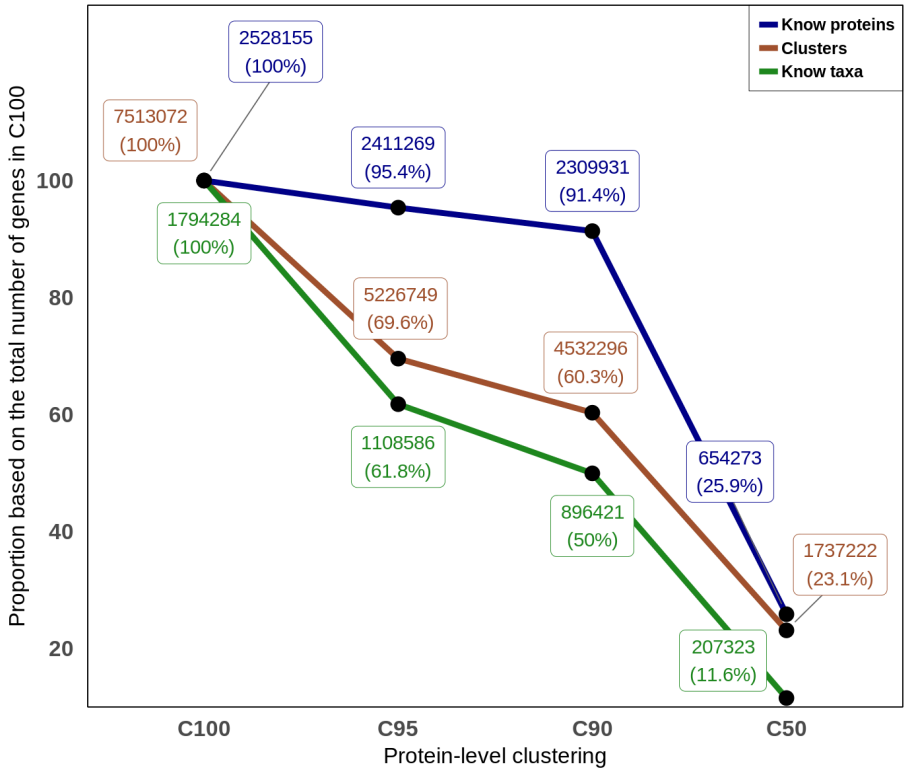

Supplementary Figure 1: Numbers of predicted genes, known proteins and taxa of four ruminal prokaryotic microbiome gene catalogs based on sequence similarity within clusters (100 to 50%). The annotation of known proteins was performed by aligning the protein sequences to the Uniprot TrEMBL. Taxonomic annotation was performed by Kraken2. The value next to the dot indicates the number of each item, and the values in parentheses indicate the proportion of each item in the total number of genes in the C100.

Taxonomic classification using Kraken2 revealed that the ruminal microbiome of Brazilian Nelore was predominantly bacterial, accounting for 96.02% of the classified genes, while archaeal genes represented 3.98%. The most abundant bacterial phyla were *Proteobacteria* (28.28%), *Firmicutes* (28.10%), *Bacteroidetes* (20.41%), and *Actinobacteria* (15.70%) (Figure 1a). Within the archaeal domain, 92.47% of the complete genes were classified as *Euryarchaeota* followed by *Candidatus Thermoplasmatota* (4.05%) and *Crenarchaeota* (2.11%) (Figure 1b). At the family level, within the bacterial domain, *Prevotellaceae* (10.39%), *Oscillospiraceae* (7.24%), *Lachnospiraceae* (7.21%), *Streptomycetaceae* (3.61%), and *Bacteroidaceae* (2.94%) were the most prominent (Figure 1c). Within the archaeal domain, the predominant families were *Methanobacteriaceae* (80.06%), *Candidatus Methanomethylophilaceae* (11.52%) and *Methanosarcinaceae* (1.83%) (Figure 1d). Details of the taxonomic classification for the NRPMG are available in Supplementary Table S2.

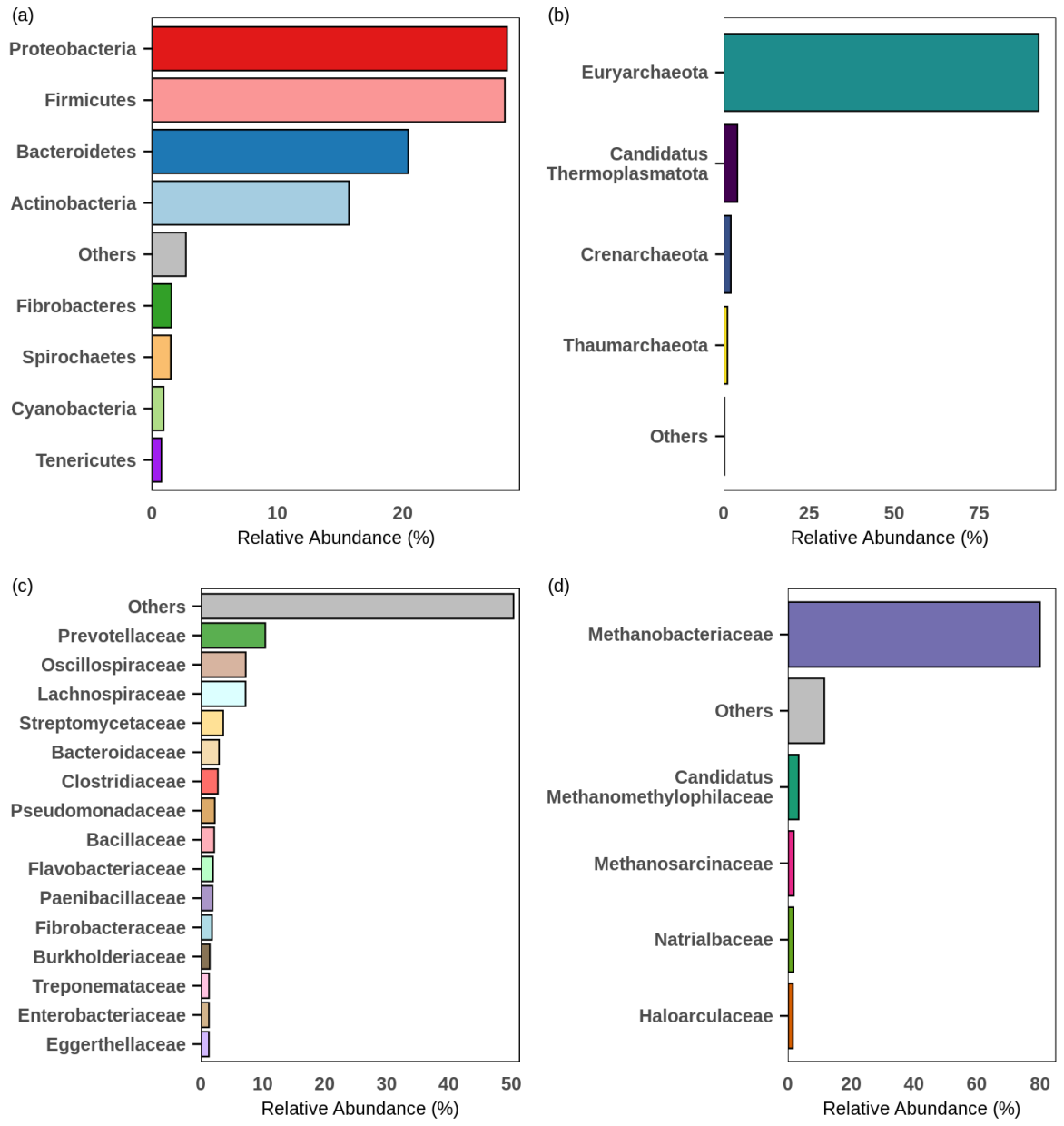

Figure 1. Taxonomic composition of the Nelore Ruminal Prokaryotic Microbiome Genes (NRPMG) catalog. Relative abundance of dominant (a) bacterial phyla (mean abundance >1%), (b) archaeal phyla (mean abundance >1%), (c) bacterial families (mean abundance >1%), and (d) archaeal families (mean abundance >1%).

The functional annotation results using the EggNOG database revealed that approximately 2.95 million (56.60%) were functionally annotated for at least one of the following databases or classification systems: COG (56.9%), KEGG (33.2%), EC (16.9%), and CAZy (1%) (Figure 2a). COG and KEGG had the highest number of unique and shared annotations (Supplementary Figure 2), highlighting their broad functional coverage and complementarity. CAZy showed limited annotations in the EggNOG database, consistent

with its specificity for carbohydrate metabolism enzymes. Thus, COG and KEGG were prioritized for further analyses. Within these, the most abundant metabolic categories were Carbohydrate (22.66%), Amino Acid (18.93%), Energy (12.07%), Coenzyme/Vitamin (11.68%), and Nucleotide metabolism (9.17%) (Figure 2b). Among non-metabolic functions (Figure 2c), the most represented were Genetic Information Processing (38.54%), Uncharacterized Functions (25.54%), and Cell Signaling and Transport (20.13%). Details of the functional classification by EggNOG for the NRPMG are available in Supplementary Table S3.

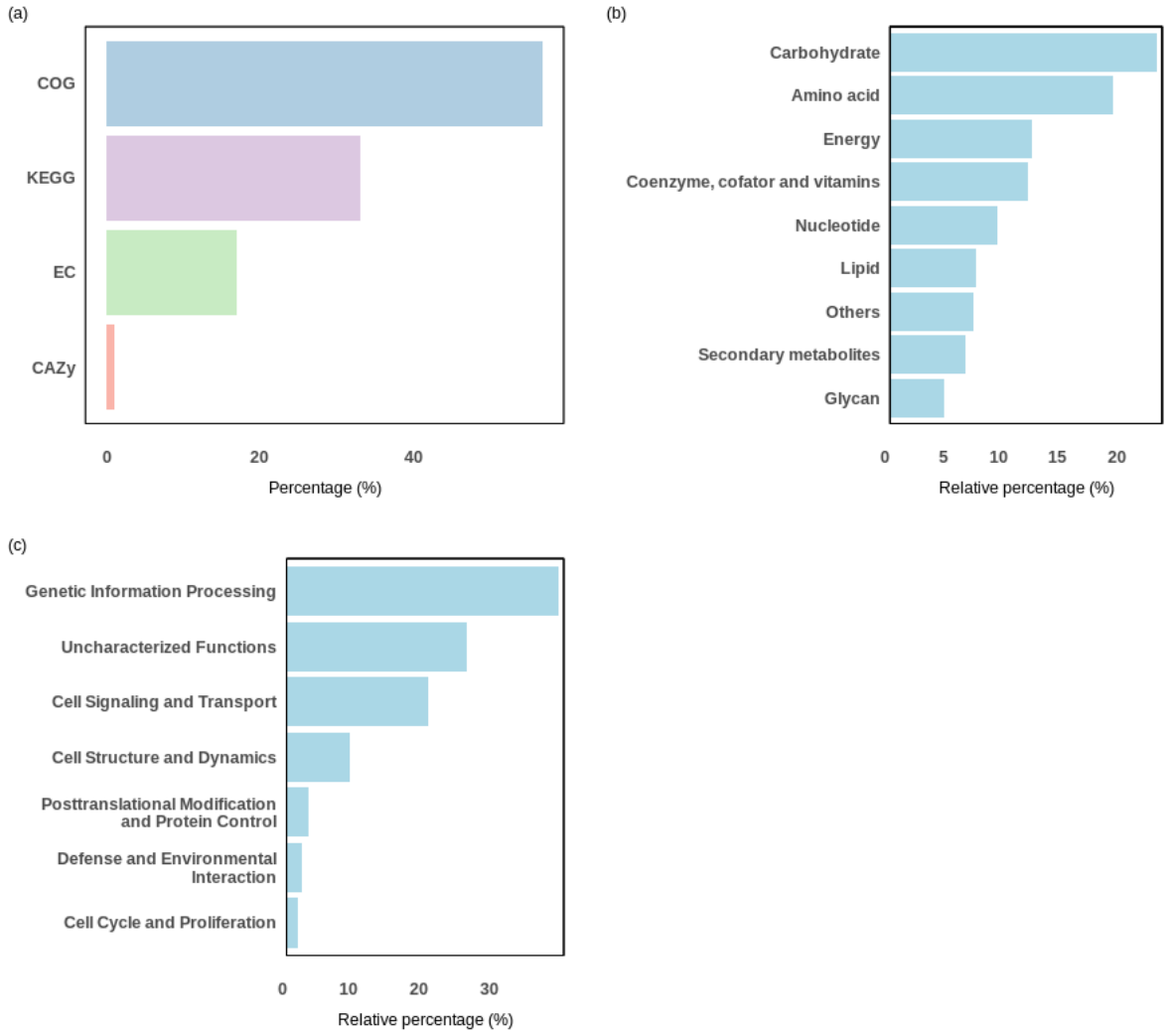

Figure 2: Functional annotation of active genes from the Nelore Ruminal Prokaryotic Microbiome Genes (NRPMG) catalog based on the EggNOG database. (a) Percentage of annotated genes assigned to COG, KEGG, EC, and CAZy (b) Abundances (%) of microbial metabolic functions based on COG categories and the KEGG hierarchy. (c) Abundances of microbial non-metabolic functions based on COG categories and the KEGG hierarchy.

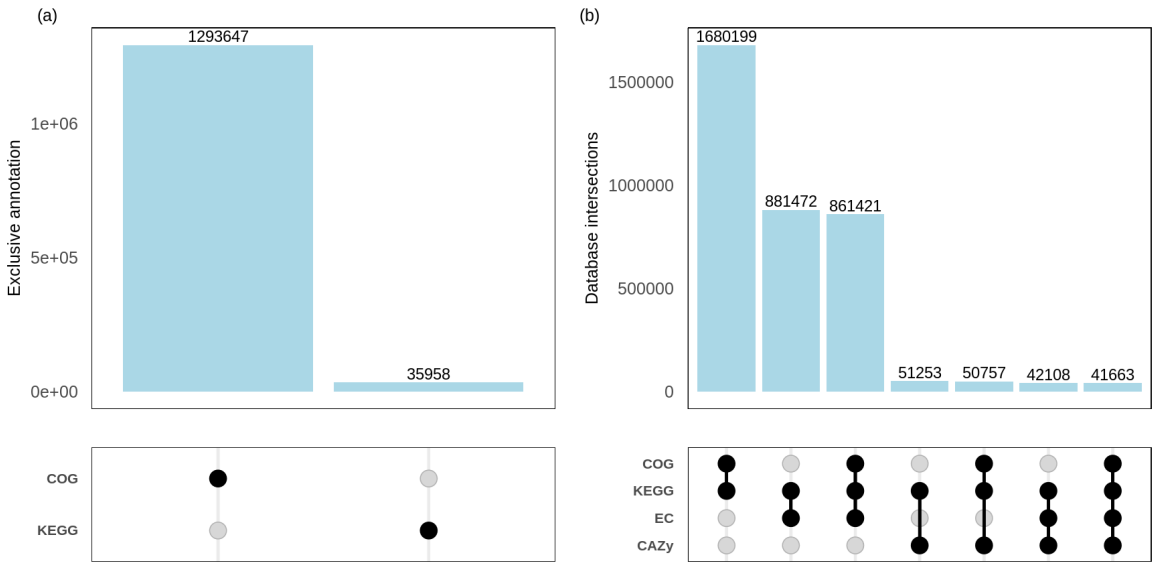

Supplementary Figure 2: Functional annotation of genes from the Nelore Ruminal Prokaryotic Microbiome Genes (NRPMG) based on eggNOG. (a) Number of exclusive annotations. (b) Shared annotations across COG, KEGG, EC, and CAZyme databases. Bars indicate the number of annotations present in each database combination. The bottom panel shows the specific combinations included in each intersection, with filled circles representing database presence.

The analysis of CAZymes revealed a large profile dominated by the glycoside hydrolases (GH) (47.17%) and glycosyltransferases (GT) (36.56%) families. These were followed by the carbohydrate esterases (CE) (9.01%), carbohydrate-binding modules (CBM) (5.36%), and polysaccharide lyases (PL) (1.80%) families, while the auxiliary activities (AA) family was the least represented, accounting for only 0.10% of the genes identified (Figure 3a). Regarding the substrates (Figure 3b-c), the most abundant was *cell wall polysaccharides*, which is related to carbohydrate degradation (58.21%). Within this category, the most prominent substrates were hemicellulose-derived polysaccharides from the plant cell wall, such as xylan (13.04%), arabinan (7.07%), and beta-glucan (6.43%). Additionally, the *Other* category (13.53%) was the second most represented, mainly comprising enzymes for polyphenols (4.86%) and alpha-glucans (2.91%) degradation. Among storage carbohydrates (10.03%) enzymes related to the degradation of starch (4.03%), trehalose (3.52%), and glycogen (2.49%) were also observed. Details of the functional classification by CAZymes for the NRPMG are available in Supplementary Table S3.

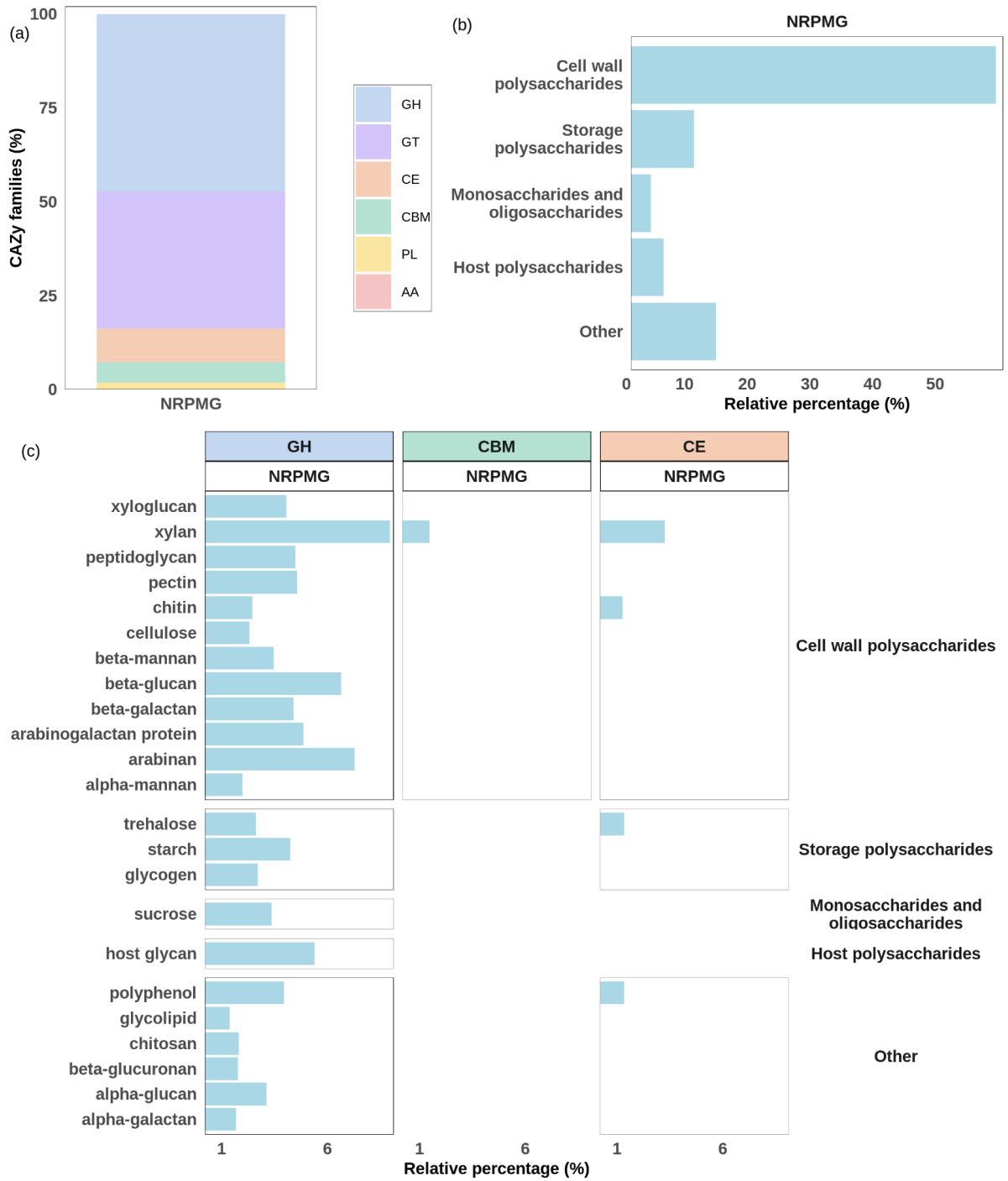

Figure 3. Classification of carbohydrate-active enzyme (CAZyme) families in the Nelore Ruminal Prokaryotic Microbiome Genes (NRPMG) catalog. (a) Relative abundance of CAZyme family classes, including glycoside hydrolases (GH), glycosyltransferases (GT), carbohydrate esterases (CE), carbohydrate-binding modules (CBM), polysaccharide lyases (PL), and auxiliary activities (AA). (b) Relative abundance of functional categories based on substrate type. (c) Detailed breakdown of CAZymes families by substrate specificity, highlighting the contribution of individual enzymes in degrading major carbohydrate groups.

3.4.2 Validation between complete genes and active consensus sequences

In order to generate a subcatalog of active genes, metatranscriptomic reads were mapped to the NRPMG reference catalog. From these mappings, we derived consensus sequences representing the expressed genes. We then compared the functional annotations of these consensus sequences with those of their corresponding complete genes in the NRPMG catalog. Confusion matrices for KEGG Orthology (KO) and Clusters of Orthologous Groups (COG) (Supplementary Figure 3) were used to evaluate whether annotation was consistent. Accuracy reached 92.73% for KO (Supplementary Figure 3a) and 98.16% for COG (Supplementary Figure 3b), indicating high concordance and supporting the use of full-length reference genes to reliably capture functional activity.

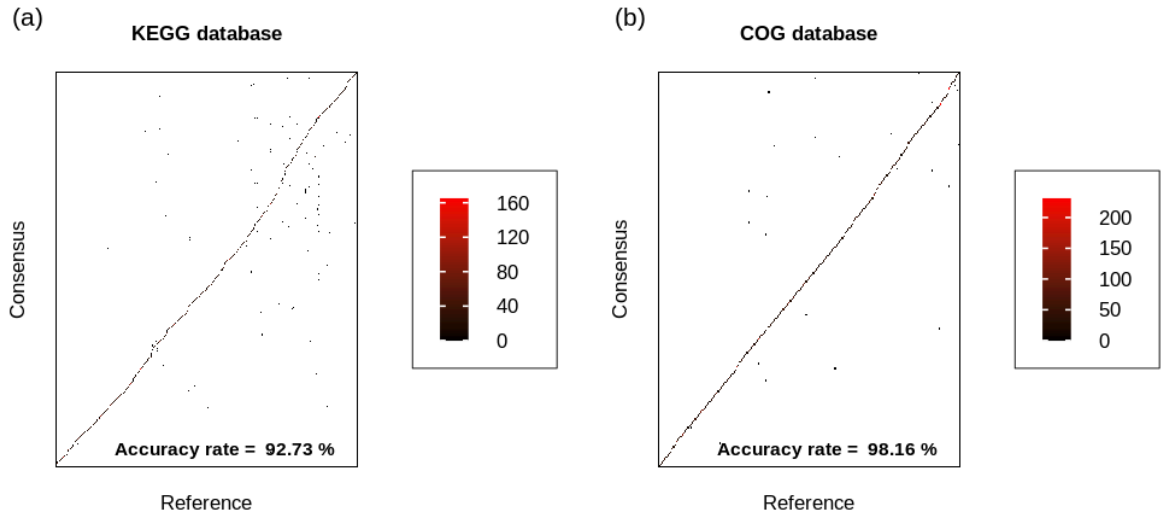

Supplementary Figure 3. Confusion matrices evaluating the agreement between the functional annotations of complete genes (reference) and their respective metatranscriptome consensus sequences, based on two functional databases: (a) KEGG Orthology (KO) Database and (b) Clusters of Orthologous Groups (COG). The density of points along the diagonal reflects the degree of agreement between predicted and reference categories, with higher densities indicating stronger concordance.

3.4.3 Active Nelore Ruminal Prokaryotic Microbiome Genes

After filtering primary alignments and applying criteria of a minimum identity of 90% and at least 80% coverage, the alignment with the metatranscriptomic reads identified 624,925 active genes in the NRPMG. Moreover, a prevalence (20%) analysis was performed resulting in a subcatalog, composed of 71,217 active genes, representing the active Nelore Ruminal Prokaryotic Microbiome Genes (aNRPMG) set. This subcatalog was used for

taxonomic classification, functional annotation analyses and associations with traits of interest, such as RME and RFI.

The taxonomic profile consisted of 93.93% Bacteria and 6.06% Archaea. These values correspond to 1.79% and 0.11%, respectively, of the classified taxonomically gene content in the NRPMG catalog. The most abundant active bacterial phyla were *Bacteroidetes* (32.45%), *Firmicutes* (31.23%), *Proteobacteria* (18.57%), *Spirochaetes* (6%) and, *Actinobacteria* (4.47%) (Figure 4a). Within the archaeal domain, the predominant phyla were *Euryarchaeota* (80.56%) followed by *Candidatus Thermoplasmatota* (13.24%), *Thaumarchaeota* (3.06%) and *Crenarchaeota* (3.06%) (Figure 4b). At the family level, within the bacterial domain (Figure 4c), *Prevotellaceae* (15.86%), *Lachnospiraceae* (7.88%), *Oscillospiraceae* (6.77%), *Treponemataceae* (5.84%), *Bacteroidaceae* (5.18%), and *Clostridiaceae* (4.35%) were the most active. Within the archaeal domain (Figure 4d), the predominant families were *Methanobacteriaceae* (73.48%), *Candidatus Methanomethylophilaceae* (10.53%) and *Methanomassiliicoccaceae* (2.61%). Also, figure 4 illustrates how these values relate to the total taxonomically classified gene content in the NRPMG catalog. Details of the unfiltered taxonomic classification for the aNRPMG are available in Supplementary Table S2.

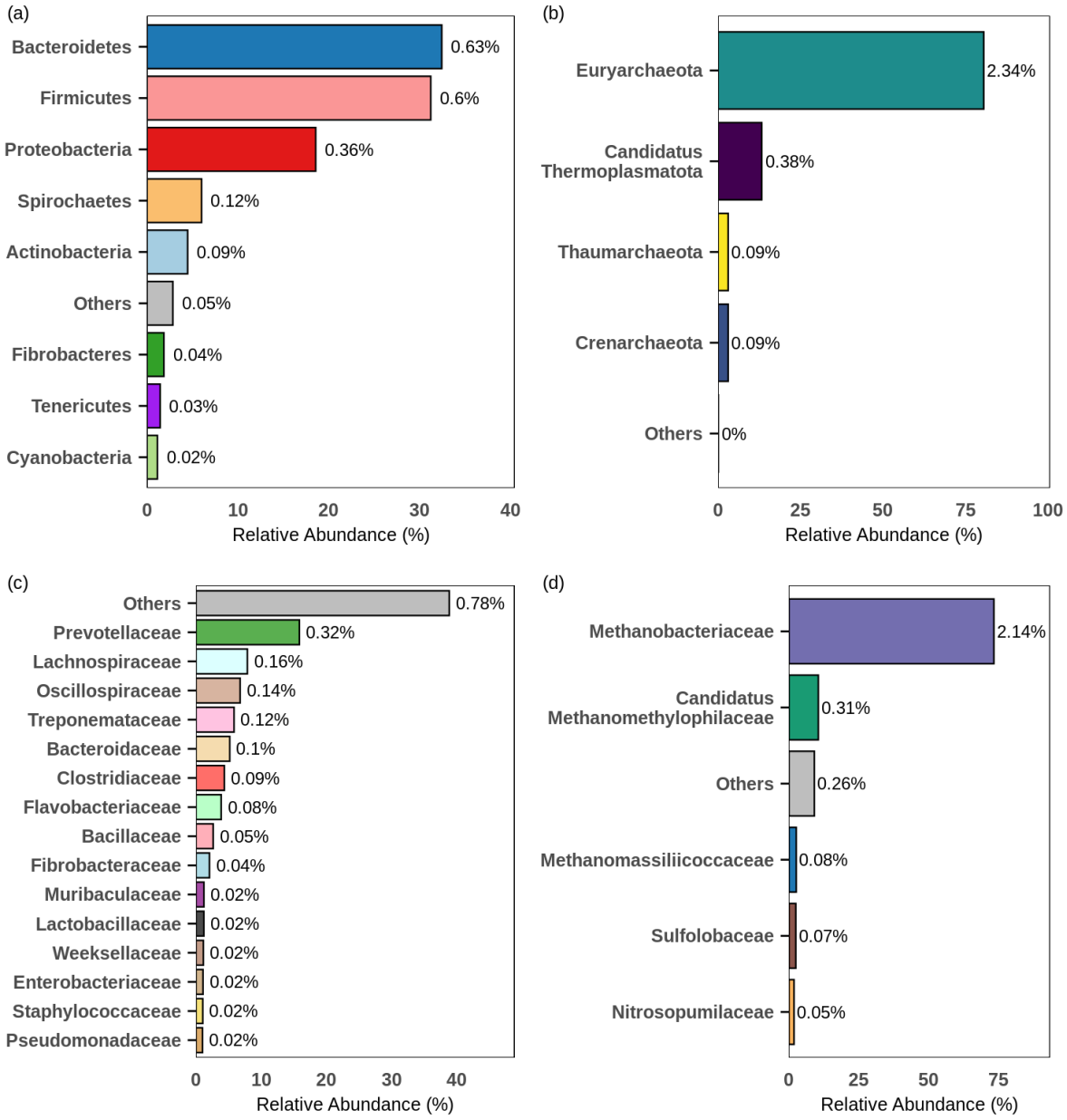

Figure 4. Taxonomic composition of the active Nelore Ruminal Prokaryotic Microbiome Genes (aNRPMG) catalog. Relative abundance of dominant (a) bacterial phyla (mean abundance >1%), (b) archaeal phyla (mean abundance >1%), (c) bacterial families (mean abundance >1%), (d) archaeal families (mean abundance >1%). The values on the x-axis represent the abundance of taxonomic classification in the aNRPMG while the panel values show their relative contribution to the total taxonomically classified gene content in the NRPMG catalog.

The functional annotation using the EggNOG database revealed 41,437 (58.18%) active genes functionally annotated for at least one of the following categories: COG (58.3%), KEGG (50.4%), EC (19.3%), and CAZy (1.6%) (Figure 5a). The aNRPMG

subcatalog accounted for 1.4% of total annotated genes in the NRPMG, and for 0.82%, 0.71%, 0.27%, and 0.022% of the annotated genes in the COG, KEGG, EC, and CAZy categories, respectively.

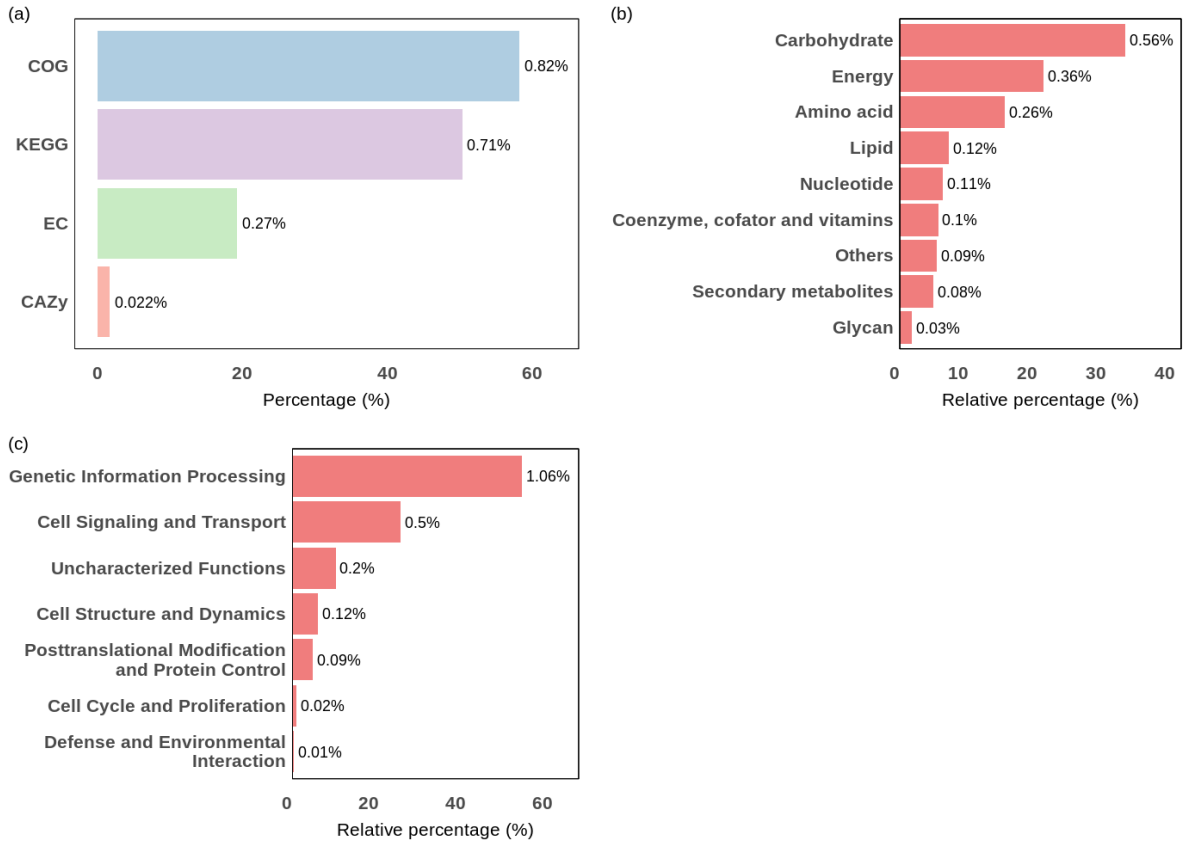

Figure 5. Functional annotation of active from the Nelore ruminal prokaryotic microbiome (aNRPMG) based on the EggNOG database (a) Annotated genes were assigned to COG, KEGG, EC, and CAZy categories. (b) Relative abundances of microbial metabolic functions based on COG categories and the KEGG hierarchy. (c) Relative abundances of microbial non-metabolic functions based on COG categories and the KEGG hierarchy. The values on the x-axis represent the abundance of functional categories in the aNRPMG while the panel values show their contribution to the total functionally classified gene content in the NRPMG catalog.

According to COG and KEGG functional annotation, the most active metabolic categories were Carbohydrate (32.74%), Energy (20.88%), Amino Acid (15.24%), Lipid (7.19%), and Nucleotide metabolism (6.22%) (Figure 5b). Compared to NRPMG, these categories accounted for 0.56%, 0.36%, 0.26%, 0.12%, and 0.11% of the annotated genes, respectively (Figure 5b). Among the non-metabolism-related functions, the most active categories were Genetic Information Processing (52.85%), Cell Signaling and Transport (25.04%), Uncharacterized Functions (9.99%), Cell Structure and Dynamics (5.91%) and, Posttranslational modification and protein control (4.73%) (Figure 5c). Compared to

NRPMG, these categories accounted for 1.06%, 0.5%, 0.2%, 0.12%, and 0.09% of the annotated genes, respectively (Figure 5c). Details on the unfiltered functional classification by EggNOG for the aNRPMG are available in Supplementary Table S3.

Considering the CAZymes categories (Figure 6) the GH family was the most abundant, comprising 60.11% of the active genes. This is followed by the CBM (14.00%), CE (10.43%), GT (9.90%), and PL (5.37%) families (Figure 6a). Compared to NRPMG, these families accounted for 1.08%, 0.25%, 0.19%, 0.18%, and 0.09% of the annotated genes by CAZymes, respectively. In the substrates categories, which are shown in Figure 6b, cell wall polysaccharides were the most abundant (67.21%), with a notable predominance of hemicellulose components such as xylan (19.87%) and beta-glucan (13.90%), followed by cellulose (7.93%) and pectin (3.71%). Additionally, enzymes related to chitin degradation were detected in low abundance (1.26%). In the Other carbohydrates category (12.48%), represented in Figure 6c, the main enzymes were alpha-glucan (5.06%), chitosan (3.71%), and glycolipids (3.71%). As for storage carbohydrates, the active fraction showed a functional convergence toward the preferential degradation of starch (6.14%) (Figure 6c). Details on the functional classification by CAZymes for the aNRPMG are available in Supplementary Table S3.

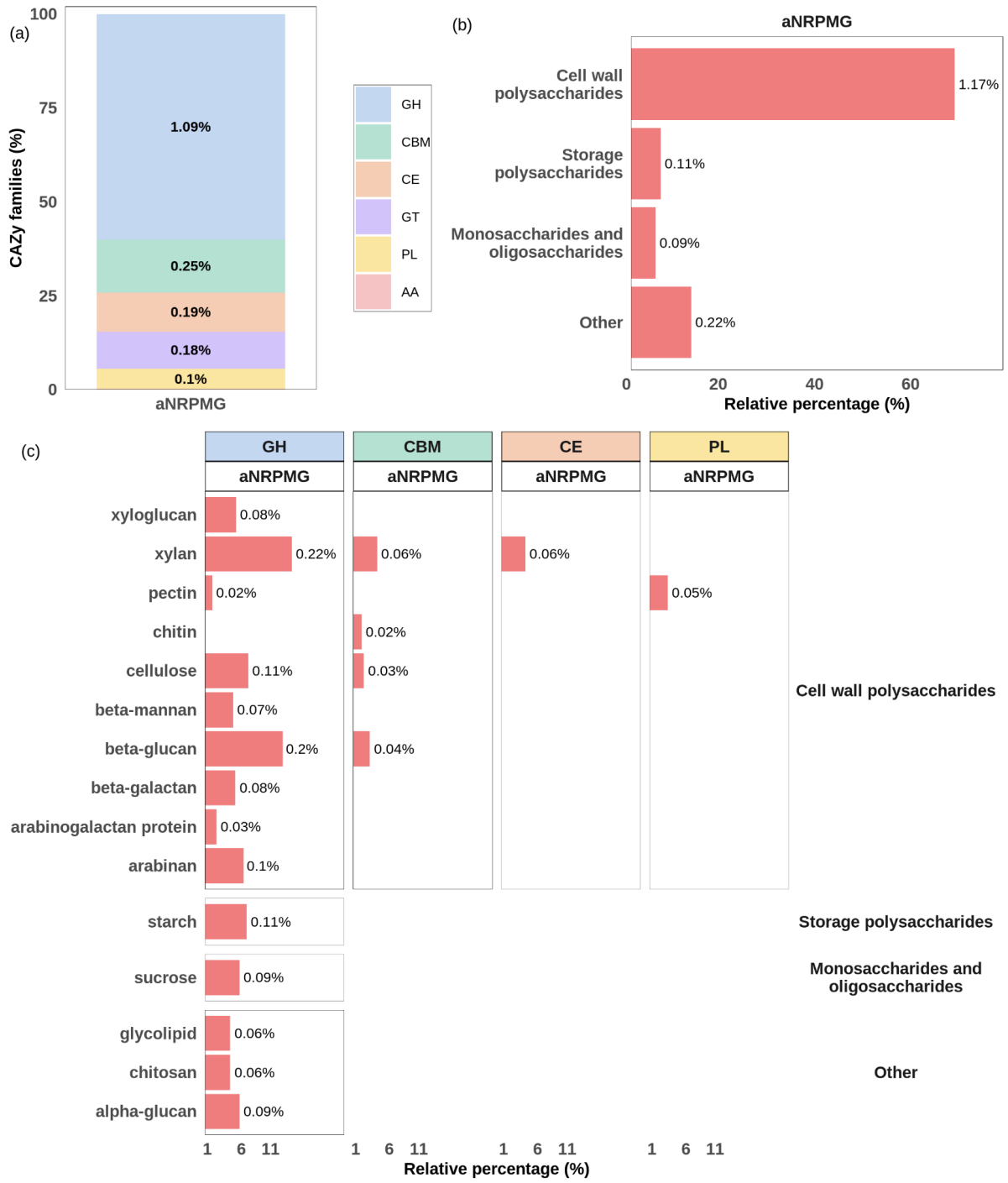

Figure 6. Functional classification of CAZy families in the active Nelore Ruminal Prokaryotic Microbiome gene (aNRPMG) subcatalog. (a) Distribution of CAZymes family classes, showing the relative abundance of glycoside hydrolases (GH), glycosyltransferases (GT), carbohydrate esterases (CE), carbohydrate-binding modules (CBM), polysaccharide lyases (PL), and auxiliary activities (AA). (b) Functional categorization based on substrate type. (c) Detailed breakdown of Cazyme families by substrate specificity, highlighting the contribution of individual enzymes to the degradation of major carbohydrate groups. The values on the

x-axis represent the abundance of CAZymes families in the aNRPMG while the panel values show their contribution to the total CAZymes classified content in the NRPMG catalog.

3.4.4 Association between bacterial genera and RME and RFI

We conducted an exploratory analysis seeking for the profile of microbial genera that could influence methane production and feed efficiency. To estimate bacterial and archaeal expression levels, RPKM values of all contigs assigned to each genus were summed, as detailed in Supplementary Table S4.

Therefore, we used the sPLS1 approach to examine the associations between bacterial genera and the phenotypic traits RME and RFI, separately. Here, we will focus on the selected variables filtered with absolute correlations greater than 0.2. Among the selected features, bacterial genera *Aquirufa*, *Mycoplasmopsis*, and *Listeria* showed positive correlations with RME, whereas *Microcystis*, *Sedimentisphaera*, and *Aneurinibacillus* were negatively correlated (Figure 7a). Within the archaeal domain, *Nitrosopumilus* was positively associated with RME, while *Halosimplex* was negatively associated (Figure 8a). The complete list of correlation values is provided in Supplementary Table S5.

In the sPLS1 model relating bacterial genera to the RFI trait, positive correlations with RFI were observed for *Hathewaya*, *Calothrix*, *Sedimentisphaera*, and *Microcystis* (Figure 7b). Considering the archaeal domain, *Halosimplex* showed a positive association, whereas *Metallosphaera* and *Promethearchaeum* were negatively associated (Figure 8b). The complete list of correlation values is provided in Supplementary Table S5.

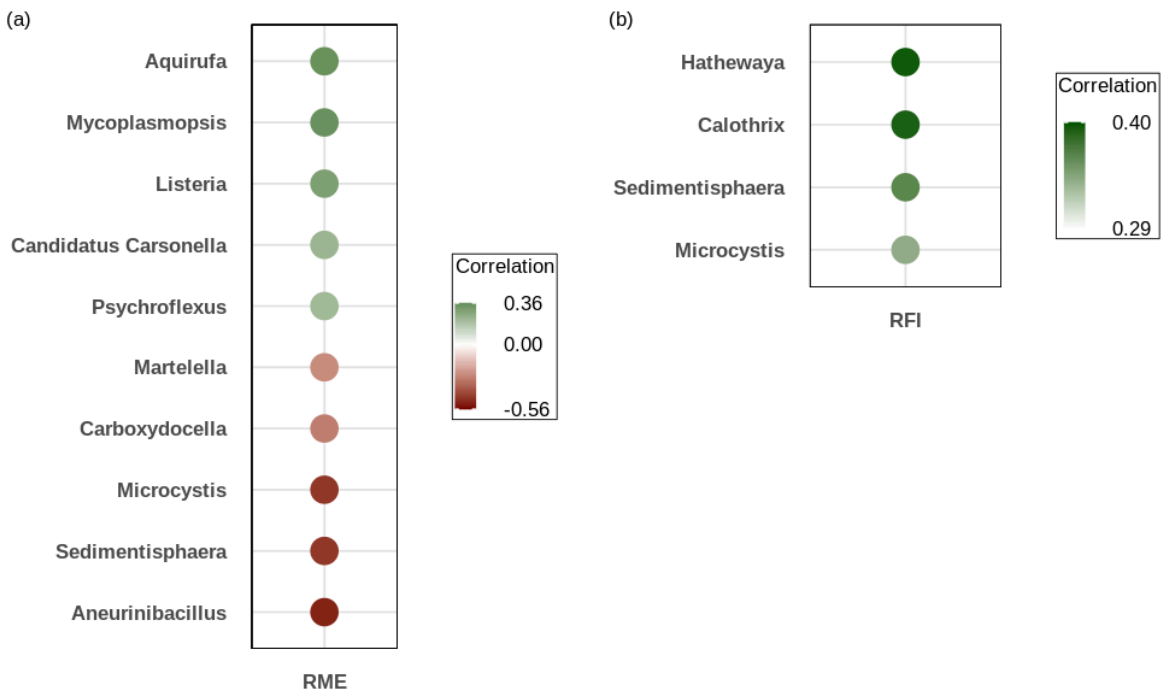

Figure 7. Bacterial genera from Nelore rumen correlated with (a) residual methane emission (RME) and (b) residual feed intake (RFI) traits using sparse Partial Least Squares 1 (sPLS1) and filtered using absolute value cutoffs of ≥ 0.20 for RME and for RFI. Positive correlations were shown in green, and negative in red.

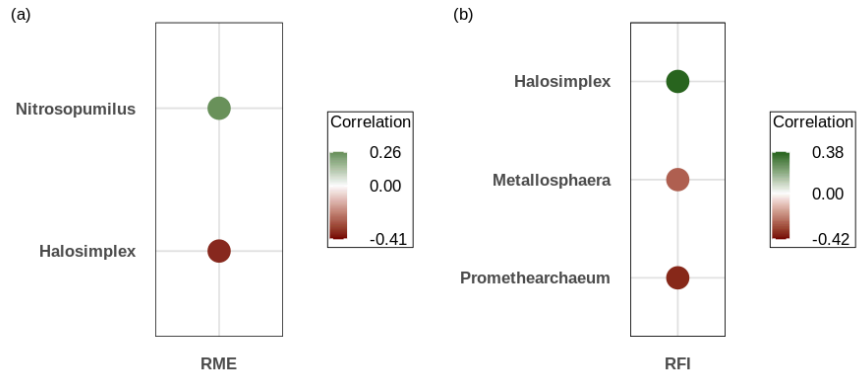

Figure 8. Archaeal genera from Nelore rumen correlated with (a) residual methane emission (RME) and (b) residual feed intake (RFI) traits using sparse Partial Least Squares 1 (sPLS1) and filtered using absolute value cutoffs of ≥ 0.20 for RME and for RFI. Positive correlations were shown in green, and negative in red.

The second association was performed to explore whether microbial taxa could influence both methane production and feed efficiency. Therefore, we applied the sPLS2 approach to identify bacterial genera associated with residual methane emissions (RME) and residual feed intake (RFI) simultaneously. The complete list of correlation values is provided in Supplementary Table S5. In total, 16 bacterial genera correlated with both RME and RFI traits, while eight genera exhibited contrasting association patterns with the two

traits (Figure 9a). For instance, *Sedimentisphaera*, *Microcystis,* and *Aneurinibacillus* showed strong negative correlations with RME and strong positive correlation with RFI. Also, *Monoglobus*, *Egibacter* and *Cronobacter* showed negative correlation with both traits. Conversely, genera such as *Metamycoplasma*, *Listeria*, *Chromobacterium*, and *Amniculibacterium* were positively correlated with both RME and RFI. In the archaeal domain, the genus Picrophilus was positively correlated with both RME and RFI, while Halosimplex was positively correlated with RFI and negatively with RME (Figure 9b).

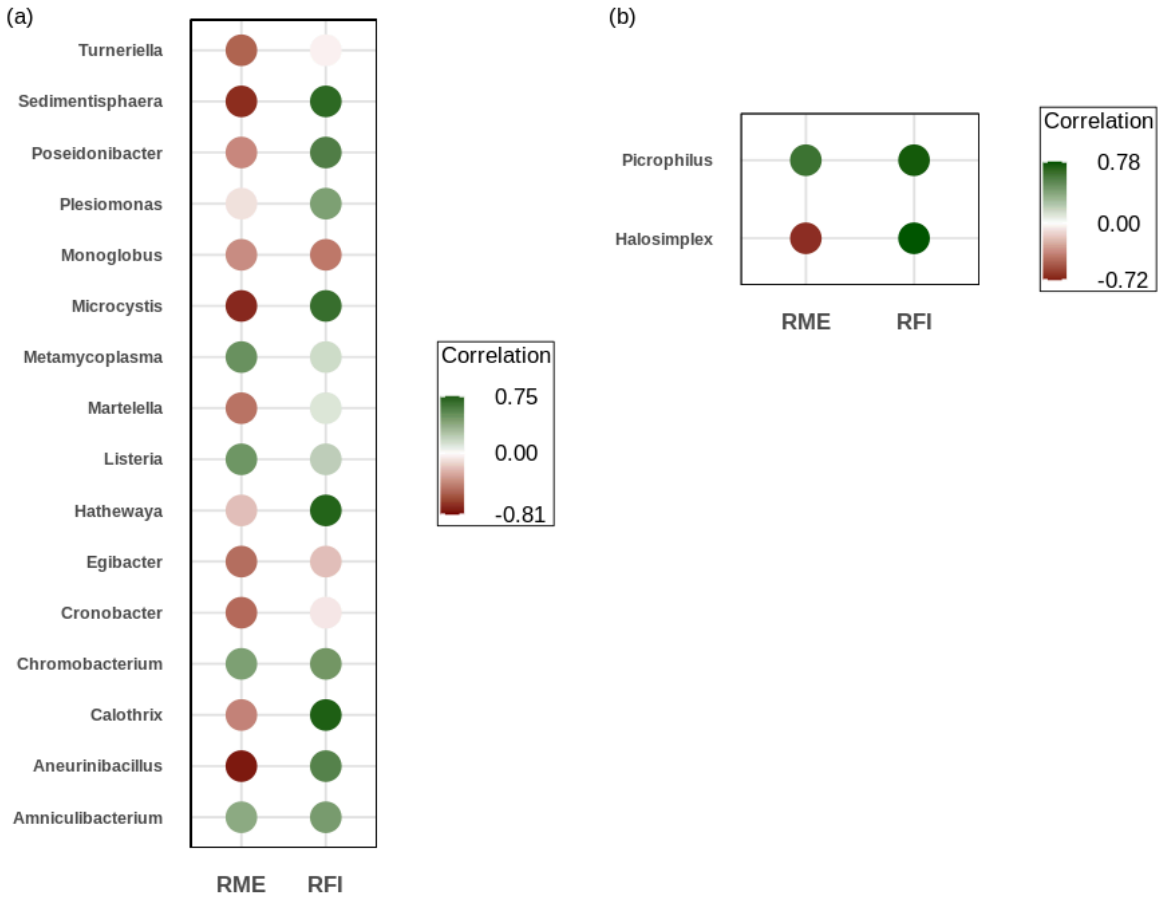

Figure 9. Microbial genera from Nelore rumen correlated with both residual methane emissions (RME) and residual feed intake (RFI) using the sparse Partial Least Squares 2 (sPLS2) approach and filtered with an absolute value cutoff of ≥ 0.45. (a) Bacterial genera (b) Archaeal genera. Positive correlations are shown in green, and negative in red.

3.4.5 Association between enzymes-coding transcripts and the phenotypic traits RME and RFI

Here we extended the analysis applied to taxonomical classification to examine correlations between the expression of enzymes-coding transcripts and the phenotypic traits RME and RFI. To estimate expression levels, RPKM values of all contigs associated with each functional identifier were summed, as detailed in Supplementary Table S4. As

illustrated in the Figure 10a, 31 enzymes were correlated with residual methane emission and, among them, eight showed positive correlations and 23 showed negative correlations (greater than $|r| \geq 0.35$). Considering feed efficiency, nine enzymes were associated with RFI, five positively and four negatively (Figure 10b; correlations greater than $|r| \geq 0.2$). The complete list of correlation values is provided in Supplementary Table S6.

The enzymes with positive correlations with RME were maltase-glucoamylase (K12407), homospermidine synthase (K00808), glucosamine-phosphate N-acetyltransferase (K00621), mannose-6-phosphate isomerase (COG0662), (R)-2-hydroxyglutarate-pyruvate transhydrogenase (K21618), 2-phosphosulfolactate phosphatase (K05799 and COG2045), and GH13_e193. Among the enzymes negatively correlated with RME, were GH3_e10, CE20_e40, GH130, GH105_e41, PL1_e77, 2-keto-4-pentenoate hydratase/2-oxohepta-3-ene-1,7-dioic acid hydratase (COG0197), and imidazoleglycerol-phosphate synthase subunit HisH (K02501 and COG0118).

The enzymes positively correlated with RFI were Isoaspartyl peptidase or L-asparaginase (COG1446), SH3-like domain (COG3807), CBM63_e6 and GH24_e226. The enzymes negatively correlated with RFI were Phosphoribosyl-AMP cyclohydrolase (K01496), GH13_14, Activator of 2-hydroxyglutaryl-CoA dehydratase (COG1924), and CO dehydrogenase/acetyl-CoA synthase (COG1614).

Figure 10: Enzymes-coding transcripts from the Nelore rumen microbiota with transcript abundance correlated with (a) residual methane emission (RME) and (b) residual feed intake (RFI) identified using the sparse Partial Least Squares 1 (sPLS1) Correlations were filtered using absolute value cutoffs of ≥ 0.35 for RME and ≥ 0.20 for RFI. Positive correlations are shown in green, negative correlations in red.

In addition, similarly to the analysis of taxa, we also applied the sPLS2 method to identify enzymes-coding transcripts that presented correlation with RFI and RME ($|r| \geq 0.2$). The complete list of correlation values is provided in Supplementary Table S6. Nineteen enzymes were significantly associated with both traits (Figure 11). Among them, those negatively correlated with RME and RFI were of particular interest, as they contribute simultaneously to reducing methane emissions and improving feed efficiency. This group includes Adenosine deaminase (K19572), GH3_e10, GH18_e118, and CE20_e40. In contrast, enzymes positively correlated with both traits were linked to increased methane emissions and reduced feed efficiency, such as Glucosamine-phosphate N-acetyltransferase (K00621), GMP reductase (K00364), Isoaspartyl peptidase or L-asparaginase (COG1446), Prephenate dehydrogenase (COG0287), and Hypoxanthine phosphoribosyltransferase

(COG2236). Other enzymes displayed opposing associations with the two traits. For example, NAD(P)H dehydrogenase (quinone) (K00355), NADP-dependent 3-hydroxy acid dehydrogenase (COG4221), SH3-like domain (COG3807), Phosphotransferase system cellobiose-specific component IIC (COG1455), as well as GH3_e10, GH24_e266, GH18_e118, GH15_e31, CE20_e40, CBM63_e6, and CBM50_e619, were associated with lower methane emissions but also with reduced feed efficiency.

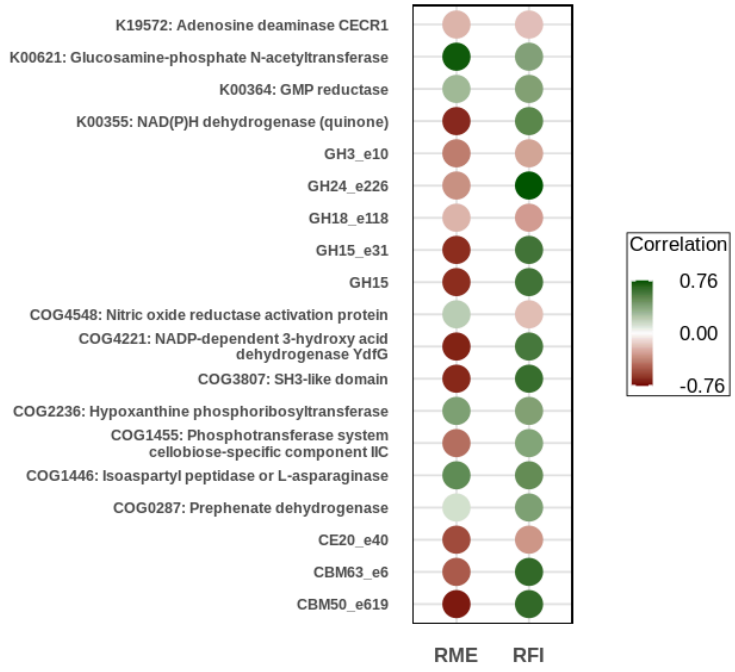

Figure 11. Enzymes-coding transcripts from Nelore rumen microbiota, with transcript abundance correlated with both residual methane emissions (RME) and residual feed intake (RFI) using the the sparse Partial Least Squares 2 (sPLS2) approach and filtered with an absolute value cutoff of ≥ 0.20. Positive correlations were shown in green, and negative in red.

3.4.6 Association among genera, enzyme and the phenotypic traits RME and RFI

Subsequent to the investigation of the associations between microbial genera and enzyme profile individually, we conducted an exploratory analysis integrating microbial genera and enzymatic functions to examine their contribution to RME and RFI variation. Therefore, we applied MB-PLS to construct separate networks for the bacterial and archaeal domains using the selected variables in the sPLS analysis. The correlation values and centrality measures for both bacterial and archaeal networks were reported in Supplementary Table S7.

Regarding the bacterial domain, the network analysis revealed a modular organization (Figure 12). The first module is strongly centered on RME, with 24 direct

connections. This module encompasses a diverse range of bacterial genera such as *Monoglobus, Cronobacter, Metamycoplasma,* and *Mycoplasmopsis,* along with highly connected enzymes including CE20_e40, GH2_e127, COG0179, GH105_e41, and GH51_e19. In contrast, the second module is anchored by the RFI phenotype, exhibiting 12 direct connections and characterized by a more distributed network structure. It features several key bacteria such as *Microcystis, Sedimentisphaera, Aneurinibacillus*, and *Calothrix*. The enzymes with the highest centrality in this module include CBM50_e619, GH15, COG4221, K00355, and GH15_e31. Beyond these connections, a specific set of nodes stands out for their direct correlation with both traits, RME and RFI. These include the enzymes COG4221, K00355, CBM50_e619, GH15, and GH15_e31, as well as the bacterial genera *Microcystis* and *Sedimentisphaera*.

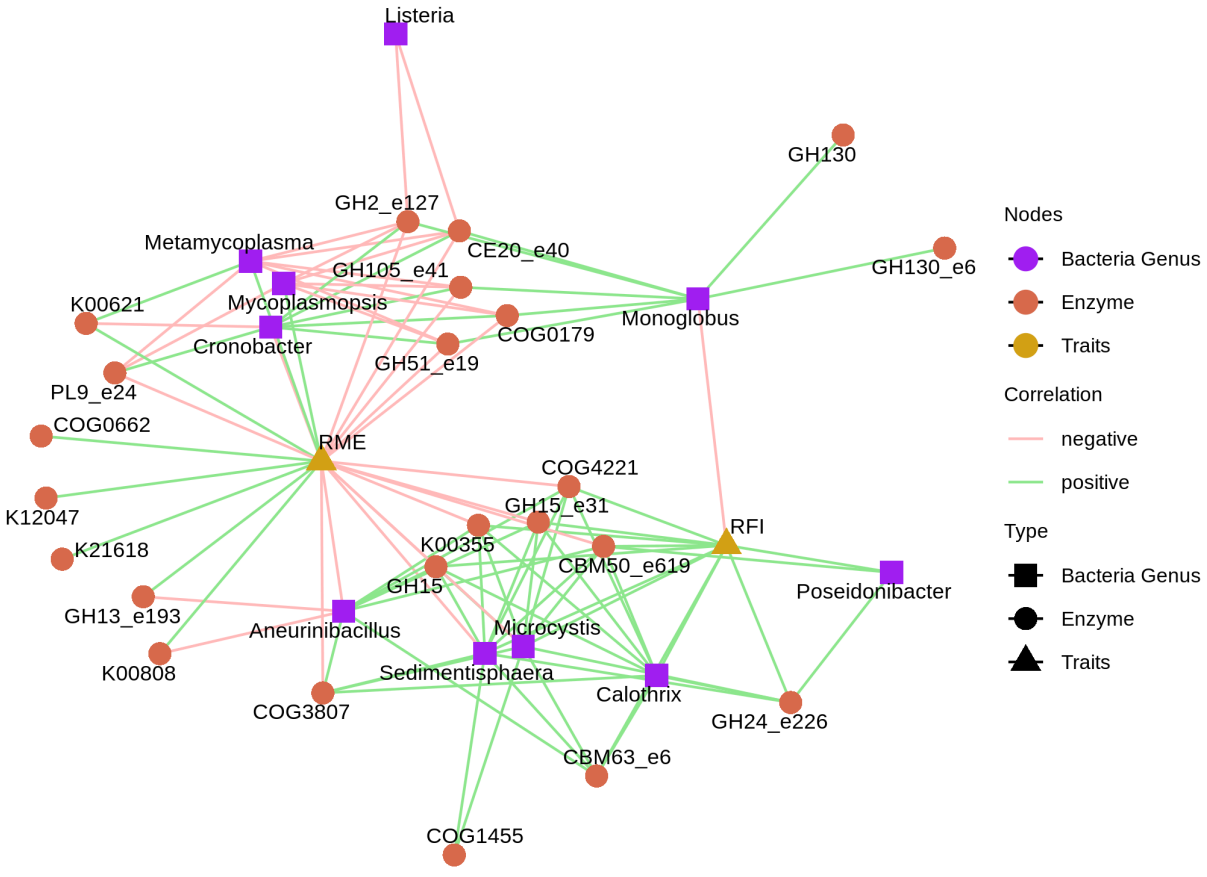

Figure 12: Network representation of the correlations among Nelore (*Bos indicus*) ruminal bacterial genera (purple squares), enzymes-coding transcripts (orange circles), and the traits Residual Methane Emission (RME) and Residual Feed Intake (RFI) (yellow triangles). The color of the edges represent the relationship between latent variables: green for positive and red for negative. Variables selected by Multiblock Partial Least Squares (MB-PLS) were represented and filtered with an absolute value cutoff of ≥ 0.60.

Regarding the archaeal domain, the network analysis, represented in Figure 13, showed the most central nodes are predominantly enzymes. Notably, enzymes such as COG1446, COG4221, K00621, COG3807, CBM50_e619, K00355, GH15_e31, and GH15 stood out due to their high connectivity. Among the archaeal genera, *Halosimplex* emerged as a key connection, associated with multiple interactions within the network.

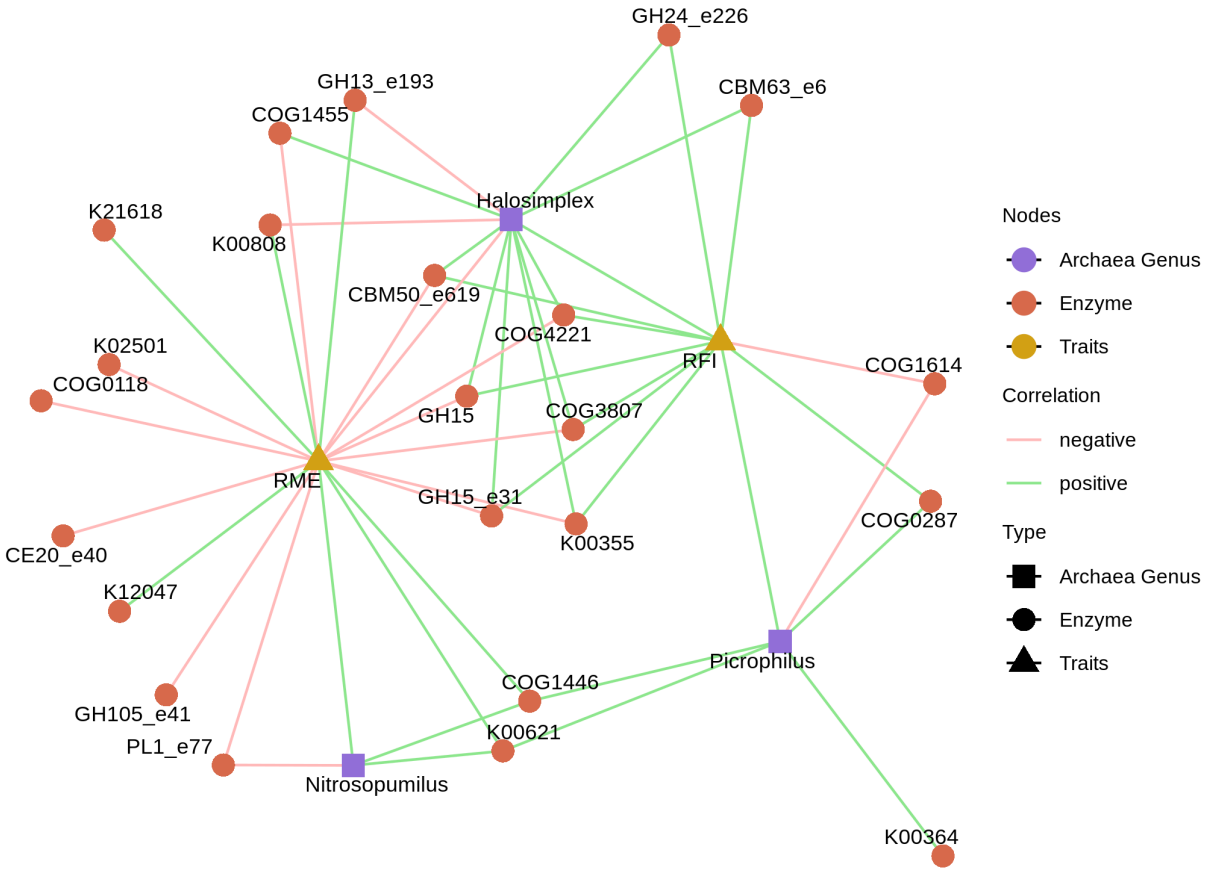

Figure 13: Network representation of the correlations among Nelore ruminal archaeal genera (purple squares), enzymes-coding transcripts (orange circles), and the traits Residual Methane Emission (RME) and Residual Feed Intake (RFI) (yellow triangles). The color of the edges represent the relationship between latent variables: green for positive and red for negative.Variables selected by Multiblock Partial Least Squares (MB-PLS) were represented and filtered with an absolute value cutoff of ≥ 0.5.

3.5 Discussion

The ruminal microbiome plays a pivotal role in ruminant nutrition, productivity, and environmental impact of production. Nonetheless, information on the ruminal microbiome of Nelore (*Bos indicus*) cattle, which dominate tropical production systems, remains scarce. To address this gap, we constructed the Nelore Ruminal Prokaryotic Microbiome Genes (NRPMG) catalog from ruminal metagenomes and integrated metatranscriptomic data from

the same animals, providing the first active gene catalog of Nelore (active Nelore Ruminal Prokaryotic Microbiome Genes - aNRPMG). This integrative approach captured both genomic potential and the expressed fraction of the microbiome, enabling the association of microbial taxa and enzymes-coding transcripts with feed efficiency and methane emission, traits directly related to sustainable livestock production.

Notably, the analysis of the active ruminal microbiome (aNRPMG) revealed a distinct profile compared to the total metagenomic catalog (NRPMG), highlighting that not all genes present in the microbiome were being expressed at a reasonable level. This distinction between functional potential and activity has also been observed in *Bos taurus* breeds (Angus, Charolais, Kinsella composite hybrid), where microbial differences were less pronounced at the metatranscriptomic than at the metagenomic level (Li et al., 2019). Noteworthy, our active gene catalog represents microbiome's gene expression under two different diets, thus potentially covering a broader diversity of diet induced functions.

At the phylum level, *Proteobacteria* and *Firmicutes* dominated the NRPMG catalog, whereas the aNRPMG revealed *Bacteroidetes*, *Firmicutes*, *Proteobacteria*, and *Spirochaetes* as the most transcriptionally active phyla. Similar patterns have been observed in *Bos taurus* active microbiome (Comtet-Marre et al., 2017; Li et al., 2019). At the family level, *Prevotellaceae*, *Lachnospiraceae*, *Oscillospiraceae* and *Treponemataceae* stood out as the most transcriptionally active bacterial families in the aNRPMG catalog. This finding is consistent with their known roles in hemicellulose degradation, short-chain fatty acid production, and protein degradation (Betancur-Murillo et al., 2022; Kaminsky et al., 2023). Interestingly, although the *Treponemataceae* family was underrepresented in the NRPMG catalog, it ranked among the five most transcriptionally active families in the aNRPMG. This high activity likely reflects its functional role in the degradation of soluble fibers, as previously reported by Bekele et al. (2011). The archaeal domain accounted for 6.06% of the classified transcripts in the active microbiome, compared with only 3.98% in the NRPMG catalog, indicating a greater representation at the transcriptional level. The consistent predominance of *Methanobacteriaceae* in both datasets highlights its common presence in the bovine rumen and its central role in hydrogenotrophic methanogenesis (Janssen and Kirs, 2008; Hook et al., 2010; Volmer et al., 2023).

Functionally, the high activity in metabolic pathways related to carbohydrates, energy, and amino acid metabolism found in our catalog are aligned with patterns reported in different beef cattle breeds (Li and Guan, 2017), dairy cows (Mann et al., 2018), and our previous metagenomic study on Nelore microbiomes (Conteville et al., 2023). Compared with the NRPMG catalog, the active microbiome exhibited higher expression of functions associated with carbohydrate, energy, and lipid metabolism, while functions related to amino acid metabolism were relatively reduced. This profile reflects the strict anaerobic

environment of the rumen, where microbial fermentation of complex dietary polysaccharides produces VFAs (Ungerfeld, 2020) that can supply up to 80% of the host's energy requirements (Sanjorjo et al., 2023). The detection of active genes involved in glycolysis and the pentose phosphate pathway synthesis (Wang et al., 2020; Ge et al., 2023) reflects the efficient microbial conversion of dietary polysaccharides into energy-rich intermediates. Also, the increase in lipid metabolism suggests enhanced microbial involvement in lipid biohydrogenation, a key process in the rumen that contributes to the formation of VFAs (Lourenço et al., 2010).

Among the non-metabolic functional categories, both catalogs exhibited a predominance of functions related to genetic information processing. However, this category was more abundant in the active rumen metagenome (aNRPMG, 52.85%) than in the NRPMG (38.54%). This disproportion suggests that the ruminal microbiome invests a substantial part of its functional activity in sustaining core processes such as transcription, translation, RNA processing and modification, as well as DNA replication and repair. This observation is consistent with Xue et al. (2022), who also reported that active rumen communities devote a larger portion of their expressed genes to genetic information processing compared to the DNA-based metagenome. In addition, functions related to cell signaling and transport were also slightly more enriched in the aNRPMG (25.04%) than in the NRPMG (20.13%), highlighting that active ruminal microbes also prioritize intercellular interactions and host–microbe communication (Wu and Luo, 2021).

Conversely, the proportion of uncharacterized functions was substantially higher in the NRPMG (25.54%) than in the aNRPMG (9.99%). This contrast indicates that the active gene fraction provides a clearer representation of the functional roles within the microbiome, thereby reducing the prevalence of genes with unknown functions. As reported before, focusing on the expressed genes thus enables a more precise functional characterization and enhances our understanding of the microbiome's role in host-associated processes (Li et al., 2019).

In the context of CAZymes, the active microbiome (aNRPMG) showed higher abundances of glycoside hydrolases (GH), carbohydrate-binding modules (CBM), and polysaccharide lyases (PL) compared to the total NRPMG. Functionally, GH and PL cleave glycosidic bonds through hydrolytic and non-hydrolytic mechanisms, respectively (Lombard et al., 2025), while CBM facilitates enzyme-substrate interactions by mediating attachment to carbohydrate substrates (Lombard et al., 2025). The preferential expression of these classes in the active microbiome highlights the central role of carbohydrate degradation in ruminal activity, reflecting the functional priority of microbes. In contrast, glycosyl transferases (GT), responsible for glycosidic bond formation (Lombard et al., 2025), were abundant in the NRPMG but expressed at much lower levels in the aNRPMG. This indicates that while the

genomic potential for glycan biosynthesis is present, it is not actively prioritized under the ruminal conditions sampled.

Our results further revealed that CAZymes in the active ruminal microbiome were predominantly specialized in degrading plant cell wall polysaccharides, including cellulose (7.93%), pectin (3.71%), and hemicelluloses such as xylan (19.87%) and β-glucan (13.90%). This result underscores the centrality of lignocellulosic degradation in rumen metabolism, as the degradation of these carbohydrates releases fermentable sugars and produces VFAs which are essential energy sources for the host (Xu et al., 2012; Sun et al., 2022; Weimer, 2022). Regarding storage carbohydrates, the aNRPMG showed exclusive activity on starch degradation (6.14%), whereas the NRPMG displayed broader substrate diversity, including trehalose and glycogen. This selective activation of starch-degrading functions observed in aNRPMG may reflect the preferential utilization of substrates that are both abundant and rapidly fermentable. According to Hua et al. (2022), starch-degrading bacteria proliferate and express amylolytic enzymes in response to starch availability, facilitating rapid fermentation and VFA production.

In cattle, fiber-degrading microbes influence fermentation pathways that produce or consume molecular hydrogen, thereby influencing methanogenesis and traits such as feed efficiency and methane emission (Hook et al., 2010; Janssen, 2010). To further explore these relationships, we constructed an integrative network linking enzyme expression, microbial genera and the traits RME and RFI.

Our results show that the enzymes CE20_e40, GH2_e127, COG0179, GH105_e41, and GH51_e19, were negatively correlated with RME and acted as hubs within the network module associated with this trait. From these, GH51 (α-L-arabinofuranosidases), GH105 and GH2 (β-galactosidases) are key in hemicellulose, cellulose and pectin degradation (Suen et al., 2011; Dai et al., 2015; Kim et al., 2019; Gharechahi et al., 2021, 2023). GH51 and GH2 families have been consistently identified as the most prevalent CAZymes families in bovine rumen metagenomes (Gharechahi et al., 2021), and their activity in our data reinforces their central role in plant cell wall deconstruction. Although fiber degradation has been reported to favor the production of acetate and butyrate, thereby increasing the availability of hydrogen for methanogenesis and potentially enhancing methane emission (Jiyana et al., 2022), our results indicate that, at the individual enzyme level, specific CAZymes may instead be associated with RME reduction. A clear example is CE20_e40, an acetyl ester hydrolase that removes acetyl groups from acetylated sugars present in plant polysaccharides, directly generating acetic acid (Aldridge, 1953). Since this process leads to the production of acetate without the production of H_2, it decreases the availability of reducing substrates for methanogens, and impacts on methanogenesis.

Also, in the second module, we observed that GH15 (α-glucosidases), GH15_e31, COG4221 (NADP-dependent 3-hydroxyacid dehydrogenase), K00355 (NAD(P)H dehydrogenase) and CBM50 (LysM domain) were positively correlated with RFI and negatively correlated with RME. The GH15 family, which includes GH15 and GH15_e31, are α-glucosidases that hydrolyze starch (Hua et al., 2022; Tian et al., 2023), and COG4221 encodes a dehydrogenase that catalyzes late steps in the formation of 3-hydroxypropionate (Kim et al., 2010), a metabolite involved in acetate metabolism (Tabita, 2009). Together, these family enzymes suggest alterations in the acetate to propionate ratio (Lin et al., 2020), since starch fermentation in the rumen promotes propionate production by reducing carbon dioxide with hydrogen. While this pathway may reduce methanogenesis (Almeida et al., 2022), excessive activation may also lead to lactate accumulation and ruminal pH decline, potentially compromising feed efficiency (Li et al., 2021a; Hua et al., 2022). The presence of the enzyme K00355, a NAD(P)H dehydrogenase (Pey et al., 2019), promotes electron transfer toward quinones rather than CO_2, thereby competing with the methanogenesis pathway (Palacios et al., 2023). The role of CBM50 (LysM domains), negatively correlated with RME and positively correlated with RFI, is unclear as it is best known for roles in bacterial peptidoglycan and chitin binding, microbial competition and fungal control (Buist et al., 2008), functions that are not characterized in the rumen.

The bacterial genus *Monoglobus, Cronobacter, Metamycoplasma* and *Mycoplasmatota* were identified as hubs within the network module associated with RME. Among them, *Monoglobus* showed a negative correlation with both methane emission and feed efficiency. This genus has been described as beneficial for host metabolism, particularly through pectin degradation and sugar utilization (Kim et al., 2019; Wang et al., 2023). In cattle, increased abundance of this genus has been associated with healthy Angus breeds (Wang et al., 2023). Notably, *Monoglobus pectinilyticus* is highly efficient in degrading pectin, as it normally encodes CAZymes such as GH51 and GH105, which contribute to the breakdown of plant fibers (Kim et al., 2019). Consistently, these enzymes were negatively correlated with RME in our study, supporting the idea that an increased abundance of *Monoglobus* may enhance fiber-degrading activity and, consequently, contribute to reduced methane emission. Additionally, the genus *Cronobacter*, known for including opportunistically human pathogens and occasionally found in bovine feces (Ogihara et al., 2019), showed a positive correlation with the enzymes CE20_e40, GH105_e41, GH51_e19, GH2_e127, and COG0179, and all of them had negative association with RME. The potential role of this genus within the rumen environment remains unclear and warrants further investigation, particularly considering its possible sanitary implications.

In contrast, the genera *Metamycoplasma* and *Mycoplasmopsis*, both of the phylum *Mycoplasmatota*, exhibited opposite associations. Both were positively associated with RME,

and *Metamycoplasma* also showed a slight positive correlation with RFI. This pattern is reinforced by the fact that these genera were negatively associated with the enzymes CE20_e40, GH105_e41, GH51_e19, GH2_e127, and COG0179, which were associated with methane reduction in our study. In addition, *Metamycoplasma* was positively associated with the enzyme K00621, a glucosamine-phosphate N-acetyltransferase involved in the biosynthesis of UDP-N-acetylglucosamine, essential for bacterial cell wall formation and division (Mio et al., 1999). This metabolite diverts glucose, along with glutamine, acetyl-coenzyme A, adenosine triphosphate, and uridine triphosphate from other fermentative processes (Rodríguez-Díaz et al., 2012; Li et al., 2021b). Beyond its structural role, UDP-GlcNAc is also related to O-GlcNAcylation, a reversible protein modification that regulates diverse intracellular signaling pathways and has been linked to neurodegeneration, cancer, cardiovascular, and metabolic disorders in humans (Li et al., 2021b). Although the role of this enzyme in the rumen and its relationship with cattle have not yet been investigated, our results suggest that the diversion of glucose into this route may reduce its availability for the host and alter fermentation balance, thereby contributing to lower feed efficiency and higher methane emissions.

In the second module, the hub genera *Microcystis*, *Sedimentisphaera*, and *Aneurinibacillus* showed positive correlations with RFI and negative correlations with RME, while *Calothrix* was positively correlated with RFI. Although *Microcystis* and *Calothrix* are aquatic cyanobacteria, both have been previously detected in the rumen of cattle (Li and Guan, 2017; Schären et al., 2017; Ilina et al., 2021). These organisms are known for producing toxins such as microcystins (Mohamed and Al Shehri, 2007; Manubolu et al., 2014), the most commonly recognized hepatotoxins (Badar et al., 2021), which could cause economic losses in beef and milk production, since liver dysfunction negatively affects growth, body condition, and cattle's overall performance (Badar et al., 2021). Although the rumen is predominantly an anaerobic system, aerobic bacteria, such as *Microcystis*, *Calothrix, Sedimentisphaera* and *Aneurinibacillus,* detected in our study, can ferment carbohydrates under residual O_2 and N_2 conditions (Neves et al., 2017). Thus, the negative correlation among these genera and RME, suggests that the residual oxygen may create a hostile environment for methanogenic archaea, thereby reducing methane production (Yuan et al., 2009). Functionally, these four genera were positively associated with the enzymes GH15 family, CBM50, COG4221 and K00355, whose potential roles in reducing methane emission and feed efficiency have already been highlighted and discussed in this study.

In the correlation network with archaeal genera, *Halosimplex* were the hub taxon, showing positive correlation with RFI and a broad set of enzymes (COG1455, GH24_e226, CBM63_e6, CBM50_e619, COG4221, COG3807, K00355, GH15_e31 and GH15) but a negative correlation with RME. *Halosimplex* is an extremely halophilic archaea that grows on

simple substrates (glycerol, acetate, pyruvate) and can not utilize sugars, proteins or nucleic acids (Vreeland et al., 2002; Mao et al., 2025). As acetate is beneficial for RFI (Lage et al., 2020) consumption of this VFA could underlie the negative impact on feed efficiency. Consistently, GH15, COG4221, K00355, and CBM50 showed potential roles in methane emission and feed efficiency as already highlighted and discussed in this study. In addition, SH3-like domains (COG3807), involved in substrate recognition and kinase downregulation (Buist et al., 2008; Kurochkina and Guha, 2012) were correlated with higher RFI and lower RME. Although the role of *Halosimplex* in the rumen has not yet been established, taken together these associations suggest that its functional repertoire may act as modulators of energy efficiency, but further studies are needed.

Picrophillus was positively correlated with RFI and with the enzymes K00364, COG0287, COG1446 and K00621, being the latest two also positively correlated to RME and to the genus *Nitrosopumilus*. The enzyme COG1446 (isoaspartyl peptidase/L-asparaginase) is particularly relevant, since it releases ammonia from asparagine (Sharma et al., 2022). Elevated levels of ammonia can enhance the hydrogenotrophic pathway, favoring methanogenic archaea that reduce CO_2 using H_2 to produce methane (Yang et al., 2018). In addition, *Picrophilus* was negatively correlated with COG1614 (CO-methylating acetyl-CoA synthase), which operates in the Wood-Ljungdahl pathway to convert CO_2 to acetyl-CoA (Ragsdale and Pierce, 2008), and consistently showed negative correlations with RFI. Since this pathway is characteristic of acetogens that compete with methanogens for hydrogen, its activity may represent a shift toward alternative hydrogen sinks, when methanogenesis is suppressed (Freetly et al., 2020). In this context, one hypothesis posits that energy spared from methane losses could be redirected toward body weight gain, thereby enhancing feed efficiency (Freetly et al., 2020), corroborating our results that show a negative correlation of the enzyme COG1614 with *Picrophilus* and RFI.

3.6 Conclusion

This study is the first to integrate metatranscriptomic and metagenomic data in Nelore cattle, expanding the understanding of tropical ruminant production systems. We identified taxonomic and functional differences between the total metagenomic catalog (NRPMG) and its transcriptionally active fraction (aNRPMG). The association of enzyme-coding transcript profiles and microbial taxa with the host traits methane emission and feed efficiency, demonstrated that metabolic activity, rather than microbial presence alone, shapes critical physiological outcomes in cattle. Our results further highlight the central role of hemicellulose and pectin degrading enzymes, alternative redox pathways, and specific bacterial and archaeal genera in modulating fermentation dynamics and host energy

use. Overall, this study offers a basis for future strategies to manipulate the ruminal microbiome, aiming to improve productivity while simultaneously reducing environmental impacts, particularly methane emissions.

3.7 Data availability

The data presented in the study are deposited in the National Center for Biotechnology Information repository. The metagenomes are available under BioProject ID PRJNA987743, and the metatranscriptomes under PRJNA1131826. Supplementary tables are available at https://encurtador.com.br/RITCK. The gene catalog of the Nelore ruminal microbiome (NRPMG) and the active catalog (aNRPMG) were deposited in Figshare under the DOIs 10.6084/m9.figshare.30257683 and 10.6084/m9.figshare.30257680, respectively. For reviewer access, the datasets are temporarily available through the following private links: https://figshare.com/s/db80e01df014b8e769d8 (NRPMG) and https://figshare.com/s/fcfe03309c96603f54aa (aNRPMG).

3.8 Supplementary Figure

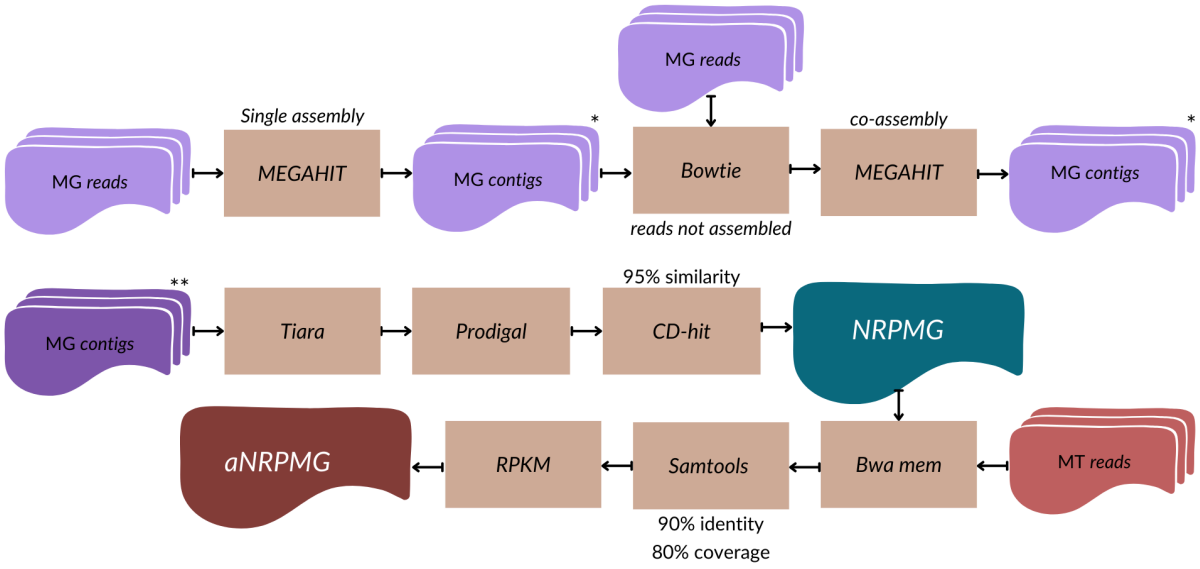

Supplementary Figure 1. Workflow illustrating the construction of the Nelore Ruminal Prokaryotic Microbiome Genes (NRPMG) catalog and its transcriptionally active fraction (active-Nelore Ruminal Prokaryotic Microbiome Genes, aNRPMG). The figure summarizes the steps used to derive the gene catalog and to identify the actively transcribed genes.

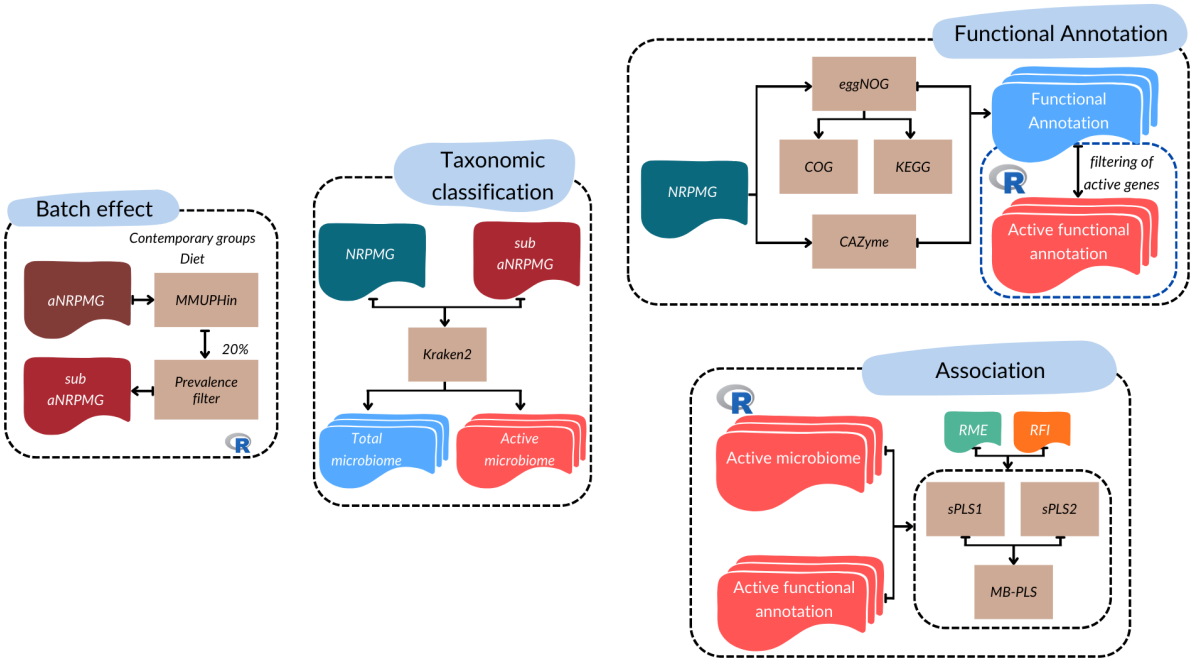

Supplementary Figure 2. Workflow summarizing batch-effect correction, taxonomic classification, functional annotation, and association analyses with residual methane emission (RME) and residual feed intake (RFI).

3.9 References

Aldridge, W. N. (1953). Serum esterases. 1. Two types of esterase (A and B) hydrolysing p -nitrophenyl acetate, propionate and butyrate, and a method for their determination. Biochem. J. 53, 110–117. doi: 10.1042/bj0530110

Almeida, K. V., Santos, G. T., Daniel, J. L. P., Nino-de-Guzman, C., Amaro, F. X., Sultana, H., et al. (2022). Effects of nitrate sources on in vitro methane production and ruminal fermentation parameters in diets differing in starch degradability. Anim. Feed Sci. Technol. 292, 115437. doi: 10.1016/j.anifeedsci.2022.115437

Andrade, B. G. N., Bressani, F. A., Cuadrat, R. R. C., Cardoso, T. F., Malheiros, J. M., De Oliveira, P. S. N., et al. (2022). Stool and Ruminal Microbiome Components Associated With Methane Emission and Feed Efficiency in Nelore Beef Cattle. Front. Genet. 13, 812828. doi: 10.3389/fgene.2022.812828

Badar, M., Batool, F., Khan, S. S., Khokhar, I., Qamar, M. K., and Yasir, C. (2021). EFFECTS OF MICROCYSTINS TOXINS CONTAMINATED DRINKING WATER ON HEPATIC PROBLEMS IN ANIMALS (COWS AND BUFFALOS) AND TOXINS REMOVAL CHEMICAL METHOD.

Badhan, A., Wang, Y., Terry, S., Gruninger, R., Guan, L. L., and McAllister, T. A. (2025). Invited review: Interplay of rumen microbiome and the cattle host in modulating feed efficiency and methane emissions. J. Dairy Sci. 108, 5489–5501. doi: 10.3168/jds.2024-26063

Basarab, J. A., Beauchemin, K. A., Baron, V. S., Ominski, K. H., Guan, L. L., Miller, S. P., et al. (2013). Reducing GHG emissions through genetic improvement for feed

efficiency: effects on economically important traits and enteric methane production. Animal 7, 303–315. doi: 10.1017/S1751731113000888

Bekele, A. Z., Koike, S., and Kobayashi, Y. (2011). Phylogenetic diversity and dietary association of rumen Treponema revealed using group-specific 16S rRNA gene-based analysis: Diversity and diet association of rumen Treponema. FEMS Microbiol. Lett. 316, 51–60. doi: 10.1111/j.1574-6968.2010.02191.x

Betancur-Murillo, C. L., Aguilar-Marín, S. B., and Jovel, J. (2022). Prevotella: A Key Player in Ruminal Metabolism. Microorganisms 11, 1. doi: 10.3390/microorganisms11010001

Buist, G., Steen, A., Kok, J., and Kuipers, O. P. (2008). LysM, a widely distributed protein motif for binding to (peptido)glycans. Mol. Microbiol. 68, 838–847. doi: 10.1111/j.1365-2958.2008.06211.x

Cammack, K. M., Austin, K. J., Lamberson, W. R., Conant, G. C., and Cunningham, H. C. (2018). RUMINNAT NUTRITION SYMPOSIUM: Tiny but mighty: the role of the rumen microbes in livestock production1. J. Anim. Sci. 96, 752–770. doi: 10.1093/jas/skx053

Cantalapiedra, C. P., Hernández-Plaza, A., Letunic, I., Bork, P., and Huerta-Cepas, J. (2021). eggNOG-mapper v2: Functional Annotation, Orthology Assignments, and Domain Prediction at the Metagenomic Scale. Mol. Biol. Evol. 38, 5825–5829. doi: 10.1093/molbev/msab293

Cao, K.-A. L., Rossouw, D., Robert-Granié, C., and Besse, P. (2008). A Sparse PLS for Variable Selection when Integrating Omics Data. Stat. Appl. Genet. Mol. Biol. 7. doi: 10.2202/1544-6115.1390

Chen, C., Zhou, Y., Fu, H., Xiong, X., Fang, S., Jiang, H., et al. (2021). Expanded catalog of microbial genes and metagenome-assembled genomes from the pig gut microbiome. Nat. Commun. 12, 1106. doi: 10.1038/s41467-021-21295-0

Comtet-Marre, S., Parisot, N., Lepercq, P., Chaucheyras-Durand, F., Mosoni, P., Peyretaillade, E., et al. (2017). Metatranscriptomics Reveals the Active Bacterial and Eukaryotic Fibrolytic Communities in the Rumen of Dairy Cow Fed a Mixed Diet. Front. Microbiol. 8. doi: 10.3389/fmicb.2017.00067

Conteville, L. C., Silva, J. V., Andrade, B. G. N., Cardoso, T. F., Bruscadin, J. J., Oliveira, P. S. N., et al. (2023). Rumen and fecal microbiomes are related to diet and production traits in Bos indicus beef cattle. Front. Microbiol. doi: https://doi.org/10.3389/fmicb.2023.1282851

Costa Jr, C. C., Wironen, M., Racette, K., and Wollenberg, E. (2021). Global Warming Potential* (GWP*): Understanding the implications for mitigating methane emissions in agriculture.

Dai, X., Tian, Y., Li, J., Su, X., Wang, X., Zhao, S., et al. (2015). Metatranscriptomic Analyses of Plant Cell Wall Polysaccharide Degradation by Microorganisms in the Cow Rumen. Appl. Environ. Microbiol. 81, 1375–1386. doi: 10.1128/AEM.03682-14

Donoghue, K. A., Bird-Gardiner, T., Arthur, P. F., Herd, R. M., and Hegarty, R. F. (2016). Genetic and phenotypic variance and covariance components for methane emission and postweaning traits in Angus cattle12. J. Anim. Sci. 94, 1438–1445. doi: 10.2527/jas.2015-0065

Freetly, H. C., Dickey, A., Lindholm-Perry, A. K., Thallman, R. M., Keele, J. W., Foote, A. P., et al. (2020). Digestive tract microbiota of beef cattle that differed in feed efficiency. J. Anim. Sci. 98, skaa008. doi: 10.1093/jas/skaa008

Ge, T., Yang, C., Li, B., Huang, X., Zhao, L., Zhang, X., et al. (2023). High-energy diet modify rumen microbial composition and microbial energy metabolism pattern in fattening sheep. BMC Vet. Res. 19, 32. doi: 10.1186/s12917-023-03592-6

Gharechahi, J., Vahidi, M. F., Bahram, M., Han, J.-L., Ding, X.-Z., and Salekdeh, G. H. (2021). Metagenomic analysis reveals a dynamic microbiome with diversified adaptive functions to utilize high lignocellulosic forages in the cattle rumen. ISME J. 15, 1108–1120. doi: 10.1038/s41396-020-00837-2

Gharechahi, J., Vahidi, M. F., Sharifi, G., Ariaeenejad, S., Ding, X.-Z., Han, J.-L., et al. (2023). Lignocellulose degradation by rumen bacterial communities: New insights from metagenome analyses. Environ. Res. 229, 115925. doi: 10.1016/j.envres.2023.115925

Herd, R. M., Arthur, P. F., Donoghue, K. A., Bird, S. H., Bird-Gardiner, T., and Hegarty, R. S. (2014). Measures of methane production and their phenotypic relationships with dry matter intake, growth, and body composition traits in beef cattle1,2. J. Anim. Sci. 92, 5267–5274. doi: 10.2527/jas.2014-8273

Hook, S. E., Wright, A.-D. G., and McBride, B. W. (2010). Methanogens: Methane Producers of the Rumen and Mitigation Strategies. Archaea 2010, 1–11. doi: 10.1155/2010/945785

Hua, D., Hendriks, W. H., Xiong, B., and Pellikaan, W. F. (2022). Starch and Cellulose Degradation in the Rumen and Applications of Metagenomics on Ruminal Microorganisms. Animals 12, 3020. doi: 10.3390/ani12213020

Hyatt, D., Chen, G.-L., LoCascio, P. F., Land, M. L., Larimer, F. W., and Hauser, L. J. (2010). Prodigal: prokaryotic gene recognition and translation initiation site identification. BMC Bioinformatics 11, 119. doi: 10.1186/1471-2105-11-119

Ilina, L. A., Filippova, V. A., Brazhnik, E. A., Dubrovin, A. V., Yildirim, E. A., Dunyashev, T. P., et al. (2021). The Comparative Analysis of the Ruminal Bacterial Population in Reindeer (Rangifer tarandus L.) from the Russian Arctic Zone: Regional and Seasonal Effects. Animals 11, 911. doi: 10.3390/ani11030911

Janssen, P. H. (2010). Influence of hydrogen on rumen methane formation and fermentation balances through microbial growth kinetics and fermentation thermodynamics. Anim. Feed Sci. Technol. 160, 1–22. doi: 10.1016/j.anifeedsci.2010.07.002

Janssen, P. H., and Kirs, M. (2008). Structure of the Archaeal Community of the Rumen. Appl. Environ. Microbiol. 74, 3619–3625. doi: 10.1128/AEM.02812-07

Jiyana, S. T., Ratsaka, M. M., Leeuw, K.-J., and Mbatha, K. R. (2022). Impacts of graded dietary fiber levels on feed efficiency and carbon footprint of two beef breeds. Livest. Sci. 258, 104867. doi: 10.1016/j.livsci.2022.104867

Kaminsky, R. A., Reid, P. M., Altermann, E., Kenters, N., Kelly, W. J., Noel, S. J., et al. (2023). Rumen Lachnospiraceae isolate NK3A20 exhibits metabolic flexibility in response to substrate and coculture with a methanogen. Appl. Environ. Microbiol. 89, e00634-23. doi: 10.1128/aem.00634-23

Karlicki, M., Antonowicz, S., and Karnkowska, A. (2022). Tiara: deep learning-based classification system for eukaryotic sequences. Bioinformatics 38, 344–350. doi: 10.1093/bioinformatics/btab672

Kim, C. C., Healey, G. R., Kelly, W. J., Patchett, M. L., Jordens, Z., Tannock, G. W., et al. (2019). Genomic insights from Monoglobus pectinilyticus : a pectin-degrading specialist bacterium in the human colon. ISME J. 13, 1437–1456. doi: 10.1038/s41396-019-0363-6

Kim, K.-S., Pelton, J. G., Inwood, W. B., Andersen, U., Kustu, S., and Wemmer, D. E. (2010). The Rut Pathway for Pyrimidine Degradation: Novel Chemistry and Toxicity Problems.

Kock, R. M., Swiger, L. A., Chamber, D., and Gregory, K. E. (1963). EFFICIENCY OF FEED USE IN BEEF CATTLE. doi: https://doi.org/10.2527/jas1963.222486x

Kurochkina, N., and Guha, U. (2012). SH3 domains: modules of protein–protein interactions. Biophys. Rev. 5, 29–39. doi: 10.1007/s12551-012-0081-z

Lage, C. F. A., Coelho, S. G., Neto, H. C. D., Malacco, V. M. R., Rodrigues, J. P. P., Sacramento, J. P., et al. (2020). Relationship between feed efficiency indexes and thermography, blood, and ruminal parameters in pre-weaning dairy heifers. PLOS ONE 15, e0236118. doi: 10.1371/journal.pone.0236118

Langmead, B., and Salzberg, S. L. (2012). Fast gapped-read alignment with Bowtie 2. Nat. Methods 9, 357–359. doi: 10.1038/nmeth.1923

Latham, E. A., Weldon, K. K., Wickersham, T. A., Coverdale, J. A., and Pinchak, W. E. (2018). Responses in the rumen microbiome of Bos taurus and indicus steers fed a low-quality rice straw diet and supplemented protein. J. Anim. Sci. 96, 1032–1044. doi: 10.1093/jas/sky023

Li, D., Liu, C.-M., Luo, R., Sadakane, K., and Lam, T.-W. (2015). MEGAHIT: an ultra-fast single-node solution for large and complex metagenomics assembly via succinct de Bruijn graph. Bioinformatics 31, 1674–1676. doi: 10.1093/bioinformatics/btv033

Li, F., and Guan, L. L. (2017). Metatranscriptomic Profiling Reveals Linkages between the Active Rumen Microbiome and Feed Efficiency in Beef Cattle. Appl. Environ. Microbiol. 83, e00061-17. doi: 10.1128/AEM.00061-17

Li, F., Hitch, T. C. A., Chen, Y., Creevey, C. J., and Guan, L. L. (2019). Comparative metagenomic and metatranscriptomic analyses reveal the breed effect on the rumen microbiome and its associations with feed efficiency in beef cattle. Microbiome 7, 6. doi: 10.1186/s40168-019-0618-5

Li, H. (2013). Aligning sequence reads, clone sequences and assembly contigs with BWA-MEM. Available at: http://arxiv.org/abs/1303.3997 (Accessed July 9, 2024).

Li, H., Handsaker, B., Wysoker, A., Fennell, T., Ruan, J., Homer, N., et al. (2009). The Sequence Alignment/Map format and SAMtools. Bioinformatics 25, 2078–2079. doi: 10.1093/bioinformatics/btp352

Li, J., Cai, X., Zhong, H., Feng, Q., Sunagawa, S., Arumugam, M., et al. (2014). An integrated catalog of reference genes in the human gut microbiome. Nat. Biotechnol. 32, 834–841. doi: 10.1038/nbt.2942

Li, J., Zhong, H., Ramayo-Caldas, Y., Terrapon, N., Lombard, V., Potocki-Veronese, G., et al. (2020). A catalog of microbial genes from the bovine rumen unveils a specialized and diverse biomass-degrading environment. GigaScience 9, giaa057. doi: 10.1093/gigascience/giaa057

Li, M. M., White, R. R., Guan, L. L., Harthan, L., and Hanigan, M. D. (2021a). Metatranscriptomic analyses reveal ruminal pH regulates fiber degradation and fermentation by shifting the microbial community and gene expression of carbohydrate-active enzymes. Anim. Microbiome 3, 32. doi: 10.1186/s42523-021-00092-6

Li, W., and Godzik, A. (2006). Cd-hit: a fast program for clustering and comparing large sets of protein or nucleotide sequences. Bioinformatics 22, 1658–1659. doi: 10.1093/bioinformatics/btl158

Li, Z., Zhang, J., and Ai, H. (2021b). Genetically Encoded Green Fluorescent Biosensors for Monitoring UDP-GlcNAc in Live Cells. ACS Cent. Sci. 7, 1763–1770. doi: 10.1021/acscentsci.1c00745

Lin, L., Lai, Z., Zhang, J., Zhu, W., and Mao, S. (2023). The gastrointestinal microbiome in dairy cattle is constrained by the deterministic driver of the region and the modified effect of diet. Microbiome 11, 10. doi: 10.1186/s40168-022-01453-2

Lin, X., Hu, Z., Zhang, S., Cheng, G., Hou, Q., Wang, Y., et al. (2020). A Study on the Mechanism Regulating Acetate to Propionate Ratio in Rumen Fermentation by Dietary Carbohydrate Type. Adv. Biosci. Biotechnol. 11, 369–390. doi: 10.4236/abb.2020.118026

Lombard, V., Golaconda Ramulu, H., Drula, E., Coutinho, P. M., and Henrissat, B. (2014). The carbohydrate-active enzymes database (CAZy) in 2013. Nucleic Acids Res. 42, D490–D495. doi: 10.1093/nar/gkt1178

Lombard, V., Henrissat, B., and Garron, M.-L. (2025). CAZac: an activity descriptor for carbohydrate-active enzymes. Nucleic Acids Res. 53, D625–D633. doi: 10.1093/nar/gkae1045

Lourenço, M., Ramos-Morales, E., and Wallace, R. J. (2010). The role of microbes in rumen lipolysis and biohydrogenation and their manipulation. Animal 4, 1008–1023. doi: 10.1017/S175173111000042X

Ma, S., Shungin, D., Mallick, H., Schirmer, M., Nguyen, L. H., Kolde, R., et al. (2022). Population structure discovery in meta-analyzed microbial communities and inflammatory bowel disease using MMUPHin. Genome Biol. 23, 208. doi: 10.1186/s13059-022-02753-4

Mann, E., Wetzels, S. U., Wagner, M., Zebeli, Q., and Schmitz-Esser, S. (2018). Metatranscriptome Sequencing Reveals Insights into the Gene Expression and Functional Potential of Rumen Wall Bacteria. Front. Microbiol. 9, 43. doi: 10.3389/fmicb.2018.00043

Manubolu, M., Madawala, S. R., C Dutta, P., and Malmlöf, K. (2014). In vitro biodegradation of cyanotoxins in the rumen fluid of cattle. BMC Vet. Res. 10, 110. doi: 10.1186/1746-6148-10-110

Mao, Y.-L., Tan, S., Wang, B.-B., Yang, X.-Y., Hou, J., and Cui, H.-L. (2025). Halosimplex

amylolyticum sp. nov., Halosimplex halobium sp. nov., Halosimplex marinum sp. nov., Halosimplex rarum sp. nov., Halovenus amylolytica sp. nov., Halovenus halobia sp. nov., and Halovenus marina sp. nov., halophilic archaea isolated from a marine tidal flat, a marine solar saltern, three coarse sea salts, and two saline lakes. Syst. Appl. Microbiol. 48, 126626. doi: 10.1016/j.syapm.2025.126626

McAllister, T. A., Thomas, K. D., Gruninger, R. J., Elshahed, M., Li, Y., and Cheng, Y. (2025). International Symposium on Ruminant Physiology: Rumen fungi, archaea, and their interactions. J. Dairy Sci. 108, 7545–7566. doi: 10.3168/jds.2024-25713

Mio, T., Yamada-Okabe, T., Arisawa, M., and Yamada-Okabe, H. (1999). Saccharomyces cerevisiae GNA1, an Essential Gene Encoding a Novel Acetyltransferase Involved in UDP-N-acetylglucosamine Synthesis. J. Biol. Chem. 274, 424–429. doi: 10.1074/jbc.274.1.424

Mohamed, Z. A., and Al Shehri, A. M. (2007). Cyanobacteria and their toxins in treated-water storage reservoirs in Abha city, Saudi Arabia. Toxicon 50, 75–84. doi: 10.1016/j.toxicon.2007.02.021

Neves, A. L. A., Li, F., Ghoshal, B., McAllister, T., and Guan, L. L. (2017). Enhancing the Resolution of Rumen Microbial Classification from Metatranscriptomic Data Using Kraken and Mothur. Front. Microbiol. 8, 2445. doi: 10.3389/fmicb.2017.02445

New, F. N., Baer, B. R., Clark, A. G., Wells, M. T., and Brito, I. L. (2022). Collective effects of human genomic variation on microbiome function. Sci. Rep. 12, 3839. doi: 10.1038/s41598-022-07632-3

Ogihara, H., Fukuda, N., Fujiwara, A., Suzuki, H., Yamamoto, H., Kyoui, D., et al. (2019). Prevalence of Cronobacter spp. in Retail Foods and Farm-associated Environments in Japan. Food Sci. Technol. Res. 25, 265–275. doi: 10.3136/fstr.25.265

Palacios, P. A., Kleikamp, H., Nielsen, J. L., Jensen, M. B., Bentien, A., and Kofoed, M. V. W. (2023). Quinone-mediated extracellular electron transfer processes in ex situ biomethanation reactors. Bioresour. Technol. Rep. 24, 101671. doi: 10.1016/j.biteb.2023.101671

Perez, H. G., Stevenson, C. K., Lourenco, J. M., and Callaway, T. R. (2024). Understanding Rumen Microbiology: An Overview. Encyclopedia 4, 148–157. doi: 10.3390/encyclopedia4010013

Pey, A. L., Megarity, C. F., and Timson, D. J. (2019). NAD(P)H quinone oxidoreductase (NQO1): an enzyme which needs just enough mobility, in just the right places. Biosci. Rep. 39, BSR20180459. doi: 10.1042/BSR20180459

Quinlan, A. R., and Hall, I. M. (2010). BEDTools: a flexible suite of utilities for comparing genomic features. Bioinformatics 26, 841–842. doi: 10.1093/bioinformatics/btq033

Ragsdale, S. W., and Pierce, E. (2008). Acetogenesis and the Wood-Ljungdahl Pathway of CO2 Fixation. Biochim. Biophys. Acta 1784, 1873–1898. doi: 10.1016/j.bbapap.2008.08.012

Rodríguez-Díaz, J., Rubio-del-Campo, A., and Yebra, M. J. (2012). Regulatory insights into the production of UDP-N-acetylglucosamine by Lactobacillus casei. Bioengineered 3, 339–342. doi: 10.4161/bioe.21271

Rohart, F., Gautier, B., Singh, A., and Lê Cao, K.-A. (2017). mixOmics: An R package for ‘omics feature selection and multiple data integration. PLOS Comput. Biol. 13, e1005752. doi: 10.1371/journal.pcbi.1005752

Sanjorjo, R. A., Tseten, T., Kang, M.-K., Kwon, M., and Kim, S.-W. (2023). In Pursuit of Understanding the Rumen Microbiome. Fermentation 9, 114. doi: 10.3390/fermentation9020114

Saunois, M., Martinez, A., Poulter, B., Zhang, Z., Raymond, P., Regnier, P., et al. (2025). Global Methane Budget 2000–2020. doi: 10.5194/essd-2024-115

Schären, M., Drong, C., Kiri, K., Riede, S., Gardener, M., Meyer, U., et al. (2017). Differential effects of monensin and a blend of essential oils on rumen microbiota composition of transition dairy cows. J. Dairy Sci. 100, 2765–2783. doi: 10.3168/jds.2016-11994

Sharma, A., Kaushik, V., and Goel, M. (2022). Insights into the Distribution and Functional Properties of l -Asparaginase in the Archaeal Domain and Characterization of Picrophilus torridus Asparaginase Belonging to the Novel Family Asp2like1. ACS Omega 7, 40750–40765. doi: 10.1021/acsomega.2c01127

Shen, W., Sipos, B., and Zhao, L. (2024). SeqKit2: A Swiss army knife for sequence and alignment processing. iMeta 3, e191. doi: 10.1002/imt2.191

Silva, J. V., Conteville, L. C., Bruscadin, J. J., Cardoso, T. F., Porto, T., Oliveira, P. S. N., Zerlotini, A., Medeiros, S. R., Mourão, G. B., Coutinho, L. L., Palhares, J. C. P., Berndt, A., Guan, L., Andrade, B. G. N., & Regitano, L. C. A. (2025). Dietary modulation of the rumen microbiome drives the expression of metabolic and methanogenic pathways in Bos indicus. mSphere. https://doi.org/10.1128/msphere.00535-25

Suen, G., Weimer, P. J., Stevenson, D. M., Aylward, F. O., Boyum, J., Deneke, J., et al. (2011). The Complete Genome Sequence of Fibrobacter succinogenes S85 Reveals a Cellulolytic and Metabolic Specialist. PLoS ONE 6, e18814. doi: 10.1371/journal.pone.0018814

Sun, X., Cheng, L., Jonker, A., Munidasa, S., and Pacheco, D. (2022). A Review: Plant Carbohydrate Types—The Potential Impact on Ruminant Methane Emissions. Front. Vet. Sci. 9, 880115. doi: 10.3389/fvets.2022.880115

Tabita, F. R. (2009). The hydroxypropionate pathway of CO2 fixation: Fait accompli. Proc. Natl. Acad. Sci. 106, 21015–21016. doi: 10.1073/pnas.0912486107

Tian, Y., Wang, Y., Zhong, Y., Møller, M. S., Westh, P., Svensson, B., et al. (2023). Interfacial Catalysis during Amylolytic Degradation of Starch Granules: Current Understanding and Kinetic Approaches. Molecules 28, 3799. doi: 10.3390/molecules28093799

Ungerfeld, E. M. (2020). Metabolic Hydrogen Flows in Rumen Fermentation: Principles and Possibilities of Interventions. Front. Microbiol. 11, 589. doi: 10.3389/fmicb.2020.00589

Volmer, J. G., McRae, H., and Morrison, M. (2023). The evolving role of methanogenic archaea in mammalian microbiomes. Front. Microbiol. 14, 1268451. doi: 10.3389/fmicb.2023.1268451

Vreeland, R., Straight, S., Krammes, J., Dougherty, K., Rosenzweig, W., and Kamekura, M.

(2002). Halosimplex carlsbadense gen. nov., sp. nov., a unique halophilic archaeon, with three 16S rRNA genes, that grows only in defined medium with glycerol and acetate or pyruvate. Extremophiles 6, 445–452. doi: 10.1007/s00792-002-0278-3

Wang, L., Wu, D., Zhang, Y., Li, K., Wang, M., and Ma, J. (2023). Dynamic distribution of gut microbiota in cattle at different breeds and health states. Front. Microbiol. 14, 1113730. doi: 10.3389/fmicb.2023.1113730

Wang, Q., Wang, Y., Wang, X., Dai, C., Tang, W., Li, J., et al. (2020). Effects of dietary energy levels on rumen fermentation, microbiota, and gastrointestinal morphology in growing ewes. Food Sci. Nutr. 8, 6621–6632. doi: 10.1002/fsn3.1955

Weimer, P. J. (2022). Degradation of Cellulose and Hemicellulose by Ruminal Microorganisms. Microorganisms 10, 2345. doi: 10.3390/microorganisms10122345

Westerhuis, J. A., Kourti, T., and MacGregor, J. F. (1998). Analysis of multiblock and hierarchical PCA and PLS models. J. Chemom. 12, 301–321. doi: 10.1002/(SICI)1099-128X(199809/10)12:5<301::AID-CEM515>3.0.CO;2-S

Wood, D. E., Lu, J., and Langmead, B. (2019). Improved metagenomic analysis with Kraken 2. Genome Biol. 20, 257. doi: 10.1186/s13059-019-1891-0

Woolson, R. F., Bean, J. A., and Rojas, P. B. (1986). Sample Size for Case-Control Studies Using Cochran's Statistic. Biometrics 42, 927. doi: 10.2307/2530706

Wu, L., and Luo, Y. (2021). Bacterial Quorum-Sensing Systems and Their Role in Intestinal Bacteria-Host Crosstalk. Front. Microbiol. 12, 611413. doi: 10.3389/fmicb.2021.611413

Xie, F., Jin, W., Si, H., Yuan, Y., Tao, Y., Liu, J., et al. (2021). An integrated gene catalog and over 10,000 metagenome-assembled genomes from the gastrointestinal microbiome of ruminants. Microbiome 9, 137. doi: 10.1186/s40168-021-01078-x

Xu, N., Zhang, W., Ren, S., Liu, F., Zhao, C., Liao, H., et al. (2012). Hemicelluloses negatively affect lignocellulose crystallinity for high biomass digestibility under NaOH and H2SO4 pretreatments in Miscanthus. Biotechnol. Biofuels 5, 58. doi: 10.1186/1754-6834-5-58

Xue, M.-Y., Xie, Y.-Y., Zhong, Y., Ma, X.-J., Sun, H.-Z., and Liu, J.-X. (2022). Integrated meta-omics reveals new ruminal microbial features associated with feed efficiency in dairy cattle. Microbiome 10, 32. doi: 10.1186/s40168-022-01228-9

Yang, Z., Wang, W., He, Y., Zhang, R., and Liu, G. (2018). Effect of ammonia on methane production, methanogenesis pathway, microbial community and reactor performance under mesophilic and thermophilic conditions. Renew. Energy 125, 915–925. doi: 10.1016/j.renene.2018.03.032

Yuan, Y., Conrad, R., and Lu, Y. (2009). Responses of methanogenic archaeal community to oxygen exposure in rice field soil. Environ. Microbiol. Rep. 1, 347–354. doi: 10.1111/j.1758-2229.2009.00036.x

Zhao, H., Bai, S., Tan, J., Liu, M., Zhao, Y., and Jiang, L. (2024). Can meta-omics revolutionize our understanding of rumen methane emissions? Anim. Nutr. 1, e14. doi: 10.1017/anr.2024.18

Zheng, J., Ge, Q., Yan, Y., Zhang, X., Huang, L., and Yin, Y. (2023). dbCAN3: automated carbohydrate-active enzyme and substrate annotation. Nucleic Acids Res. 51, W115–W121. doi: 10.1093/nar/gkad328

4 Host–Microbiome data integration: integrating metatranscriptomics and rumen wall microRNA to unravel functional interactions within the *Bos indicus* holobiont

This chapter investigates the interactions between the *Bos indicus* (Nelore) bovine host and its ruminal microbiota through an integrative approach that combines metatranscriptomic, and microRNA data. Based on the concept of the holobiont, which considers the animal and its associated microorganisms as an ecological and functional unit, the study aims to understand how microbial and host gene regulatory mechanisms interact. This multi-omics integration provides a comprehensive view of the *Bos indicus* holobiont and contributes to a deeper understanding of the molecular interactions that support the host–microbiota symbiosis in *Bos indicus.* This section includes excerpts from the manuscript in preparation, "Host-Microbiome data integration: integrating metatranscriptomics and host microRNA to unravel functional interactions within the *Bos indicus* holobiont".

Title: Host-Microbiome data integration: integrating metatranscriptomics and host microRNA to unravel functional interactions within the *Bos indicus* holobiont

Juliana Virginio da Silva, Liliane Costa Conteville, Thanny Porto, Tainã Figueiredo Cardoso, Gerson Barreto Mourão, Luiz Lehmann Coutinho, Adhemar Zerlotini, Bruno Gabriel Nascimento Andrade, LeLuo Guan, Luciana Correia de Almeida Regitano

4.1 Introduction

The global demand for animal-derived food products, particularly meat and milk, is projected to rise substantially by 2050 (Henchion et al., 2021; Badhan et al., 2025). In response, livestock systems are under mounting pressure to adopt more sustainable and efficient production practices, especially those that optimize nutrient utilization from forage-based diets while reducing environmental impacts (Cole et al., 2018). In this context, ruminants, particularly the *Bos indicus* Nelore breed, which represents nearly 80% of the Brazilian cattle herd, play a central role in sustaining Brazil's position as a global leader in beef production and exports (Barbosa et al., 2014; Da Silva et al., 2023).

A key element of ruminant productivity lies in the functionality of the rumen, a fermentation chamber that allows the conversion of fibrous plant material into high-quality animal protein (Malmuthuge et al., 2019). This process is driven by a diverse microbial community, comprising bacteria, archaea, protozoa, and fungi, that produces enzymes to degrade structural polysaccharides. Fermentation produces short-chain volatile fatty acids (VFAs), providing more than 70% of the host's energy (Henderson et al., 2015; Malmuthuge et al., 2019). However, hydrogen released during fermentation is consumed by

methanogenic archaea to form methane (CH_4), resulting in an energy loss of 2–12% through gaseous emissions (Hook et al., 2010). For this reason, improving the efficiency of ruminal digestion is essential to increase productivity and mitigate environmental impacts (Badhan et al., 2025).

Beyond microbial composition and enzymatic functionality, increasing attention has been given to the molecular mechanisms underlying host-microbiome interactions. These interactions are framed by the concepts of the holobiont and hologenome, which view the host and its associated microbiota as a single, integrated biological and genetic unit (Margulis and Fester, 1991; Rosenberg et al., 2007). Within this context, microRNAs (miRNAs) have emerged as key mediators of host-microbe communication. First described in 1993, in eukaryotes, miRNAs were shown to regulate gene expression by binding to complementary sequences in the 3′-untranslated regions (3′-UTRs) of target mRNAs (Lee et al., 1993; Wightman et al., 1993). Since then, it has become clear that miRNAs can also interact with coding regions, thereby exerting a tight post-transcriptional control regulation of gene expression (Ojo and Kreuzer-Redmer, 2023). A single miRNA can modulate the expression of hundreds of genes, thereby influencing a wide array of cellular functions, including immune response, gut barrier integrity, and inflammation (Liu et al., 2016; Ricci et al., 2022).

In the gastrointestinal tract (GIT), a major site of host–microbe interactions, miRNAs have been implicated in modulating microbial activity and shaping community composition (Liang et al., 2014; Liu et al., 2016; Ricci et al., 2022). In ruminants, emerging evidence suggests that miRNAs contribute to host-microbe interactions by modulating nutrient absorption, metabolism, and immune responses in the digestive system (Liang et al., 2014; Ricci et al., 2022; Ojo and Kreuzer-Redmer, 2023). Additionally, host-derived miRNAs are capable of modulating bacterial gene expression at the post-transcriptional level, potentially altering the microbial community abundance or function (Cuinat et al., 2025). They may also be internalized by bacterial cells through endocytosis, where they selectively regulate gene transcripts and impact bacterial proliferation (Datta et al., 2023).

Importantly, this cross-talk can be bidirectional. While the host can shape microbial communities through miRNAs, bacteria can also influence the host through small RNAs (sRNAs) (Koeppen et al., 2016). Some bacterial species have been shown to release sRNAs capable of modulating host gene expression, not only altering host miRNA profiles but also directly impacting transcriptional responses (Yuan et al., 2018). Some studies have shown that bacteria can actively modulate host miRNA expression to favor their own survival or function (Das et al., 2016; Aguilar et al., 2019). Also, miRNA expression profiles are influenced by the composition of the microbiota (Viennois et al., 2019), reinforcing the bidirectional nature of this interaction.

In cattle, miRNAs produced by rumen epithelial cells can be secreted into rumen fluid (*e.g.* via exosomes) and thus come into contact with microbes (Ricci et al., 2022). These authors were the first to identify hundreds of host-derived miRNAs in the rumen of Holstein cows, with specific miRNAs showing associations with microbial taxa or functions. For example, the bta-miR-487b was correlated with *Ruminococcus* abundance, and with methane metabolism, indicating a potential role of miRNA regulating methane production. In a Nelore population, fecal miRNAs showed significant correlations with bacterial taxa such as *Prevotella*, *Bifidobacterium*, and *Coriobacteriaceae* suggesting that miRNAs may act as regulators of microbiome composition and contribute to feed efficiency phenotypes in beef cattle (Oliveira et al., 2024). In line with this, a study in dairy calves revealed temporal and regional changes in miRNA expression and a correlation between miRNA expression and microbial population in the GIT during early life, which provides evidence for the role of host-microbial interactions in regulating gut development (Liang et al., 2014). Also, the capacity of host miRNAs to respond to microbial signals has been documented in other tissues. In bovine mammary epithelium, for instance, the presence of *Staphylococcus aureus* was shown to modulate host responses through altered miRNA expression. The downregulation of miR-31 and miR-205, alongside the upregulation of miR-223, suggests transcriptional adaptations aimed at controlling inflammation, initiating immune responses, or repairing tissue damage (Li et al., 2012).

Despite this emerging evidence in model organisms (Dalmasso et al., 2011; Liu et al., 2016) and *Bos taurus* (Li et al., 2012; Ricci et al., 2022), the role of host-derived miRNAs in modulating the active rumen microbiome, particularly in *Bos indicus* cattle, remains largely unexplored. Considering the intricate and mutualistic relationship between the rumen microbiota and its host, and the evolutionary importance of this symbiosis for feed digestion and animal performance, an integrative multi-omic approach is warranted. The integration of metatranscriptomics and host miRNA expression profiles offers a powerful framework to elucidate functional interactions within the *Bos indicus* holobiont. Such integration may uncover novel molecular mechanisms underpinning microbial adaptation, host nutrient utilization, and ultimately, productive efficiency and environmental sustainability in tropical beef systems.

4.2 Methodology

4.2.1 Animals and sample collection

All experimental procedures followed the Animal Welfare and Humane Slaughter guidelines and were approved by EMBRAPA Livestock Science Ethics Committee on Animal Experimentation, São Carlos, São Paulo, Brazil (Protocol No. 09/2016). The experiment was

conducted in the feedlot facilities of Embrapa Pecuária Sudeste, involving 46 non-castrated Nelore males born in 2014 and slaughtered in 2016. These animals were descendants of 28 commercial Nelore bulls, with an average of 1.78 offspring per bull.

Due to initial body weight heterogeneity, heavier and lighter animals were evenly allocated within each diet group (conventional and by-product). The feedlot experiment lasted for 90 or 121 days, depending on the initial body weight. This included 10 days for animal adaptation to the feedlot, 29 days for heavy animals and 55 days for light animals in the growing phase, 51 days for heavy animals and 56 days for light animals in the finishing phase. The animals were sent to slaughter at 23-24 months of age after fasting from food and water for 16 hours, according to the current Brazilian Ministry of Agriculture, Livestock, and Food Supply (MAPA) regulations.

Approximately 50 mL of ruminal content was collected immediately after slaughter, frozen in liquid nitrogen and stored at −80 °C before DNA and RNA extraction. For the rumen wall samples, the collection position was standardized from the lateral wall of the rumen, approximately 5 cm below the esophagus and just after the edge of the reticulum, including all rumen wall layers, using the esophageal opening and reticulum as references. This procedure was described in detail by Fernandes et al (2024). The rumen wall samples were also frozen in liquid nitrogen and stored at −80 °C before analysis.

4.2.2 Taxonomic and functional profile of ruminal microbiome

The taxonomic and functional profiles analyzed in this study were derived from the active fraction of the Nelore Ruminal Prokaryotic Microbiome Gene Catalog (aNRPMG), as previously described in chapter 3 of this thesis. In brief, to identify transcriptionally active genes, metatranscriptomic reads were mapped to the Nelore Ruminal Prokaryotic Microbiome Gene (NRPMG) catalog, a comprehensive non-redundant gene catalog constructed from ruminal metagenomes of Nelore cattle. Gene expression was normalized using a modified Reads Per Kilobase per Million mapped reads (RPKM) approach that accounts for the total number of sequenced reads per sample. To ensure robustness, a prevalence filter was applied to the aNRPMG, retaining only genes expressed in at least 20% of the samples. Expression values were then corrected for potential batch effects using the MMUPHin adjust_batch model (Ma et al., 2022), accounting for confounding factors such as dietary treatment and contemporary groups (*e.g.*, weighing and slaughter groups).

Taxonomic classification of aNRPMG was conducted by subsetting the NRPMG to retain only the transcriptionally active CDS. The resulting sequences were classified using Kraken2 v. 2.1.2 (Wood et al., 2019) against the NCBI RefSeq bacterial and archaeal genomes, and taxonomic assignments were aggregated at the genus level. Genus-level expression was calculated by summing RPKM values of all constituent genes.

Low-abundance genera (<1% relative abundance across all samples) were filtered out separately for bacterial and archaeal datasets.

Functional annotation was first performed in the NRPMG to establish the global functional repertoire. Assignment of Clusters of Orthologous Groups (COGs) and KEGG Orthologies (KOs) was carried out with eggnog-mapper v2.1.12 (Cantalapiedra et al., 2021). In parallel, identification of Carbohydrate-Active enZymes (CAZymes) was accomplished using the run_dbcan3 pipeline (Lombard et al., 2014; Zheng et al., 2023), retaining only those CAZyme predictions supported by at least two out of three detection methods. From this dataset, the corresponding annotations of genes with transcriptional activity were retrieved and retained, as the functional annotation of the aNRPMG. Functional expression profiles were then calculated by summing the RPKM values of genes assigned to each COG, KO, or CAZyme IDs.

4.2.3 miRNA data

To extract total RNA from the ruminal wall, approximately 100 mg of frozen tissue was ground, and RNA was isolated using TRIzol® (Carlsbad, CA, USA), following the standard protocol (Carlsbad, CA, USA). The RNA concentration and integrity were evaluated with a Bioanalyzer 2100® (Santa Clara, CA, USA). Only samples with RNA Integrity Number (RIN) > 6 were selected. In this step, four samples were eliminated. miRNA library preparation and sequencing were conducted at the Genomics Center at ESALQ (Piracicaba, São Paulo, Brazil) according to the protocol described by Illumina. Single-end sequencing of 42 bp fragments was carried out on an Illumina MiSeq sequencer (San Diego, CA, USA) via the MiSeq Reagent Kit v3 (150 cycles).

Read quality was assessed with FastQC v.0.11.9 (Andrews, 2010). Quality and length filtering were then performed with FASTX-Toolkit v.0.0.14 (Gordon, 2009), discarding reads with a Phred quality score <28 and <18 nt. The remaining reads were subjected to the miRDeep2 software v. 2.0.1.2 (Friedländer et al., 2012) and aligned to the ARS-UCD1.2 bovine reference genome using default parameters. Mature bovine and human miRNA sequences were retrieved from miRBase v.22 (Griffiths-Jones, 2006) and used as reference.

The miRNA raw counts were also adjusted for potential batch effects, accounting for confounding factors such as dietary treatment and contemporary groups, which encompassed weighing and slaughter batches. Subsequently, the counts were normalized using the counts per million (CPM) method implemented by NOISeq software v. 3.11 (Tarazona et al., 2015). Features with low expression (CPM < 1 in 50% of the samples) were filtered out.

4.2.4 Module construction and Host-Microbiome data integration

Coexpression modules were first constructed independently for each of the three molecular profiles: active microbial enzymes, active microbial genera, and miRNAs expressed in the rumen wall, using the Weighted Correlation Network Analysis (WGCNA) package (Langfelder and Horvath, 2008). For each dataset, the standard WGCNA pipeline was applied, including the selection of the soft-thresholding power (pickSoftThreshold), construction of the adjacency matrix (adjacency) and the topological overlap matrix (TOMsimilarity), followed by hierarchical clustering (hclust) and module detection (*cutreeDynamic).* After module identification, the module eigengene, that represents the first principal component of each module, was calculated using *moduleEigengenes* function. The correlation between each feature and its respective module eigengene was computed using the *signedKME* function, yielding kME values. Intramodular connectivity metrics (kWithin, kTotal, kOut, and kDiff) were obtained using the *intramodularConnectivity* function. For each module, the main hub was identified using *chooseTopHubInEachModule* function.

Additionally, highly representative features were selected for kME ≥ 0.90, ranked by their kWithin values and labeled with their respective kME in parentheses. The final summary table for each module included the module color, the total number of features, the main hub, and the list of top representative features. The gray module, which contains unassigned enzymes, was not included in further analyses.

After constructing the individual networks for each feature set, we assessed the relationships between microbial and host miRNAs modules. Thus, pairwise coexpression networks were constructed for enzyme–miRNA and genus–miRNA datasets using WGCNA (Langfelder and Horvath, 2008). To assess cross-omics relationships, we calculated the correlation between module eigengenes (Langfelder and Horvath, 2007, 2008; Lin et al., 2023). Modules were considered associated when the absolute value of the correlation coefficient (|r|) was greater than 0.3 and p-value ≤ 0.05.

4.3 Results

4.3.1 Enzyme coexpression module

The final processed dataset comprised 3,306 enzyme features, which were grouped into 14 coexpression modules. The largest module was the *turquoise*, comprising 934 enzymes, followed by the *blue* (N = 856), *brown* (N = 349), *yellow* (N = 223), and *green* (N = 180) modules (Table 1). Among the identified hub enzymes were Glycoside Hydrolase Family 127 (GH127; turquoise, kME = 0.968), Glycosyltransferase Family 51 subfamily e160 (GT51_e160; blue, kME = 0.987), arCOG04870 (brown, kME = 0.947), Glycoside Hydrolase

Family 3 subfamily e0 (GH3_e0; yellow, kME = 0.909), and Carbohydrate-Binding Module Family 89 (CBM89; green, kME = 0.935).

Table 1: Summary of enzyme-coding transcripts co-expression modules identified by WGCNA from Nelore rumen prokaryote microbiome. The table reports the module label, the number of enzymes assigned to each module, the hub enzyme, and enzymes with strong module membership (kME ≥ 0.90).

Module	Number of enzymes	Hub	Enzymes with kME ≥ 0.90
turquoise	934	GH127	GH127 (0.968), GH127_e0 (0.968), CBM77_e0 (0.959), GH5_e293 (0.964), GH125 (0.945), GH125_e1 (0.945), COG4225 (0.946), COG3000 (0.944), GH74_e0 (0.95), K11204 (0.942), PL1 (0.944), GH5_e156 (0.945), GH74 (0.946), CBM67 (0.935), CBM67_e28 (0.935), COG1982 (0.945), GH78 (0.933), COG0457 (0.936), COG4642 (0.936), CBM37 (0.939), GH13_e122 (0.947), GH31 (0.939), COG1278 (0.932), COG0003 (0.95), GH32_e16 (0.941), GH5_4 (0.937), PL8 (0.93), CBM77 (0.93), PL1_e59 (0.93), GH27 (0.943), GH43_4 (0.939), GH43_e149 (0.939), PL33_1 (0.927), PL33_e11 (0.927), GH5_e70 (0.925), GH27_e14 (0.941), CE3_e10 (0.926), GH43_24 (0.935), GH43_e144 (0.935), arCOG00695 (0.93), COG3866 (0.932), GH78_e83 (0.923), PL31_e6 (0.927), GH19_e50 (0.933), K11417 (0.922), GH105_e39 (0.926), GH43_22 (0.937), COG1538 (0.919), K04720 (0.919), GH5_27 (0.931), GH31_e66 (0.922), K13712 (0.914), CBM13_e240 (0.92), PL31 (0.926), CE3 (0.926), GH78_e80 (0.914), GH9_e27 (0.922), K01728 (0.927), K01904 (0.924), GH31_e94 (0.915), GH124 (0.925), GH124_e0 (0.925), CBM50_e826 (0.917), COG0402 (0.929), GH2_e136 (0.92), CE7 (0.923), GH19 (0.911), CBM13 (0.915), GH5_e236 (0.912), K00922 (0.906), GH9 (0.91), K01179 (0.918), GH30_5 (0.922), GH5_e22 (0.906), K04710 (0.913), K11936 (0.903), COG5050 (0.907), K00993 (0.907), K00994 (0.907), K13644 (0.907), K05291 (0.92), GH105 (0.911), COG0024 (0.903), K01108 (0.915), COG0814 (0.919), K12960 (0.911), GH154 (0.901), GH154_e2 (0.901), COG0194 (0.901), COG4677 (0.907), K02225 (0.912), GH3 (0.911), GH97_e18 (0.9)
blue	856	GT51_e160	GT51_e160 (0.987), COG3407 (0.986), K01597 (0.986), COG0490 (0.984), GT51 (0.983), GH89_e5 (0.98), GT4_e2848 (0.982), COG0502 (0.983), K01012 (0.983), K07043 (0.981), GT83 (0.98), GT83_e87 (0.98), COG3669 (0.98), COG0475 (0.976), GH3_e217 (0.98), K00980 (0.977), GT9_e147 (0.981), COG3142 (0.977), COG0801 (0.977), GH20 (0.977), CBM50_e207 (0.975), CBM50_e954 (0.975), GH23_e731 (0.975), GH92 (0.973), GH92_e0 (0.973), K19294 (0.972), GT4_e1153 (0.977), GT4_e2572 (0.977),

			K01241 (0.971), K00950 (0.972), K00869 (0.973), GH33 (0.974), GH33_e107 (0.974), K13019 (0.973), K10774 (0.973), COG1680 (0.971), arCOG02559 (0.974), arCOG03264 (0.974), arCOG03771 (0.974), COG4945 (0.974), COG2103 (0.972), K07106 (0.972), COG2171 (0.97), K00674 (0.97), COG3104 (0.968), K00748 (0.965), GT19 (0.965), GT19_e2 (0.965), COG0382 (0.969), K03179 (0.969), K00790 (0.966), K11754 (0.965), K13766 (0.963), COG1572 (0.965), K05515 (0.963), K01916 (0.96), GH109_e5 (0.962), COG1577 (0.965), COG0609 (0.961), COG1418 (0.961), K01480 (0.96), K19302 (0.956), COG1611 (0.954), COG0414 (0.955), K01918 (0.955), CE4_e293 (0.958), COG0343 (0.954), COG1729 (0.957), COG4783 (0.957), COG0438 (0.958), COG2986 (0.957), K01745 (0.957), COG2067 (0.956), COG1179 (0.958), COG3155 (0.955), GH29 (0.954), K13566 (0.955), COG0260 (0.956), K01255 (0.956), CBM32_e126 (0.954), GH29_e30 (0.954), K18011 (0.951), arCOG01033 (0.954), K12234 (0.954), COG0853 (0.959), K01579 (0.959), GT9 (0.954), K00812 (0.954), COG0284 (0.947), K01591 (0.947), COG1166 (0.949), GH3_e88 (0.947), COG2877 (0.947), GH97_e22 (0.949), GT2 (0.947), COG0635 (0.955), COG1126 (0.95), COG1646 (0.945), K07094 (0.945), COG0701 (0.947), COG2031 (0.948), K01479 (0.945), COG2812 (0.944), GH97_e1 (0.95), GT4_e2745 (0.95), COG0041 (0.951), K01588 (0.951), GT4_e1850 (0.95), COG3808 (0.94), K01692 (0.941), K20036 (0.941), K03857 (0.942), GT4_e608 (0.942), K00100 (0.941), K07029 (0.943), COG1770 (0.943), GT4_e4035 (0.938), GH23_e567 (0.942), COG0517 (0.939), GT30 (0.934), GT30_e38 (0.934), K03274 (0.94), COG0413 (0.943), K00606 (0.943), COG1228 (0.944), K01468 (0.944), CBM32_e198 (0.934), K03269 (0.936), K02517 (0.936), COG1283 (0.944), K01969 (0.93), COG0665 (0.932), GH23 (0.94), GH73_e88 (0.937), COG1539 (0.939), K01633 (0.939), GH2_e1 (0.936), COG4232 (0.936), COG1505 (0.937), COG2957 (0.93), K10536 (0.93), COG3537 (0.93), K15866 (0.927), COG1428 (0.937), COG0659 (0.934), COG1703 (0.938), GT3 (0.926), GT3_e2 (0.926), COG0095 (0.933), K03800 (0.933), COG1477 (0.931), COG0285 (0.923), GT4 (0.929), COG2356 (0.922), K21574 (0.929), K00657 (0.928), K09474 (0.925), COG3176 (0.925), K00819 (0.926), K17828 (0.92), K00796 (0.922), K04486 (0.924), K00798 (0.919), COG0043 (0.918), K03272 (0.917), COG1109 (0.922), GH73 (0.92), COG1521 (0.918), COG2987 (0.91), K01712 (0.91), COG0603 (0.913), K03273 (0.917), K01186 (0.918), K01139 (0.92), K03525 (0.917), K00177 (0.915), K02536 (0.919), COG0047 (0.919), COG0809 (0.908), COG0204 (0.927), COG1257 (0.912), K00054 (0.912), K13016 (0.908), COG0168 (0.908), K06949 (0.923), COG2374 (0.915), COG0171 (0.907), COG1183 (0.909), K17103 (0.909), K13788 (0.909), K02843 (0.917), COG2878 (0.912), K00266 (0.911), K06881 (0.909),

			COG1280 (0.907), K09001 (0.905), COG0279 (0.914), K03271 (0.914), K00625 (0.917), COG1143 (0.907), K00175 (0.902), COG1213 (0.91), COG1014 (0.904), COG0138 (0.903), K00602 (0.903), K03783 (0.904), K10026 (0.908), K02563 (0.905), COG1636 (0.901), K00831 (0.906), COG4992 (0.904), COG0297 (0.903), K13821 (0.901), K00757 (0.901), COG2226 (0.903)
brown	349	arCOG04870	arCOG04870 (0.947), COG4059 (0.947), K00581 (0.947), arCOG01549 (0.944), COG0374 (0.941), arCOG03225 (0.937), COG4056 (0.937), K03421 (0.937), arCOG02653 (0.928), K00125 (0.928), arCOG04336 (0.922), COG1962 (0.922), K00584 (0.922), arCOG02410 (0.926), COG2141 (0.926), K00320 (0.926), COG1941 (0.916), arCOG00292 (0.919), K11260 (0.919), K14126 (0.9), arCOG04461 (0.903), COG1229 (0.903), K00200 (0.903), arCOG04869 (0.903), COG4060 (0.903), K00580 (0.903)
yellow	223	GH3_e0	GH3_e0 (0.909), COG0129 (0.918), COG1312 (0.919), COG0458 (0.905)
green	180	CBM89	CBM89 (0.935), CBM89_e0 (0.935), GH10_e38 (0.935), PL11_1 (0.932), PL11_e0 (0.932), CE8_e50 (0.93), GT51_e17 (0.925), GT9_e65 (0.934), GH23_e330 (0.93), GH2_e20 (0.921), GH25_e166 (0.92), PL1_2 (0.921), CBM13_e332 (0.917), GH105_e30 (0.91), GH28_e80 (0.91), COG1524 (0.91), PL1_e60 (0.911), GH2_e137 (0.911), GH28_e44 (0.912), GH43_e327 (0.912), GH28_e101 (0.905), CBM91_e37 (0.904), GH43_e163 (0.904), COG0428 (0.904), GH43_e68 (0.901), COG0337 (0.903), K01735 (0.903), COG3589 (0.901)
red	152	GH13_8	GH13_8 (0.945), GH13_e20 (0.945), CBM48_e32 (0.942), K00658 (0.93), GH24 (0.925), GH24_e26 (0.918), COG0346 (0.92), COG0033 (0.919), GH32 (0.925), GH32_e1 (0.922), COG3772 (0.922), CBM48 (0.906), K00700 (0.921), K00853 (0.91), COG3584 (0.919), K01835 (0.901)
black	143	COG5026	COG5026 (0.933), K00844 (0.933), GH142 (0.934), K13713 (0.92), K00841 (0.907), COG0114 (0.906), K01679 (0.906), COG0326 (0.913)
pink	108	GH77_e27	GH77_e27 (0.907), GH13_9 (0.906), GH13_e200 (0.906), CBM48_e2 (0.905)
magenta	103	K11180	K11180 (0.919), K11181 (0.908), COG2046 (0.905), K00958 (0.905), K13811 (0.905), K00395 (0.906)
purple	82	COG0301	COG0301 (0.957), K03151 (0.957), GT1_e483 (0.961), CBM13_e170 (0.959), GH28_e111 (0.952), K22410 (0.93), PL1_e73 (0.939), K00411 (0.922), GT1 (0.923), K19270 (0.916), GH43_e298 (0.916)
greenyellow	52	GH5_e281	GH5_e281 (0.921), CE6_e3 (0.92), K16951 (0.906)
tan	46	arCOG03009	arCOG03009 (0.96), COG2333 (0.96), CBM6_e71 (0.901)
salmon	41	K17716	K17716 (0.978), K06131 (0.97), K21030 (0.959), K10811

			(0.957), K04107 (0.957), COG0821 (0.947), K03526 (0.947), K19970 (0.922), K21053 (0.919), K00073 (0.917), K03431 (0.923), arCOG03999 (0.909), COG0344 (0.902), K08591 (0.902)
cyan	32	COG1049	COG1049 (0.953), K01682 (0.953), GH13_37 (0.947), GH13_e203 (0.947), COG2959 (0.916), K02496 (0.916), K00795 (0.927), COG3071 (0.92), COG3633 (0.923), GH13_e69 (0.904), COG1562 (0.918), K00801 (0.918)

4.3.2 miRNA coexpression module

Of the 385 miRNAs obtained from the rumen wall, two coexpression modules were identified. The turquoise module included 123 miRNAs, while the blue module contained 52 miRNAs (Table 2). The main hub miRNAs were bta-miR-378 in the turquoise module (kME = 0.913) and bta-miR-181c in the blue module (kME = 0.97).

Table 2: Summary of miRNA co-expression modules identified by WGCNA from Nelore rumen wall. The table reports the module label, the number of miRNA assigned to each module, the hub miRNA, and the miRNA with strong module membership (kME ≥ 0.90).

Module	Number of miRNA	Hub	miRNA with kME ≥ 0.90
turquoise	123	bta-miR-378	bta-miR-378 (0.913), bta-miR-93 (0.966), bta-miR-92a (0.938), bta-miR-425-5p (0.965), bta-miR-106b (0.934), bta-miR-182 (0.902), bta-miR-15b (0.964), bta-miR-17-3p (0.945), bta-miR-20a (0.918), bta-miR-25 (0.918), bta-miR-17-5p (0.905), bta-miR-15a (0.924), bta-miR-92b (0.919), bta-miR-16b (0.910)
blue	52	bta-miR-181c	bta-miR-181c (0.97), bta-miR-133a (0.953), bta-miR-1 (0.933), bta-miR-100 (0.942), bta-miR-181d (0.964), bta-miR-490 (0.931), bta-miR-143 (0.907), bta-miR-145 (0.913), bta-miR-192 (0.951), bta-miR-29d-5p (0.903), bta-miR-194 (0.902), bta-miR-29c (0.928), bta-miR-10182-5p (0.914), bta-miR-28 (0.91)

4.3.3 Genera coexpression module

A total of 507 active microbial genera were included in the analysis, comprising 458 bacteria and 49 archaea. Coexpression analysis grouped these genera into five modules, with turquoise being the largest (187 genera), followed by blue (119), brown (89), yellow (65), and green (36) (Table 3). Hub genera identified within these modules were *Bulleidia*

(turquoise, kME = 0.961), *Oscillibacter* (blue, kME = 0.906), *Bosea* (brown, kME = 0.98), *Ilyobacter* (yellow, kME = 0.964), and *Rodentibacter* (green, kME = 0.935).

Table 3: Summary of active microbiota genera co-expression modules identified by WGCNA from Nelore rumen. The table reports the module label, the number of genera assigned to each module, the hub genera, and the genera with strong module membership (kME ≥ 0.90).

Module	**Number of Genera**	**Hub**	**Genera with kME ≥ 0.90**
turquoise	187	*Bulleidia*	*Bulleidia (0.961), Marinitoga (0.953), Agrobacterium (0.94), Fictibacillus (0.932), Lactiplantibacillus (0.939), Mesoplasma (0.912), Scytonema (0.921), Mariniplasma (0.924), Sedimentibacter (0.915), Weissella (0.929), Stygiolobus (0.906), Olleya (0.915), Halorhabdus (0.905), Mariniflexile (0.904), Finegoldia (0.9)*
blue	119	*Oscillibacter*	*Oscillibacter (0.906), Faecalibacterium (0.921), Flavonifractor (0.91), Enterocloster (0.902)*
brown	89	*Bosea*	*Bosea (0.98), Candidatus Vallotiella (0.97), Geobacter (0.973), Alkalitalea (0.965), Janibacter (0.963), Candidatus Atelocyanobacterium (0.959), Lawsonia (0.958), Alistipes (0.967), Loigolactobacillus (0.957), Dokdonia (0.954), Methylomusa (0.953), Syntrophotalea (0.955), Sphingobacterium (0.956), Butyricimonas (0.956), Wenyingzhuangia (0.938), Sulfuritortus (0.936), Niabella (0.937), Formosa (0.933), Salinivirga (0.933), Wenzhouxiangella (0.927), Salegentibacter (0.922), Dongshaea (0.927), Pseudopedobacter (0.919), Photorhabdus (0.922), Mycolicibacterium (0.914), Microvirga (0.915), Paraburkholderia (0.913), Agarivorans (0.903), Lysinibacillus (0.901), Deinococcus (0.908), Spirosoma (0.906)*
yellow	65	*Ilyobacter*	*Ilyobacter (0.964), Brachyspira (0.921), Bordetella (0.944), Lacibacter (0.933), Melissococcus (0.905), Candidatus Endomicrobiellum (0.935), Mesorhizobium (0.922), Pyrococcus (0.914), Crassaminicella (0.919), Picrophilus (0.902), Halobacteriovorax (0.914), Geoalkalibacter (0.901)*
green	36	*Rodentibacter*	*Rodentibacter (0.935), Succinivibrio (0.955), Aggregatibacter (0.904)*

4.3.4 Coexpression between enzyme and miRNAs modules

The coexpression network integrating ruminal enzymes and host miRNAs revealed three significant coexpression modules (|r| ≥ 0.3 and p ≤ 0.05; Figure 1). The enzyme *blue*

module was negatively correlated with the miRNA *blue* module (cor = −0.31, p = 0.04) and positively correlated with the *turquoise* miRNA module (cor = 0.31, p = 0.04). The enzyme *yellow* module showed a negative correlation with the *blue* miRNA module (cor = −0.33, p = 0.03). The gray modules, which contain features that could not be assigned to any co-expression cluster, are shown for completeness but were not included in subsequent analyses.

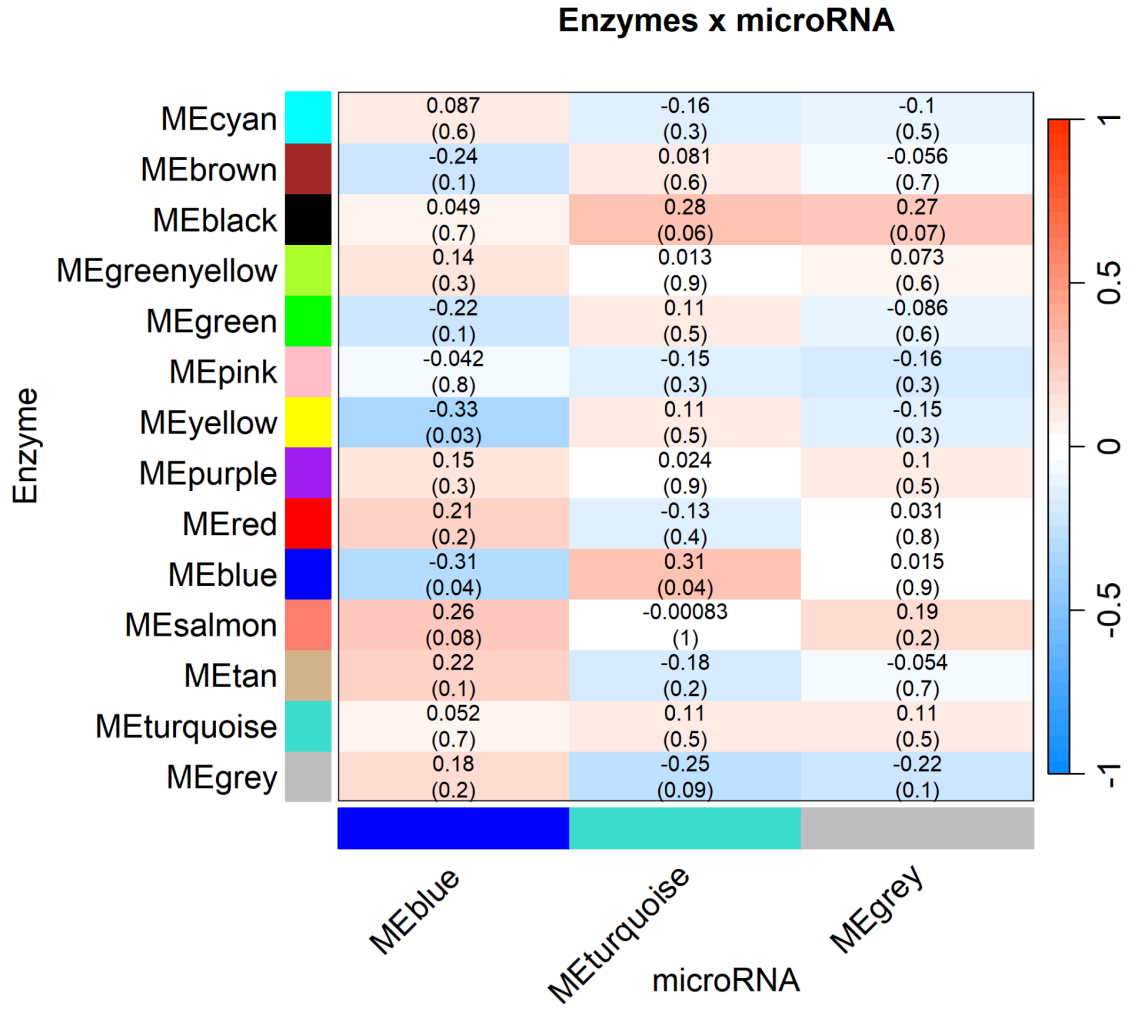

Figure 1: Correlation between enzyme and microRNA modules identified by WGCNA. Heatmap shows correlations between module eigengenes. Each cell displays the correlation coefficient, with the corresponding *p*-value shown in parentheses. Red and blue indicate positive and negative associations, respectively, and color intensity reflects correlation strength.

4.3.5 Coexpression between miRNA and genus modules

The integrated coexpression analysis between host miRNAs and ruminal genera uncovered two significant modules, considering |r| ≥ 0.3; p ≤ 0.05; Figure 2): the miRNA blue

module was negatively associated with the genera brown module (cor = −0.31, p = 0.03) and miRNA turquoise module was positively associated with the genera brown module (cor = −0.29, p = 0.05). The gray modules, which contain features that could not be assigned to any co-expression cluster, are shown for completeness but were not included in subsequent analyses.

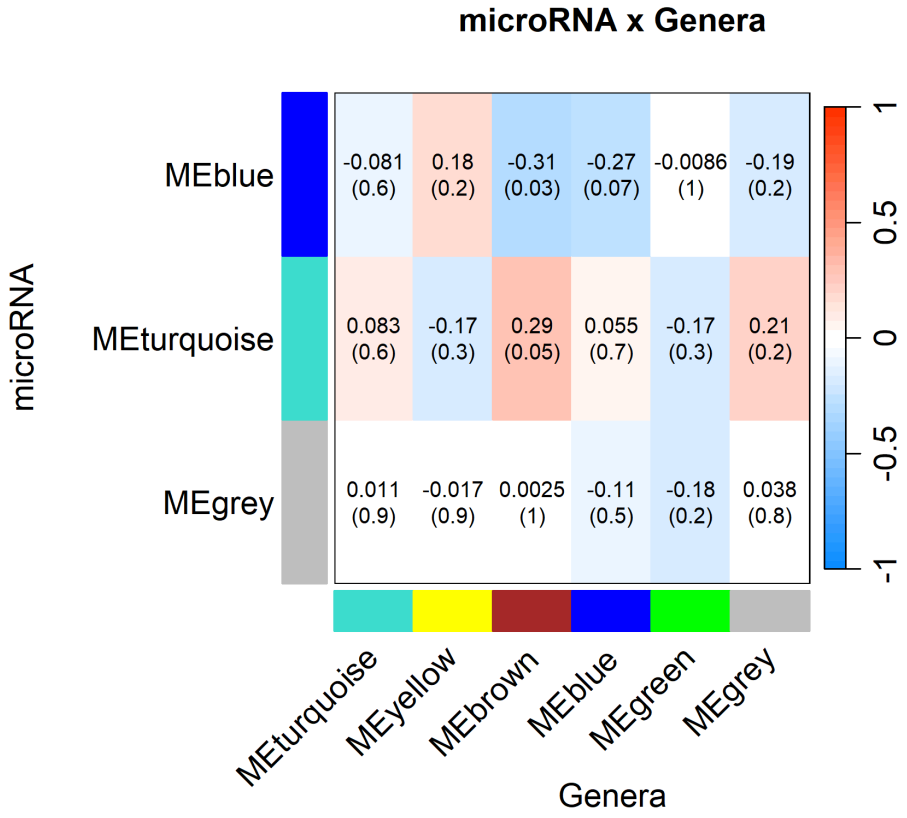

Figure 2: Correlation between genera and microRNA modules identified by WGCNA. Heatmap shows correlations between module eigengenes. Each cell displays the correlation coefficient, with the corresponding *p*-value shown in parentheses. Red and blue indicate positive and negative associations, respectively, and color intensity reflects correlation strength.

4.4 Discussion

In this study, we identified microbiota enzymatic and genera coexpression, alongside host rumen wall miRNA coexpression within the rumen environment. Our integrative network analysis revealed significant associations among these molecular features, suggesting a complex regulatory interplay among enzymes, miRNAs, and microbial genera. Our findings provide the first exploratory mapping of correlations between these layers in the Nelore rumen, highlighting candidate components of the multilayered regulatory framework that may

influence rumen function. These results offer a foundation for future studies aimed at validating the observed relationships under controlled in vitro conditions and exploring their potential implications for ruminal metabolism and host–microbiome interactions.

4.4.1 Coexpressed miRNAs, enzymes and taxa are linked to lipid metabolism

Our results showed a positive correlation between miRNA turquoise and enzyme blue modules. The miRNA turquoise module hub, bta-miR-378, has been described as playing an important role in regulating bovine muscle differentiation and function (Tong et al., 2018) and was highly expressed in bovines with high backfat thickness (Jin et al., 2010). In contrast, several members of the turquoise module, including miR-93, miR-92, miR-106b, miR-25, and cluster miR-17-92 (members bta-miR-17-3p/5p), were enriched in animals with low backfat thickness (Jin et al., 2010). In addition, miR-15a/b, also present in this module, plays an important role in adipocyte development and lipid metabolism in adipocytes (Andersen et al., 2010; Zhang et al., 2013). Therefore, our results suggest that members of the miRNA turquoise module could be involved in a coordinated regulatory role in ruminal tissue with potential impact on traits such as fat deposition and metabolic efficiency.

Accordingly, the enzyme blue module, which was positively correlated with miRNA turquoise, has several enzymes related with lipid metabolism, encompassing both lipid biosynthesis (e.g., HMG-CoA reductase, mevalonate kinase) (Goldstein and Brown, 1990; Kovacs et al., 2002; Jo and DeBose-Boyd, 2010) and lipid transport/utilization (e.g., enoyl-CoA hydratase, long-chain fatty acid transport protein) (Stahl et al., 2001; Agnihotri and Liu, 2003). Notably, key enzymes of the mevalonate pathway, such as HMG-CoA reductase, mevalonate kinase, and mevalonate pyrophosphate decarboxylase, are known to be modulated by miRNAs (Najafi-Shoushtari et al., 2010; Rottiers et al., 2011; Khan et al., 2020). Therefore, the positive correlation observed with the turquoise miRNA module may reflect a coordinated or compensatory regulation of lipid metabolism in the rumen.

In addition, the same turquoise miRNA module showed positive correlation with the brown microbial genera module. Notably, this module included *Alistipes*, a genus commonly reported in the bovine microbiome (Dowd et al., 2008; Callaway et al., 2010; Holman and Gzyl, 2019; Andrade et al., 2022; Conteville et al., 2023) whose species can produce propionate, acetate and/or succinate as a fermentation end product (Parker et al., 2020). Among these metabolites, acetate plays a central lipogenic role (Morrison and Preston, 2016) and, in mice, *Alistipes timonensis* has been shown to reduce plasma triglyceride concentrations, suggesting that it may modulate the host lipidome (Older et al., 2024). In ruminants, acetate is recognized as the main substrate for de novo fatty acid synthesis,

particularly in the mammary gland and adipose tissue, where it underpins milk production and fat deposition, respectively (Vernon, 1980; Lee et al., 2000; Lin et al., 2022). Consistently, our previous studies with Nelore cattle demonstrated that animals receiving the conventional diet had both higher ruminal abundance of *Alistipes* (Conteville et al., 2023) and increased acetate concentrations (Malheiros et al., 2023), reinforcing the link between this genus and lipid metabolic pathways in the rumen ecosystem. Thus, we hypothesize that the increased abundance of acetate-producing bacteria induces the expression of lipogenic miRNAs in the turquoise module, thus explaining the positive correlation. Together, these processes could explain the hologenomic regulation of lipogenesis in Nelore.

4.4.2 Rumen miRNA-Enzyme antagonism in amino acids and carbohydrate metabolism

The miRNA blue module, which included bta-miR-143, bta-miR-192, bta-miR-194, and bta-miR-145, was associated negatively with the enzymes blue and yellow modules. These miRNAs are highly expressed in intestinal tissues, where they modulate genes associated with tissue proliferation and gastrointestinal development in *Bos taurus* (Liang et al., 2014; Do et al., 2019). Additionally, Do et al. (2019) identified the bta-miR-145 as the hub miRNA of a module whose predicted target genes were mainly associated with negative regulation of the protein digestion and absorption, and lipid transport.

The enzyme blue module contains enzymes involved in lipogenesis and amino acid metabolism. Among the enzymes involved in lipogenesis there was sialidase (K01186), that is related with sphingolipids metabolism (Marquês et al., 2018; Eneva et al., 2021) which can modulate host lipid metabolism (Heaver et al., 2018). In *Bos taurus* calves, a positive correlation between bta-miR-100 and sphingolipid metabolism has been reported (Ricci et al., 2022). In contrast, in our study, the miRNA blue module, that includes bta-miR-100, showed a negative correlation with the module of enzymes related to sphingolipid metabolism, suggesting that this relationship might depend on microbiota composition and host development stage. In addition, among the enzymes involved in amino acid metabolism, there were enoyl-CoA hydratase (K01692), RHH-type transcriptional regulator / proline dehydrogenase / delta 1-pyrroline-5-carboxylate dehydrogenase (K13821), phosphoserine aminotransferase (K00831), and lysine 5,6-aminomutase beta subunit (K18011). Lysine 5,6 aminomutase is directly linked to the ability of some bacteria to use lysine to produce acetate via fermentation (Berkovitch et al., 2004). Furthermore, the multifunctional enzyme PutA (K13821) is involved in the oxidation of proline to glutamate in many bacteria (Liu et al., 2017). These results suggest that miRNA can play a central role in shaping amino acid metabolism in *Bos indicus*.

The yellow enzyme module, also negatively correlated with the blue miRNA module, comprises a set of enzymes primarily associated with catabolic processes and alternative metabolic pathways. Among these, notable examples include dihydroxyacid dehydratase/phosphogluconate dehydratase, involved in both branched-chain amino acid metabolism and sugar degradation through pathways such as Entner-Doudoroff (Gao et al., 2018; Evans et al., 2024); D-mannonate dehydratase, typically active in the breakdown of uronic acids derived from plant cell walls (Wichelecki et al., 2014); carbamoylphosphate synthase, essential for the biosynthesis of pyrimidines and arginine (Nyunoya and Lusty, 1983); and GH3, a glycoside hydrolase implicated in hemicellulose degradation (Gharechahi et al., 2023). Taken together, the functional profile of this module suggests a stronger association with carbohydrate degradation, particularly targeting plant-derived polysaccharides and sugars. Consistently, previous studies have reported examples of carbohydrate metabolism regulation mediated by miRNAs belonging to the blue module identified in our analysis. For example, suppression of miR-145, miR-143 or miR-29c increased glucose uptake (Lan and Albinsson, 2020) and fatty acid oxidation (Massart et al., 2017). In this context, our results suggest that there is a negative correlation between ruminal wall miRNA and microbial enzyme activity, influencing amino acid and carbohydrate metabolism in *Bos indicus*.

4.4.3 miRNA-microbiota interactions involving potentially pathogenic taxa

The miRNA blue module was negatively associated with the brown microbial genera module, which includes several pathogenic or opportunistic microorganisms with potential impacts on metabolism and muscle development. Among these, *Candidatus Atelocyanobacterium* is a member of cyanobacteria that are known to produce hepatotoxins and neurotoxins (Manubolu et al., 2014). *Lawsonia*, particularly *L. intracellularis*, is associated with proliferative enteropathy in swine, leading to mild to severe diarrhea, reduced weight gain, and impaired nutrient absorption (Campillo et al., 2021). *Photorhabdus*, which includes *P. asymbiotica,* capable of causing soft tissue infections and inducing apoptosis in human muscle cells (Mulley et al., 2015). Other genera such as *Butyricimonas* and *Alistipes* has been linked to intestinal inflammation and dysbiosis (Enemchukwu et al., 2016; Parker et al., 2020).

In the miRNA blue module, bta-miR-192 is clustered with members of the bta-miR-29 family (bta-miR-29d-5p and bta-miR-29c), which have been previously associated with immune-related processes in the digestive tract of *Bos taurus* (Coutinho et al., 2007; Zi et al., 2018; Do et al., 2019). For example, bta-miR-192 expression was significantly downregulated in MDBK cells upon infection with enterotoxigenic *Escherichia coli*, and the

absence of bta-miR-192 was associated with altered expression of genes involved in immune regulation, cancer, and viral infections (Zi et al., 2018). This supports the hypothesis that miRNAs within the blue module may contribute to host defense processes, and their negative association with the brown microbial genera module, which contains several pathogenic or opportunistic taxa, could reflect a regulatory mechanism aimed at limiting harmful microbial proliferation and its detrimental effects on metabolism and muscle development.

4.5 Conclusion

This study provides novel insights into the multilayered regulatory framework of the ruminal environment in *Bos indicus*, integrating enzymatic, miRNA, and microbial coexpression networks. We identified associations that may influence lipid metabolism, amino acid catabolism, and carbohydrate utilization, connecting both host and microbial levels. These exploratory findings generate hypotheses and highlight candidate interactions that warrant validation in controlled experimental settings. Together, these findings expand our understanding of host-microbiome regulatory interactions in the rumen of *Bos indicus* and open avenues for functional studies and biotechnologies aimed at improving metabolic efficiency and animal health.

4.6 References

Agnihotri, G., and Liu, H. (2003). Enoyl‐CoA Hydratase: Reaction, Mechanism, and Inhibition. *ChemInform* 34, chin.200314288. doi: 10.1002/chin.200314288

Aguilar, C., Mano, M., and Eulalio, A. (2019). Multifaceted Roles of microRNAs in Host-Bacterial Pathogen Interaction. *Microbiol. Spectr.* 7, 7.3.13. doi: 10.1128/microbiolspec.BAI-0002-2019

Andersen, D. C., Jensen, C. H., Schneider, M., Nossent, A. Y., Eskildsen, T., Hansen, J. L., et al. (2010). MicroRNA-15a fine-tunes the level of Delta-like 1 homolog (DLK1) in proliferating 3T3-L1 preadipocytes. *Exp. Cell Res.* 316, 1681–1691. doi: 10.1016/j.yexcr.2010.04.002

Andrade, B. G. N., Bressani, F. A., Cuadrat, R. R. C., Cardoso, T. F., Malheiros, J. M., De Oliveira, P. S. N., et al. (2022). Stool and Ruminal Microbiome Components Associated With Methane Emission and Feed Efficiency in Nelore Beef Cattle. *Front. Genet.* 13, 812828. doi: 10.3389/fgene.2022.812828

Andrews, S. (2010). FastQC A Quality Control tool for High Throughput Sequence Data. Available at: https://www.bioinformatics.babraham.ac.uk/projects/fastqc/ (Accessed August 18, 2025).

Badhan, A., Wang, Y., Terry, S., Gruninger, R., Guan, L. L., and McAllister, T. A. (2025). Invited review: Interplay of rumen microbiome and the cattle host in modulating feed efficiency and methane emissions. *J. Dairy Sci.* 108, 5489–5501. doi: 10.3168/jds.2024-26063

Barbosa, B. R. P., Santos, S. A., Abreu, U. G. P. D., Egito, A. A., Comastri Filho, J. A., Juliano, R. S., et al. (2014). Tolerância ao calor em bovinos das raças Nelore branco, Nelore vermelho e Pantaneira. *Rev. Bras. Saúde E Produção Anim.* 15, 854–865. doi: 10.1590/S1519-99402014000400010

Berkovitch, F., Behshad, E., Tang, K.-H., Enns, E. A., Frey, P. A., and Drennan, C. L. (2004). A locking mechanism preventing radical damage in the absence of substrate, as revealed by the x-ray structure of lysine 5,6-aminomutase. *Proc. Natl. Acad. Sci.* 101, 15870–15875. doi: 10.1073/pnas.0407074101

Callaway, T. R., Dowd, S. E., Edrington, T. S., Anderson, R. C., Krueger, N., Bauer, N., et al. (2010). Evaluation of bacterial diversity in the rumen and feces of cattle fed different levels of dried distillers grains plus solubles using bacterial tag-encoded FLX amplicon pyrosequencing1. *J. Anim. Sci.* 88, 3977–3983. doi: 10.2527/jas.2010-2900

Campillo, M., Smith, S. H., Gally, D. L., and Opriessnig, T. (2021). Review of methods for the detection of *Lawsonia intracellularis* infection in pigs. *J. Vet. Diagn. Invest.* 33, 621–631. doi: 10.1177/10406387211003551

Cantalapiedra, C. P., Hernández-Plaza, A., Letunic, I., Bork, P., and Huerta-Cepas, J. (2021). eggNOG-mapper v2: Functional Annotation, Orthology Assignments, and Domain Prediction at the Metagenomic Scale. *Mol. Biol. Evol.* 38, 5825–5829. doi: 10.1093/molbev/msab293

Cole, M. B., Augustin, M. A., Robertson, M. J., and Manners, J. M. (2018). The science of food security. *Npj Sci. Food* 2, 14. doi: 10.1038/s41538-018-0021-9

Conteville, L. C., Silva, J. V., Andrade, B. G. N., Cardoso, T. F., Bruscadin, J. J., Oliveira, P. S. N., et al. (2023). Rumen and fecal microbiomes are related to diet and production traits in Bos indicus beef cattle. *Front. Microbiol.* doi: https://doi.org/10.3389/fmicb.2023.1282851

Coutinho, L. L., Matukumalli, L. K., Sonstegard, T. S., Van Tassell, C. P., Gasbarre, L. C., Capuco, A. V., et al. (2007). Discovery and profiling of bovine microRNAs from immune-related and embryonic tissues. *Physiol. Genomics* 29, 35–43. doi: 10.1152/physiolgenomics.00081.2006

Cuinat, C., Pan, J., and Comelli, E. M. (2025). Host-dependent alteration of the gut microbiota: the role of luminal microRNAs. *Microbiome Res. Rep.* 4. doi: 10.20517/mrr.2024.46

Da Silva, W. A. L., Da Costa E Silva, E. V., Ferreira, M. G. C. R., Gheller, J. M., Poehland, R., and Melo-Sterza, F. D. A. (2023). Effect of shading on the physiological and reproductive parameters in Nelore cows. *Trop. Anim. Health Prod.* 55, 374. doi: 10.1007/s11250-023-03774-2

Dalmasso, G., Nguyen, H. T. T., Yan, Y., Laroui, H., Charania, M. A., Ayyadurai, S., et al. (2011). Microbiota Modulate Host Gene Expression via MicroRNAs. *PLoS ONE* 6, e19293. doi: 10.1371/journal.pone.0019293

Das, K., Garnica, O., and Dhandayuthapani, S. (2016). Modulation of Host miRNAs by Intracellular Bacterial Pathogens. *Front. Cell. Infect. Microbiol.* 6. doi: 10.3389/fcimb.2016.00079

Datta, N., Johnson, C., Kao, D., Gurnani, P., Alexander, C., Polytarchou, C., et al. (2023).

MicroRNA-based therapeutics for inflammatory disorders of the microbiota-gut-brain axis. *Pharmacol. Res.* 194, 106870. doi: 10.1016/j.phrs.2023.106870

Do, D. N., Dudemaine, P.-L., Fomenky, B. E., and Ibeagha-Awemu, E. M. (2019). Integration of miRNA weighted gene co-expression network and miRNA-mRNA co-expression analyses reveals potential regulatory functions of miRNAs in calf rumen development. *Genomics* 111, 849–859. doi: 10.1016/j.ygeno.2018.05.009

Dowd, S. E., Callaway, T. R., Wolcott, R. D., Sun, Y., McKeehan, T., Hagevoort, R. G., et al. (2008). Evaluation of the bacterial diversity in the feces of cattle using 16S rDNA bacterial tag-encoded FLX amplicon pyrosequencing (bTEFAP). *BMC Microbiol.* 8, 125. doi: 10.1186/1471-2180-8-125

Enemchukwu, C. U., Ben-Faras, H., Gialanella, P., Szymczak, W. A., Nosanchuk, J. D., and Madaline, T. F. (2016). Butyricimonas virosa bacteraemia and bowel disease: case report and review. *New Microbes New Infect.* 13, 34–36. doi: 10.1016/j.nmni.2016.05.004

Eneva, R., Engibarov, S., Abrashev, R., Krumova, E., and Angelova, M. (2021). Sialic acids, sialoconjugates and enzymes of their metabolism in fungi. *Biotechnol. Biotechnol. Equip.* 35, 346–357. doi: 10.1080/13102818.2021.1879678

Evans, S. E., Franks, A. E., Bergman, M. E., Sethna, N. S., Currie, M. A., and Phillips, M. A. (2024). Plastid ancestors lacked a complete Entner-Doudoroff pathway, limiting plants to glycolysis and the pentose phosphate pathway. *Nat. Commun.* 15. doi: 10.1038/s41467-024-45384-y

Fernandes, A. C., Reverter, A., Keogh, K., Alexandre, P. A., Afonso, J., Palhares, J. C. P., et al. (2024). Transcriptional response to an alternative diet on liver, muscle, and rumen of beef cattle. *Sci. Rep.* 14, 13682. doi: 10.1038/s41598-024-63619-2

Friedländer, M. R., Mackowiak, S. D., Li, N., Chen, W., and Rajewsky, N. (2012). miRDeep2 accurately identifies known and hundreds of novel microRNA genes in seven animal clades. *Nucleic Acids Res.* 40, 37–52. doi: 10.1093/nar/gkr688

Gao, H., Azam, T., Randeniya, S., Couturier, J., Rouhier, N., and Johnson, M. K. (2018). Function and maturation of the Fe–S center in dihydroxyacid dehydratase from Arabidopsis. *J. Biol. Chem.* 293, 4422–4433. doi: 10.1074/jbc.ra117.001592

Gharechahi, J., Vahidi, M. F., Sharifi, G., Ariaeenejad, S., Ding, X.-Z., Han, J.-L., et al. (2023). Lignocellulose degradation by rumen bacterial communities: New insights from metagenome analyses. *Environ. Res.* 229, 115925. doi: 10.1016/j.envres.2023.115925

Goldstein, J. L., and Brown, M. S. (1990). Regulation of the mevalonate pathway. *Nature* 343, 425–430. doi: 10.1038/343425a0

Gordon, A. (2009). FASTX-Toolkit. Available at: http://hannonlab.cshl.edu/fastx_toolkit/ (Accessed August 18, 2025).

Griffiths-Jones, S. (2006). miRBase: microRNA sequences, targets and gene nomenclature. *Nucleic Acids Res.* 34, D140–D144. doi: 10.1093/nar/gkj112

Heaver, S. L., Johnson, E. L., and Ley, R. E. (2018). Sphingolipids in host–microbial interactions. *Curr. Opin. Microbiol.* 43, 92–99. doi: 10.1016/j.mib.2017.12.011

Henchion, M., Moloney, A. P., Hyland, J., Zimmermann, J., and McCarthy, S. (2021). Review: Trends for meat, milk and egg consumption for the next decades and the role played by livestock systems in the global production of proteins. *Animal* 15, 100287. doi: 10.1016/j.animal.2021.100287

Henderson, G., Cox, F., Ganesh, S., Jonker, A., Young, W., Global Rumen Census Collaborators, et al. (2015). Rumen microbial community composition varies with diet and host, but a core microbiome is found across a wide geographical range. *Sci. Rep.* 5, 14567. doi: 10.1038/srep14567

Holman, D. B., and Gzyl, K. E. (2019). A meta-analysis of the bovine gastrointestinal tract microbiota. *FEMS Microbiol. Ecol.* 95, fiz072. doi: 10.1093/femsec/fiz072

Hook, S. E., Wright, A.-D. G., and McBride, B. W. (2010). Methanogens: Methane Producers of the Rumen and Mitigation Strategies. *Archaea* 2010, 1–11. doi: 10.1155/2010/945785

Jin, W., Dodson, M. V., Moore, S. S., Basarab, J. A., and Guan, L. L. (2010). Characterization of microRNA expression in bovine adipose tissues: a potential regulatory mechanism of subcutaneous adipose tissue development. *BMC Mol. Biol.* 11. doi: 10.1186/1471-2199-11-29

Jo, Y., and DeBose-Boyd, R. A. (2010). Control of Cholesterol Synthesis through Regulated ER-Associated Degradation of HMG CoA Reductase. *Crit. Rev. Biochem. Mol. Biol.* 45, 185–198. doi: 10.3109/10409238.2010.485605

Khan, A. A., Agarwal, H., Reddy, S. S., Arige, V., Natarajan, B., Gupta, V., et al. (2020). MicroRNA 27a Is a Key Modulator of Cholesterol Biosynthesis. *Mol. Cell. Biol.* 40. doi: 10.1128/mcb.00470-19

Koeppen, K., Hampton, T. H., Jarek, M., Scharfe, M., Gerber, S. A., Mielcarz, D. W., et al. (2016). A Novel Mechanism of Host-Pathogen Interaction through sRNA in Bacterial Outer Membrane Vesicles. *PLOS Pathog.* 12, e1005672. doi: 10.1371/journal.ppat.1005672

Kovacs, W. J., Olivier, L. M., and Krisans, S. K. (2002). Central role of peroxisomes in isoprenoid biosynthesis. *Prog. Lipid Res.* 41, 369–391. doi: 10.1016/S0163-7827(02)00002-4

Lan, S., and Albinsson, S. (2020). Regulation of IRS-1, insulin signaling and glucose uptake by miR-143/145 in vascular smooth muscle cells. *Biochem. Biophys. Res. Commun.* 529, 119–125. doi: 10.1016/j.bbrc.2020.05.148

Langfelder, P., and Horvath, S. (2007). Eigengene networks for studying the relationships between co-expression modules. *BMC Syst. Biol.* 1, 54. doi: 10.1186/1752-0509-1-54

Langfelder, P., and Horvath, S. (2008). WGCNA: an R package for weighted correlation network analysis. *BMC Bioinformatics* 9, 559. doi: 10.1186/1471-2105-9-559

Lee, R. C., Feinbaum, R. L., and Ambros, V. (1993). The C. elegans heterochronic gene lin-4 encodes small RNAs with antisense complementarity to lin-14. *Cell* 75, 843–854. doi: 10.1016/0092-8674(93)90529-y

Lee, S. C., Lee, H. J., Kim, D. W., Park, J. G., and Han, I. K. (2000). Effects of Carbon Precursors and Hormones on the Lipogenesis and Lipolysis of Hanwoo Cattle

Adipose Tissues. *Asian-Australas. J. Anim. Sci.* 13, 300–306. doi: 10.5713/ajas.2000.300

Li, L., Huang, J., Zhang, X., Ju, Z., Qi, C., Zhang, Y., et al. (2012). One SNP in the 3′-UTR of HMGB1 gene affects the binding of target bta-miR-223 and is involved in mastitis in dairy cattle. *Immunogenetics* 64, 817–824. doi: 10.1007/s00251-012-0641-1

Liang, G., Malmuthuge, N., McFadden, T. B., Bao, H., Griebel, P. J., Stothard, P., et al. (2014). Potential Regulatory Role of MicroRNAs in the Development of Bovine Gastrointestinal Tract during Early Life. *PLoS ONE* 9, e92592. doi: 10.1371/journal.pone.0092592

Lin, M., Jiang, M., Yang, T., Tan, D., Hu, G., Zhao, G., et al. (2022). Acetate-Induced Milk Fat Synthesis Is Associated with Activation of the mTOR Signaling Pathway in Bovine Mammary Epithelial Cells. *Animals* 12, 2616. doi: 10.3390/ani12192616

Lin, Y., Li, Y., Chen, H., Meng, J., Li, J., Chu, J., et al. (2023). Weighted gene co-expression network analysis revealed T cell differentiation associated with the age-related phenotypes in COVID-19 patients. *BMC Med. Genomics* 16, 59. doi: 10.1186/s12920-023-01490-2

Liu, L.-K., Becker, D. F., and Tanner, J. J. (2017). Structure, function, and mechanism of proline utilization A (PutA). *Arch. Biochem. Biophys.* 632, 142–157. doi: 10.1016/j.abb.2017.07.005

Liu, S., da Cunha, A. P., Rezende, R. M., Cialic, R., Wei, Z., Bry, L., et al. (2016). The Host Shapes the Gut Microbiota via Fecal MicroRNA. *Cell Host Microbe* 19, 32–43. doi: 10.1016/j.chom.2015.12.005

Lombard, V., Golaconda Ramulu, H., Drula, E., Coutinho, P. M., and Henrissat, B. (2014). The carbohydrate-active enzymes database (CAZy) in 2013. *Nucleic Acids Res.* 42, D490–D495. doi: 10.1093/nar/gkt1178

Ma, S., Shungin, D., Mallick, H., Schirmer, M., Nguyen, L. H., Kolde, R., et al. (2022). Population structure discovery in meta-analyzed microbial communities and inflammatory bowel disease using MMUPHin. *Genome Biol.* 23, 208. doi: 10.1186/s13059-022-02753-4

Malheiros, J. M., Correia, B. S. B., Ceribeli, C., Bruscadin, J. J., Diniz, W. J. S., Banerjee, P., et al. (2023). Ruminal and feces metabolites associated with feed efficiency, water intake and methane emission in Nelore bulls. *Sci. Rep.* 13, 18001. doi: 10.1038/s41598-023-45330-w

Malmuthuge, N., Liang, G., and Guan, L. L. (2019). Regulation of rumen development in neonatal ruminants through microbial metagenomes and host transcriptomes. *Genome Biol.* 20, 172. doi: 10.1186/s13059-019-1786-0

Manubolu, M., Madawala, S. R., C Dutta, P., and Malmlöf, K. (2014). In vitro biodegradation of cyanotoxins in the rumen fluid of cattle. *BMC Vet. Res.* 10, 110. doi: 10.1186/1746-6148-10-110

Margulis, L., and Fester, R. (1991). *Symbiosis as a Source of Evolutionary Innovation*. Cambrigde: The MIT Press.

Marquês, J. T., Marinho, H. S., and de Almeida, R. F. M. (2018). Sphingolipid hydroxylation

in mammals, yeast and plants – An integrated view. *Prog. Lipid Res.* 71, 18–42. doi: 10.1016/j.plipres.2018.05.001

Massart, J., Sjögren, R. J. O., Lundell, L. S., Mudry, J. M., Franck, N., O'Gorman, D. J., et al. (2017). Altered miR-29 Expression in Type 2 Diabetes Influences Glucose and Lipid Metabolism in Skeletal Muscle. *Diabetes* 66, 1807–1818. doi: 10.2337/db17-0141

Morrison, D. J., and Preston, T. (2016). Formation of short chain fatty acids by the gut microbiota and their impact on human metabolism. *Gut Microbes* 7, 189–200. doi: 10.1080/19490976.2015.1134082

Mulley, G., Beeton, M. L., Wilkinson, P., Vlisidou, I., Ockendon-Powell, N., Hapeshi, A., et al. (2015). From Insect to Man: Photorhabdus Sheds Light on the Emergence of Human Pathogenicity. *PLOS ONE* 10, e0144937. doi: 10.1371/journal.pone.0144937

Najafi-Shoushtari, S. H., Kristo, F., Li, Y., Shioda, T., Cohen, D. E., Gerszten, R. E., et al. (2010). MicroRNA-33 and the SREBP Host Genes Cooperate to Control Cholesterol Homeostasis. *Science* 328, 1566–1569. doi: 10.1126/science.1189123

Nyunoya, H., and Lusty, C. J. (1983). The carB gene of Escherichia coli: a duplicated gene coding for the large subunit of carbamoyl-phosphate synthetase. *Proc. Natl. Acad. Sci.* 80, 4629–4633. doi: 10.1073/pnas.80.15.4629

Ojo, O. E., and Kreuzer-Redmer, S. (2023). MicroRNAs in Ruminants and Their Potential Role in Nutrition and Physiology. *Vet. Sci.* 10, 57. doi: 10.3390/vetsci10010057

Older, E. A., Mitchell, M. K., Campbell, A., Lian, X., Madden, M., Wang, Y., et al. (2024). Human gut commensal *Alistipes timonensis* modulates the host lipidome and delivers anti-inflammatory outer membrane vesicles to suppress colitis in an *Il10* -deficient mouse model. doi: 10.1101/2024.10.23.619966

Oliveira, P. S. N. D., Andrade, B. G. N., Cardoso, T. F., Conteville, L. C., Pena, G. A. C., Malago-Jr, W., et al. (2024). miRNA-microbiome interplay is related to Bos indicus feed efficiency. doi: 10.21203/rs.3.rs-4744784/v1

Parker, B. J., Wearsch, P. A., Veloo, A. C. M., and Rodriguez-Palacios, A. (2020). The Genus Alistipes: Gut Bacteria With Emerging Implications to Inflammation, Cancer, and Mental Health. *Front. Immunol.* 11, 906. doi: 10.3389/fimmu.2020.00906

Ricci, S., Petri, R. M., Pacífico, C., Castillo-Lopez, E., Rivera-Chacon, R., Sener-Aydemir, A., et al. (2022). Characterization of presence and activity of microRNAs in the rumen of cattle hints at possible host-microbiota cross-talk mechanism. *Sci. Rep.* 12, 13812. doi: 10.1038/s41598-022-17445-z

Rosenberg, E., Koren, O., Reshef, L., Efrony, R., and Zilber-Rosenberg, I. (2007). The role of microorganisms in coral health, disease and evolution. *Nat. Rev. Microbiol.* 5, 355–362. doi: 10.1038/nrmicro1635

Rottiers, V., Najafi-Shoushtari, S. H., Kristo, F., Gurumurthy, S., Zhong, L., Li, Y., et al. (2011). MicroRNAs in Metabolism and Metabolic Diseases. *Cold Spring Harb. Symp. Quant. Biol.* 76, 225–233. doi: 10.1101/sqb.2011.76.011049

Stahl, A., Gimeno, R. E., Tartaglia, L. A., and Lodish, H. F. (2001). Fatty acid transport proteins: a current view of a growing family. *Trends Endocrinol. Metab.* 12, 266–273. doi: 10.1016/S1043-2760(01)00427-1

Tarazona, S., Furió-Tarí, P., Turrà, D., Pietro, A. D., Nueda, M. J., Ferrer, A., et al. (2015). Data quality aware analysis of differential expression in RNA-seq with NOISeq R/Bioc package. *Nucleic Acids Res.*, gkv711. doi: 10.1093/nar/gkv711

Tong, H., Jiang, R., Liu, T., Wei, Y., Li, S., and Yan, Y. (2018). bta-miR-378 promote the differentiation of bovine skeletal muscle-derived satellite cells. *Gene* 668, 246–251. doi: 10.1016/j.gene.2018.03.102

Vernon, R. G. (1980). Lipid metabolism in the adipose tissue of ruminant animals. *Prog. Lipid Res.* 19, 23–106. doi: 10.1016/0163-7827(80)90007-7

Viennois, E., Chassaing, B., Tahsin, A., Pujada, A., Wang, L., Gewirtz, A. T., et al. (2019). Host-derived fecal microRNAs can indicate gut microbiota healthiness and ability to induce inflammation. *Theranostics* 9, 4542–4557. doi: 10.7150/thno.35282

Wichelecki, D. J., Vendiola, J. A. F., Jones, A. M., Al-Obaidi, N., Almo, S. C., and Gerlt, J. A. (2014). Investigating the Physiological Roles of Low-Efficiency D-Mannonate and D-Gluconate Dehydratases in the Enolase Superfamily: Pathways for the Catabolism of L-Gulonate and L-Idonate. *Biochemistry* 53, 5692–5699. doi: 10.1021/bi500837w

Wightman, B., Ha, I., and Ruvkun, G. (1993). Posttranscriptional regulation of the heterochronic gene lin-14 by lin-4 mediates temporal pattern formation in C. elegans. *Cell* 75, 855–862. doi: 10.1016/0092-8674(93)90530-4

Wood, D. E., Lu, J., and Langmead, B. (2019). Improved metagenomic analysis with Kraken 2. *Genome Biol.* 20, 257. doi: 10.1186/s13059-019-1891-0

Yuan, C., Burns, M. B., Subramanian, S., and Blekhman, R. (2018). Interaction between Host MicroRNAs and the Gut Microbiota in Colorectal Cancer. *mSystems* 3, e00205-17. doi: 10.1128/mSystems.00205-17

Zhang, Y., Cheng, X., Lu, Z., Wang, J., Chen, H., Fan, W., et al. (2013). Upregulation of miR-15b in NAFLD models and in the serum of patients with fatty liver disease. *Diabetes Res. Clin. Pract.* 99, 327–334. doi: 10.1016/j.diabres.2012.11.025

Zheng, J., Ge, Q., Yan, Y., Zhang, X., Huang, L., and Yin, Y. (2023). dbCAN3: automated carbohydrate-active enzyme and substrate annotation. *Nucleic Acids Res.* 51, W115–W121. doi: 10.1093/nar/gkad328

Zi, C., Zeng, D., Zhou, J., Dai, J., Jiang, L., Xue, F., et al. (2018). Selected microRNA-192 mutant indicates association with several function genes in bovine cells. *Genes Genomics* 40, 361–371. doi: 10.1007/s13258-017-0635-3

5 Conclusion

This study analyzed metatranscriptomic data and integrated it with metagenomic and microRNA expression data to investigate, for the first time, the functional mechanisms connecting diet, the rumen microbiome, and productive traits in Nelore cattle. Initially, we demonstrated that different diets can functionally modulate the rumen microbiome. Furthermore, we showed that diets formulated with agro-industrial by-products, such as citrus pulp and peanut meal, can promote alternative metabolic pathways that compete with methanogenesis. These findings highlight the potential of such diets to reduce feeding costs and greenhouse gas emissions, contributing to more sustainable production systems.

In a second approach, by comparing the total metagenomic catalog with the set of transcriptionally active genes (aNRPMG) from the rumen microbiome, we showed that microbial activity, not merely its presence, is a key factor in mitigating methane emissions and improving feed efficiency. Enzymes involved in hemicellulose and pectin degradation, alternative redox pathways, and the specific activity of certain microbial genera emerged as key elements in modulating ruminal fermentation and the energetic utilization of the diet. Finally, we explored a novel frontier at the interface between host genomics and the rumen microbiome. By identifying co-expression patterns between ruminal microRNAs, microbial enzymes, and genera, we suggest that microRNAs may act as central regulators of microbial functionality in the rumen, opening innovative perspectives for genetic improvement and precision nutritional management strategies.

Taken together, the findings of this study significantly advance our understanding of the molecular mechanisms underlying productive and environmental efficiency in beef cattle raised under tropical systems. The evidence gathered provides a strong foundation for the development of technologies aimed at modulating the rumen microbiome through diet, targeted additives, or genomic selection of more efficient and better-adapted animals.